Electronic Supplementary Information

Mechanochemical applications of magnesium nitride to fullerene chemistry: synthesis of pyrroline-fused tetra-functionalized [60]fullerene derivatives

Jun-Shen Chen,[a] Wen-Jie Qiu,[a] Li-Feng Guo[a] and Guan-Wu Wang*[abc]

[a] *Department of Chemistry, University of Science and Technology of China, Hefei, Anhui 230026, P. R. China.*

Fax: +86 551 63607864; Tel: +86 551 63607864

E-mail: gwang@ustc.edu.cn

[b] *Key Laboratory of Functional Molecular Solids, Ministry of Education, Anhui Laboratory of Molecule-Based Materials, and School of Chemistry and Materials Science, Anhui Normal University, Wuhu, Anhui 241002, P. R. China.*

[c] *State Key Laboratory of Natural Product Chemistry, Lanzhou University, Lanzhou, Gansu 730000, P. R. China.*

Table of Contents

1. General Information

Tetra-*n*-butylammonium perchlorate (n-Bu_4NClO_4), used as an electrolyte, was recrystallised from absolute ethanol and dried under vacuum at 50 °C prior to use. Other chemicals were obtained commercially and used without further purification. NMR spectra were recorded on a 400 MHz NMR spectrometer (400 MHz for ^1H NMR; 101 MHz for ^{13}C NMR) or a 500 MHz NMR spectrometer (500 MHz for ^1H NMR; 126 MHz for ^{13}C NMR). ^1H NMR chemical shifts were determined relative to TMS or residual $C_2H_2Cl_4$ (δ 5.90 ppm). ^{13}C NMR chemical shifts were determined relative to TMS or $C_2D_2Cl_4$ (δ 72.85 ppm). Data for ^1H NMR and ^{13}C NMR are reported as follows: chemical shift (δ, ppm), multiplicity (s = singlet, d = doublet, t = triplet, q = quartet, m = multiplet). High-resolution mass spectra (HRMS) were measured with MALDI-TOF in negative mode. Ball-milling reactions were performed in a GT 600 mixer mill, using a stainless-steel jar (5 mL, 282.2 g) along with 4 stainless-steel balls (5 mm in diameter, 0.5 g) and milled vigorously at room temperature (~25 °C). The custom-made GT 600 mixer mill is a product of Beijing Grinder Instrument Co., Ltd.

Fig. S1 Photo of the custom-made GT 600 mixer mill.

2. Synthesis and Spectral Data of 2a-n′

General Procedure for Mechanosynthesis: A mixture of [60]fullerene (C_{60}) (0.04 mmol), Mg_3N_2 (0.20 mmol), **1** (0.60 mmol or 0.40 mmol), AgCl (0.04 mmol) and silica gel (36.0 mg) together with 4 stainless-steel balls (5 mm in diameter) was introduced into a stainless-steel jar (5 mL) and milled vigorously (35 Hz) in a GT 600 mixer mill at room temperature for 1 h. After that, the reaction mixture was suspended in carbon disulfide (CS_2), transferred on the top of a silica gel column and then separated by column chromatography with CS_2 as the eluent to provide unreacted C_{60}, further elution with dichloromethane (CH_2Cl_2)/CS_2 afforded **2**.

Procedure for Liquid-Phase Synthesis of 2a: C_{60} (0.04 mmol), Mg_3N_2 (0.20 mmol), **1a** (0.60 mmol), AgCl (0.04 mmol), silica gel (36.0 mg) and toluene were added into a Schlenk tube and stirred for 1 h vigorously at room temperature. After the reaction was complete, the reaction mixture was extracted with CS_2 and separated by column chromatography on silica gel with CS_2 as the eluent to provide unreacted C_{60}, further elution with CH_2Cl_2/CS_2 afforded **2a**.

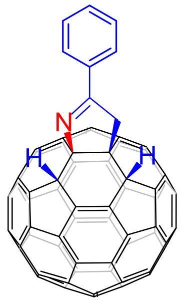

Synthesis and Spectral Data of 2a: By following the general procedure, a mixture of C_{60} (0.04 mmol, 28.8 mg), Mg_3N_2 (0.20 mmol, 20.1 mg), **1a** (0.60 mmol, 72.0 mg), AgCl (0.04 mmol, 5.8 mg) and silica gel (36.0 mg) was milled vigorously (35 Hz) for 1 h to afford unreacted C_{60} (7.7 mg, 27%) and **2a** (12.5 mg, 37%) as an amorphous brown solid. ^{1}H NMR (500 MHz, $CS_2/CDCl_3$) δ 8.24–8.16 (m, 2H), 7.59–7.53 (m, 3H), 6.28 (d, J = 1.8 Hz, 1H), 6.19 (d, J = 1.8 Hz, 1H), 4.72 (d, J = 18.2 Hz, 1H), 4.57 (d, J = 18.2 Hz, 1H); ^{13}C NMR (126 MHz, $CS_2/CDCl_3$, all 1C unless indicated) δ 169.49 (*C*=N), 150.39, 149.88, 149.17, 149.14, 148.98, 148.40, 148.31, 148.23, 148.18 (2C), 147.20, 146.93, 146.84, 146.66 (2C), 146.44, 146.33, 146.22, 145.69, 145.64, 145.62, 145.11 (2C), 144.80, 144.74, 144.72, 144.60 (2C), 144.36, 144.24, 144.17, 144.15, 144.10, 144.09, 144.04, 143.79, 143.58, 143.30, 143.26, 143.03, 142.96, 142.88, 142.75, 142.63, 142.38, 142.29, 142.22, 142.06, 141.55, 141.17, 141.02, 139.29, 136.84, 136.43, 136.10, 134.49, 133.35 (aryl *C*), 131.48 (aryl *C*), 128.73 (2C, aryl *C*), 128.27 (2C, aryl *C*), 94.00 (sp^3-*C* of C_{60}), 60.88 (sp^3-*C* of C_{60}), 59.66 (sp^3-*C* of C_{60}), 58.95, 56.68 (sp^3-*C* of C_{60}); FT-IR ν/cm^{-1} (KBr) 1616, 1442, 1421, 1339, 1183, 902, 757, 729, 688, 587, 575, 545, 526; UV–vis ($CHCl_3$) λ_{max}/nm (log ε) 257 (4.94), 330 (4.38), 431 (3.64), 705 (2.53); MALDI-TOF MS m/z calcd for $C_{68}H_9N$ $[M]^-$ 839.0740, found 839.0731.

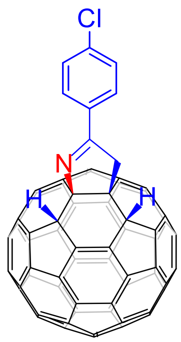

Synthesis and Spectral Data of 2b: By following the general procedure, a mixture of C_{60} (0.04 mmol, 28.9 mg), Mg_3N_2 (0.20 mmol, 20.0 mg), **1b** (0.60 mmol, 92.7 mg), AgCl (0.04 mmol, 5.7 mg) and silica gel (36.0 mg) was milled vigorously (35 Hz) for 1 h to afford unreacted C_{60} (15.2 mg, 53%) and **2b** (12.5 mg, 36%) as an amorphous brown solid. ^{1}H NMR (400 MHz, $CS_2/C_2D_2Cl_4$) δ 8.15 (d, J = 8.5 Hz, 2 H), 7.54 (d, J = 8.5 Hz, 2 H), 6.27 (d, J = 1.7 Hz, 1H), 6.17 (d, J = 1.7 Hz, 1H), 4.67 (d, J = 18.4 Hz, 1H), 4.51 (d, J = 18.4 Hz, 1H); ^{13}C NMR (101 MHz, $CS_2/C_2D_2Cl_4$, all 1C unless indicated) δ 167.66 (*C*=N), 149.33, 148.87, 148.10 (2C), 147.90, 147.35, 147.16, 147.13, 147.12, 147.07, 146.02, 145.86, 145.78, 145.60 (2C), 145.38, 145.26, 145.16, 144.57, 144.53, 144.38, 144.06, 144.01, 143.72, 143.68, 143.65, 143.53 (2C), 143.31, 143.14, 143.09 (2C), 143.01, 143.00 (2C), 142.70, 142.53, 142.24, 142.17, 141.99, 141.88, 141.78, 141.66, 141.57, 141.32, 141.21, 141.15, 140.95, 140.49, 140.09, 139.95, 138.15, 136.86 (aryl *C*), 135.74, 135.22, 134.97, 133.49, 130.72 (aryl *C*), 128.52 (2C, aryl *C*), 128.02 (2C, aryl *C*), 92.96 (sp^3-*C* of C_{60}), 59.69 (sp^3-*C* of C_{60}), 58.72 (sp^3-*C* of C_{60}), 57.66, 55.50 (sp^3-*C* of C_{60}); FT-IR ν/cm^{-1} (KBr) 1620, 1508, 1492, 1421, 1190, 1091, 1012, 825, 779, 745, 588, 572, 565, 556, 539, 529, 523; UV–vis ($CHCl_3$) λ_{max}/nm (log ε) 258 (4.97), 332 (4.39), 431 (3.66), 706 (2.30); MALDI-TOF MS m/z calcd for $C_{68}H_8{}^{35}ClN$ $[M]^-$ 873.0350, found 873.0357.

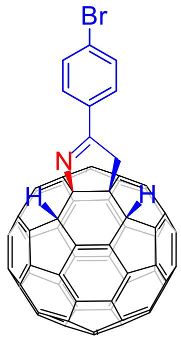

Synthesis and Spectral Data of 2c: By following the general procedure, a mixture of C_{60} (0.04 mmol, 28.8 mg), Mg_3N_2 (0.20 mmol, 20.2 mg), **1c** (0.40 mmol, 80.0 mg), AgCl (0.04 mmol, 5.6 mg) and silica gel (36.0 mg) was milled vigorously (35 Hz) for 1 h to afford unreacted C_{60} (18.5 mg, 64%) and **2c** (10.6 mg, 29%) as an amorphous brown solid. ^{1}H NMR (500 MHz, $CS_2/C_2D_2Cl_4$) δ 8.08 (d, *J* = 8.5 Hz, 2H), 7.70 (d, *J* = 8.5 Hz, 2H), 6.26 (d, *J* = 1.7 Hz, 1H), 6.16 (d, *J* = 1.7 Hz, 1H), 4.67 (d, *J* = 18.3 Hz, 1H), 4.51 (d, *J* = 18.3, 1H); ^{13}C NMR (101 MHz, $CS_2/C_2D_2Cl_4$, all 1C unless indicated) δ 167.73 (*C*=N), 149.29, 148.84, 148.08 (2C), 147.86, 147.33, 147.14, 147.12, 147.10, 147.01, 145.99, 145.84, 145.76, 145.59, 145.56, 145.37, 145.24, 145.14, 144.56, 144.52, 144.30, 144.04, 143.99, 143.70, 143.66, 143.64, 143.52 (2C), 143.29, 143.13, 143.07 (2C), 143.00, 142.98 (2C), 142.69, 142.51, 142.23, 142.15, 141.97, 141.87, 141.78, 141.65, 141.55, 141.30, 141.20, 141.14, 140.93, 140.47, 140.08, 139.94, 138.14, 135.73, 135.20, 134.95, 133.48, 131.12 (aryl *C*), 130.98 (2C, aryl *C*), 128.67 (2C, aryl *C*), 125.54 (aryl *C*), 92.97 (sp^3-*C* of C_{60}), 59.68 (sp^3-*C* of C_{60}), 58.68 (sp^3-*C* of C_{60}), 57.60, 55.46 (sp^3-*C* of C_{60}); FT-IR ν/cm^{-1} (KBr) 1620, 1586, 1421, 1395, 1331, 1188, 1068, 1008, 816, 749, 587, 571, 566, 533, 528, 523; UV–vis ($CHCl_3$) λ_{max}/nm (log ε) 259 (4.90), 331 (4.33), 431 (3.59), 707 (2.31); MALDI-TOF MS m/z calcd for $C_{68}H_8{}^{79}BrN$ $[M]^-$ 916.9845, found 916.9837.

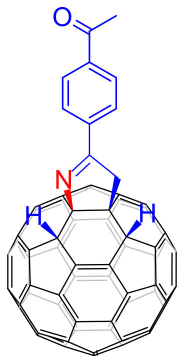

Synthesis and Spectral Data of 2d: By following the general procedure, a mixture of C_{60} (0.04 mmol, 28.8 mg), Mg_3N_2 (0.20 mmol, 20.2 mg), **1d** (0.40 mmol, 64.8 mg), AgCl (0.04 mmol, 5.6 mg) and silica gel (36.0 mg) was milled vigorously (35 Hz) for 1 h to afford unreacted C_{60} (5.9 mg, 20%) and **2d** (20.8 mg, 59%) as an amorphous brown solid. ^{1}H NMR (500 MHz, $CS_2/C_2D_2Cl_4$) δ 8.31 (d, J = 8.4 Hz, 2H), 8.12 (d, J = 8.4 Hz, 2H), 6.29 (d, J = 1.8 Hz, 1H), 6.19 (d, J = 1.8 Hz, 1H), 4.73 (d, J = 18.3 Hz, 1H), 4.58 (d, J = 18.3, 1H), 2.68 (s, 3H); ^{13}C NMR (126 MHz, $CS_2/C_2D_2Cl_4$, all 1C unless indicated) δ 194.68 (*C*=O), 167.67 (*C*=N), 149.08, 148.68, 148.02, 148.00, 147.69, 147.27, 147.05 (2C), 147.00, 146.78, 145.86, 145.78, 145.70, 145.54, 145.44, 145.32, 145.18, 145.08, 144.52, 144.49, 143.98, 143.96, 143.91, 143.61, 143.59, 143.58 (2C), 143.47, 143.23, 143.05, 143.02 (2C), 142.95, 142.91 (2C), 142.63, 142.45, 142.20, 142.07, 141.88, 141.83, 141.76, 141.62, 141.52, 141.25, 141.15, 141.08, 140.87, 140.40, 140.06, 139.93, 138.10, 137.82 (aryl *C*), 136.03 (aryl *C*), 135.74, 135.15, 134.89, 133.44, 127.45 (2C, aryl *C*), 127.35 (2C, aryl *C*), 93.05 (sp^3-*C* of C_{60}), 59.64 (sp^3-*C* of C_{60}), 58.55 (sp^3-*C* of C_{60}), 57.70, 55.36 (sp^3-*C* of C_{60}), 25.30; FT-IR ν/cm^{-1} (KBr) 1685, 1618, 1420, 1405, 1262, 1189, 1047, 946, 883, 744, 586, 571, 566, 559, 533, 528, 523; UV–vis ($CHCl_3$) λ_{max}/nm (log ε) 260 (4.88), 332 (4.32), 431 (3.57), 707 (2.22); MALDI-TOF MS m/z calcd for $C_{70}H_{11}NO$ [M]$^-$ 881.0846, found 881.0841.

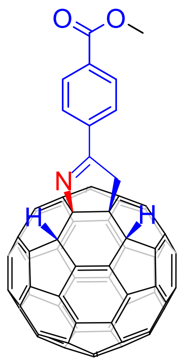

Synthesis and Spectral Data of 2e: By following the general procedure, a mixture of C_{60} (0.04 mmol, 28.8 mg), Mg_3N_2 (0.20 mmol, 20.2 mg), **1e** (0.40 mmol, 71.2 mg), AgCl (0.04 mmol, 5.7 mg) and silica gel (36.0 mg) was milled vigorously (35 Hz) for 1 h to afford unreacted C_{60} (8.3 mg, 29%) and **2e** (10.7 mg, 30%) as an amorphous brown solid. Owing to the low solubility of **2e** in common organic solvents, no ^{13}C NMR spectrum with acceptable signal/noise ratio could be recorded. ^{1}H NMR (500 MHz, $CS_2/C_2D_2Cl_4$) δ 8.28 (d, J = 8.5 Hz, 2H), 8.21 (d, J = 8.5 Hz, 2H), 6.29 (d, J = 1.7 Hz, 1H), 6.19 (d, J = 1.7 Hz, 1H), 4.73 (d, J = 18.3 Hz, 1H), 4.57 (d, J = 18.3, 1H), 3.96 (s, 3H); FT-IR *ν*/cm^{-1} (KBr) 1719, 1624, 1433, 1279, 1191, 1108, 1018, 780, 769, 587, 572, 566, 529, 523; UV–vis ($CHCl_3$) λ_{max}/nm (log ε) 259 (4.89), 333 (4.29), 431 (3.55), 707 (2.33); MALDI-TOF MS m/z calcd for $C_{70}H_{11}NO_2$ $[M]^-$ 897.0795, found 897.0793.

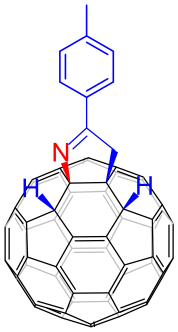

Synthesis and Spectral Data of 2f: By following the general procedure, a mixture of C_{60} (0.04 mmol, 28.8 mg), Mg_3N_2 (0.20 mmol, 20.2 mg), **1f** (0.60 mmol, 80.3 mg), AgCl (0.04 mmol, 5.7 mg) and silica gel (36.0 mg) was milled vigorously (35 Hz) for 1 h to afford unreacted C_{60} (16.5 mg, 57%) and **2f** (8.8 mg, 26%) as an amorphous brown solid. ^{1}H NMR (500 MHz, $CS_2/C_2D_2Cl_4$) *δ* 8.08 (d, *J* = 8.0 Hz, 2H), 7.36 (d, *J* = 8.0 Hz, 2H), 6.27 (d, *J* = 1.8 Hz, 1H), 6.17 (d, *J* = 1.8 Hz, 1H), 4.68 (d, *J* = 18.2 Hz, 1H), 4.52 (d, *J* = 18.2 Hz, 1H), 2.50 (s, 3H); ^{13}C NMR (126 MHz, $CS_2/C_2D_2Cl_4$, all 1C unless indicated) *δ* 168.34 (*C*=N), 149.43, 148.89, 148.05, 148.02 (2C), 147.38, 147.28, 147.14, 147.11, 147.06, 146.17, 145.81, 145.72, 145.60, 145.53, 145.31, 145.21, 145.10, 144.86, 144.52, 144.49, 144.03, 144.00, 143.69, 143.68, 143.61, 143.47 (2C), 143.25, 143.14, 143.04 (2C), 142.98, 142.97, 142.93, 142.66, 142.47, 142.16 (2C), 141.96, 141.82, 141.73, 141.61, 141.50, 141.26, 141.16, 141.11, 140.94, 140.79 (aryl *C*), 140.45, 140.02, 139.87, 138.15, 135.62, 135.27, 135.00, 133.38, 129.58 (aryl *C*), 128.42 (2C, aryl *C*), 127.24 (2C, aryl *C*), 92.83 (sp^3-*C* of C_{60}), 59.75 (sp^3-*C* of C_{60}), 58.57 (sp^3-*C* of C_{60}), 57.82, 55.65 (sp^3-*C* of C_{60}), 20.65; FT-IR *ν*/cm^{-1} (KBr) 1619, 1607, 1420, 1337, 1182, 1050, 1019, 816, 748, 587, 566, 572, 561, 543, 530, 524; UV–vis ($CHCl_3$) λ_{max}/nm (log ε) 258 (4.96), 333 (4.37), 431 (3.64), 707 (2.13); MALDI-TOF MS m/z calcd for $C_{69}H_{11}N$ $[M]^-$ 853.0896, found 853.0891.

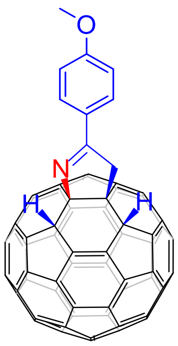

Synthesis and Spectral Data of 2g: By following the general procedure, a mixture of C_{60} (0.04 mmol, 28.7 mg), Mg_3N_2 (0.20 mmol, 20.0 mg), **1g** (0.40 mmol, 60.0 mg), AgCl (0.04 mmol, 5.7 mg) and silica gel (36.0 mg) was milled vigorously (35 Hz) for 1 h to afford unreacted C_{60} (17.4 mg, 61%) and **2g** (7.2 mg, 21%) as an amorphous brown solid. ^{1}H NMR (500 MHz, $CS_2/C_2D_2Cl_4$) δ 8.13 (d, J = 8.8 Hz, 2H), 7.04 (d, J = 8.8 Hz, 2H), 6.27 (d, J = 1.8 Hz, 1H), 6.16 (d, J = 1.8 Hz, 1H), 4.66 (d, J = 18.1 Hz, 1H), 4.51 (d, J = 18.1, 1H), 3.91 (s, 3H); ^{13}C NMR (126 MHz, $CS_2/C_2D_2Cl_4$, all 1C unless indicated) δ 167.62 (*C*=N), 161.00 (aryl *C*), 149.47, 148.88, 148.03 (2C), 148.00, 147.42, 147.26, 147.12, 147.09, 147.03, 146.19, 145.79, 145.70, 145.58, 145.50, 145.29, 145.19, 145.08, 145.03, 144.50, 144.47, 144.01, 143.99, 143.70, 143.66, 143.59, 143.45 (2C), 143.22, 143.14, 143.01 (2C), 142.964, 142.955, 142.90, 142.64, 142.44, 142.14, 142.12, 141.93, 141.80, 141.72, 141.59, 141.48, 141.24, 141.14, 141.09, 140.93, 140.43, 140.00, 139.83, 138.16, 135.54, 135.28, 134.99, 133.33, 128.88 (2C, aryl *C*), 124.91 (aryl *C*), 112.97 (2C, aryl *C*), 92.74 (sp^3-*C* of C_{60}), 59.77 (sp^3-*C* of C_{60}), 58.63 (sp^3-*C* of C_{60}), 57.76, 55.73 (sp^3-*C* of C_{60}), 53.99; FT-IR ν/cm^{-1} (KBr) 1603, 1513, 1420, 1341, 1254, 1169, 1028, 872, 827, 749, 585, 571, 566, 544, 531, 521; UV–vis ($CHCl_3$) λ_{max}/nm (log ε) 258 (4.96), 333 (4.41), 431 (3.69), 707 (2.38); MALDI-TOF MS m/z calcd for $C_{69}H_{11}NO$ [M]$^-$ 869.0846, found 869.0840.

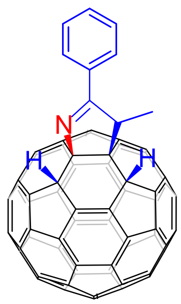

Synthesis and Spectral Data of 2h: By following the general procedure, a mixture of C_{60} (0.04 mmol, 28.8 mg), Mg_3N_2 (0.20 mmol, 20.3 mg), **1h** (0.60 mmol, 80.5 mg), AgCl (0.04 mmol, 5.9 mg) and silica gel (36.0 mg) was milled vigorously (35 Hz) for 1 h to afford unreacted C_{60} (9.9 mg, 34%) and **2h** (10.7 mg, 31%) as an amorphous brown solid. ^{1}H NMR (400 MHz, $CS_2/C_2D_2Cl_4$) δ 8.09–8.04 (m, 2H), 7.60–7.53 (m, 3H), 6.21 (s, 2H), 4.81 (q, J = 7.6 Hz, 1H), 1.71 (d, J = 7.6, 3H); ^{13}C NMR (101 MHz, $CS_2/C_2D_2Cl_4$, all 1C unless indicated) δ 173.00 (*C*=N), 149.30, 149.06, 148.10, 148.08, 148.00, 147.29, 147.24, 147.20, 147.12, 146.28, 146.21, 145.85, 145.72, 145.60, 145.40, 145.27, 145.16, 144.88, 144.54 (2C), 144.50, 144.04, 144.01, 143.75, 143.70, 143.68, 143.51, 143.47, 143.33, 143.26, 143.10, 143.00, 142.98, 142.93, 142.91, 142.67, 142.51, 142.13, 142.03, 141.91, 141.82, 141.77, 141.62, 141.54, 141.32, 141.19, 141.11, 140.95, 140.52, 140.20, 139.91, 137.66, 135.58, 135.51, 135.23, 134.87, 132.29 (aryl *C*), 129.97 (aryl *C*), 127.74 (2C, aryl *C*), 127.55 (2C, aryl *C*), 90.91 (sp^3-*C* of C_{60}), 64.17 (sp^3-*C* of C_{60}), 61.49 (sp^3-*C* of C_{60}), 60.73, 55.73 (sp^3-*C* of C_{60}), 16.42; FT-IR ν/cm^{-1} (KBr) 2957, 2924, 2848, 1620, 1447, 1427, 1383, 1193, 1093, 765, 694, 566, 529, 522; UV–vis ($CHCl_3$) λ_{max}/nm (log ε) 256 (4.91), 331 (4.34), 431 (3.60), 708 (2.13); MALDI-TOF MS m/z calcd for $C_{69}H_{11}N$ [M]$^-$ 853.0896, found 853.0889.

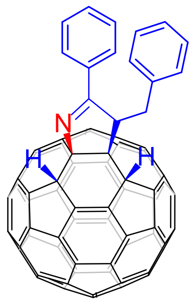

Synthesis and Spectral Data of 2i: By following the general procedure, a mixture of C_{60} (0.04 mmol, 28.8 mg), Mg_3N_2 (0.20 mmol, 20.2 mg), **1i** (0.40 mmol, 84.1 mg), AgCl (0.04 mmol, 5.7 mg) and silica gel (36.0 mg) was milled vigorously (40 Hz) for 1.5 h to afford unreacted C_{60} (13.4 mg, 47%) and **2i** (7.3 mg, 20%) as an amorphous brown solid. ^{1}H NMR (400 MHz, $CS_2/C_2D_2Cl_4$) δ 8.13–8.05 (m, 2H), 7.61–7.54 (m, 3H), 7.47 (d, J = 7.5 Hz, 2H), 7.32 (t, J = 7.7 Hz, 2H), 7.19 (t, J = 7.4 Hz, 1H), 6.20 (d, J = 1.7 Hz, 1H), 6.13 (d, J = 1.7 Hz, 1H), 5.30 (dd, J = 11.4, 3.2 Hz, 1H), 3.69 (dd, J = 15.9, 3.2 Hz, 1H), 3.03 (dd, J = 15.9, 11.4 Hz, 1H); ^{13}C NMR (101 MHz, $CS_2/C_2D_2Cl_4$, all 1C unless indicated) δ 172.19 (*C*=N), 149.04, 148.76, 148.01 (2C), 147.79, 147.22, 147.15, 147.05, 146.94, 146.34, 145.87, 145.75, 145.64, 145.55, 145.39, 145.12, 145.10, 144.52, 144.25, 144.17, 143.99, 143.66, 143.65, 143.52, 143.43 (2C), 143.29, 143.20, 143.07, 142.98, 142.91, 142.85 (2C), 142.82, 142.78, 142.60, 142.51, 142.11, 142.03, 141.96, 141.78, 141.60, 141.55, 141.48, 141.19, 141.10 (2C), 140.91, 140.17, 139.95, 139.91, 137.37, 137.20, 136.40 (aryl *C*), 135.45, 135.21, 135.12, 132.40 (aryl *C*), 129.85 (aryl *C*), 127.75 (2C, aryl *C*), 127.73 (2C, aryl *C*), 127.70 (2C, aryl *C*), 127.46 (2C, aryl *C*), 125.80 (aryl *C*), 91.46 (sp^3-*C* of C_{60}), 66.24, 63.82 (sp^3-*C* of C_{60}), 61.15 (sp^3-*C* of C_{60}), 55.67 (sp^3-*C* of C_{60}), 35.73; FT-IR ν/cm^{-1} (KBr) 2960, 2922, 2845, 1621, 1510, 1490, 1443, 1190, 1028, 763, 693, 575, 566, 530, 523, 520; UV–vis ($CHCl_3$) λ_{max}/nm (log ε) 257 (4.97), 334 (4.40), 431 (3.68), 78 (2.17); MALDI-TOF MS m/z calcd for $C_{75}H_{15}N$ $[M]^-$ 929.1209, found 929.1201.

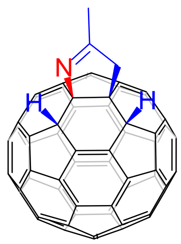

Synthesis and Spectral Data of 2j: By following the general procedure, a mixture of C_{60} (0.04 mmol, 28.8 mg), Mg_3N_2 (0.20 mmol, 20.1 mg), **1j** (0.80 mmol, 46.0 mg), AgCl (0.04 mmol, 5.7 mg) and silica gel (36.0 mg) was milled vigorously (35 Hz) for 1 h to afford unreacted C_{60} (7.1 mg, 25%) and **2j** (12.6 mg, 41%) as an amorphous brown solid. ^{1}H NMR (500 MHz, $CS_2/CDCl_3$, $Cr(acac)_3$ as relaxation reagent) δ 6.14 (d, J = 1.8 Hz, 1H), 6.07 (d, J = 1.8 Hz, 1H), 4.25 (d, J = 18.7 Hz, 1H), 4.11 (d, J = 18.7 Hz, 1H), 2.52 (s, 3H); ^{13}C NMR (126 MHz, $CS_2/C_2D_2Cl_4$, $Cr(acac)_3$ as relaxation reagent, all 1C unless indicated) δ 170.75 (*C*=N), 149.31, 148.71, 148.00, 147.97, 147.92, 147.23, 147.21, 147.06, 147.03, 147.01, 146.01, 145.76, 145.67, 145.54, 145.50, 145.26, 145.15, 145.04, 144.75, 144.45, 144.42, 143.94, 143.93, 143.62, 143.56, 143.55, 143.43 (2C), 143.19, 143.06, 142.99, 142.98, 142.92, 142.90, 142.88, 142.60, 142.42, 142.09 (2C), 141.88, 141.74, 141.68, 141.55, 141.46, 141.22, 141.12, 141.05, 140.85, 140.38, 139.98, 139.83, 138.02, 135.49, 135.11, 134.91, 133.33, 92.78 (sp^3-*C* of C_{60}), 61.40, 59.45 (sp^3-*C* of C_{60}), 58.89 (sp^3-*C* of C_{60}), 55.32 (sp^3-*C* of C_{60}), 18.70; FT-IR *ν*/cm^{-1} (KBr) 1653, 1508, 1421, 1180, 586, 571, 565, 559, 529, 521; UV–vis ($CHCl_3$) λ_{max}/nm (log ε) 257 (4.99), 331 (4.44), 431 (3.72), 706 (2.65); MALDI-TOF MS m/z calcd for $C_{63}H_7N$ [M]$^-$ 777.0583, found 777.0574

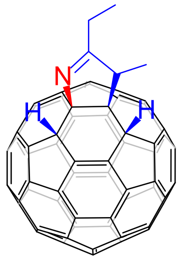

Synthesis and Spectral Data of 2k: By following the general procedure, a mixture of C_{60} (0.04 mmol, 28.8 mg), Mg_3N_2 (0.20 mmol, 20.2 mg), **1k** (0.60 mmol, 51.6 mg), AgCl (0.04 mmol, 5.7 mg) and silica gel (36.0 mg) was milled vigorously (35 Hz) for 1 h to afford unreacted C_{60} (12.3 mg, 43%) and **2k** (14.5 mg, 45%) as an amorphous brown solid. ^{1}H NMR (500 MHz, $CS_2/C_2D_2Cl_4$) *δ* 6.10 (d, *J* = 1.8 Hz, 1H), 6.04 (d, *J* = 1.8 Hz, 1H), 4.18 (q, *J* = 7.6 Hz, 1H), 2.77–2.61 (m, 2H), 1.69 (d, *J* = 7.6 Hz, 3H), 1.53 (t, *J* = 7.4 Hz, 3H); ^{13}C NMR (101 MHz, $CS_2/C_2D_2Cl_4$, all 1C unless indicated) *δ* 177.09 (*C*=N), 149.24, 148.85, 148.19, 148.02, 147.98, 147.21, 147.17, 147.11, 147.00, 146.32, 145.92, 145.75, 145.66, 145.56, 145.49, 145.30, 145.19, 145.08, 144.59, 144.49, 144.38, 143.97, 143.92, 143.65, 143.64, 143.59, 143.43, 143.41, 143.25, 143.21, 143.02, 142.91 (2C), 142.82, 142.80, 142.58, 142.44, 142.06, 141.88, 141.79, 141.72 (2C), 141.53, 141.46, 141.22, 141.14, 141.03, 140.92, 140.41, 140.15, 139.78, 137.63, 135.66, 135.22, 135.11, 134.84, 90.11 (sp^3-*C* of C_{60}), 63.90, 63.71 (sp^3-*C* of C_{60}), 60.57 (sp^3-*C* of C_{60}), 55.36 (sp^3-*C* of C_{60}), 24.20, 14.43, 9.85. FT-IR *ν*/cm^{-1} (KBr) 2965, 2923, 1646, 1457, 1418, 1376, 1182, 786, 757, 588, 578, 565, 528; UV–vis ($CHCl_3$) λ_{max}/nm (log ε) 256 (4.93), 331 (4.38), 431 (3.67), 707 (2.19); MALDI-TOF MS m/z calcd for $C_{65}H_{11}N$ [M]$^-$ 805.0896, found 805.0890.

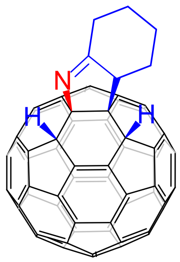

Synthesis and Spectral Data of 2l: By following the general procedure, a mixture of C_{60} (0.04 mmol, 28.8 mg), Mg_3N_2 (0.20 mmol, 20.2 mg), **1l** (0.60 mmol, 58.9 mg), AgCl (0.04 mmol, 5.7 mg) and silica gel (36.0 mg) was milled vigorously (35 Hz) for 1 h to afford unreacted C_{60} (4.1 mg, 14%) and **2l** (11.8 mg, 36%) as an amorphous brown solid. ^{1}H NMR (500 MHz, $CS_2/CDCl_3$) *δ* 6.11–6.05 (m, 2H), 3.98 (dd, *J* = 12.9, 6.2 Hz, 1H), 3.19–3.09 (m, 1H), 2.75 (td, J = 13.9, 7.9 Hz, 1H), 2.72–2.67 (m, 1H), 2.27–2.19 (m, 1H), 2.19–2.12 (m, 1H), 1.88 (qt, J = 13.2, 3.3 Hz, 1H), 1.69–1.55 (m, 2H); ^{13}C NMR (101 MHz, $CS_2/C_2D_2Cl_4$, all 1C unless indicated) δ 175.17 (*C*=N), 149.25, 148.68, 148.13, 148.01, 147.99, 147.22, 147.14 (2C), 147.02, 146.09, 146.04, 145.78, 145.65, 145.52, 145.30, 145.26, 145.19, 145.09, 144.54, 144.49, 144.41, 143.97, 143.94, 143.63, 143.60 (2C), 143.44 (2C), 143.21, 143.20, 143.03, 142.93, 142.91, 142.86, 142.83, 142.60, 142.44, 142.11, 141.91, 141.81, 141.70, 141.69, 141.54, 141.48, 141.25, 141.15, 141.05, 140.88, 140.42, 140.15, 139.82, 137.71, 135.41, 135.15, 135.06, 134.91, 90.93 (sp^3-*C* of C_{60}), 67.54, 63.08 (sp^3-*C* of C_{60}), 60.39 (sp^3-*C* of C_{60}), 55.31 (sp^3-*C* of C_{60}), 31.21, 31.19, 25.29, 24.75. FT-IR ν/cm^{-1} (KBr) 2922, 2849, 1655, 1460, 1443, 1424, 1315, 1192, 989, 783, 755, 587, 565, 544, 528; UV–vis ($CHCl_3$) λ_{max}/nm (log ε) 257 (4.91), 332 (4.35), 431 (3.62), 707 (2.18); MALDI-TOF MS m/z calcd for $C_{66}H_{11}N$ $[M]^-$ 817.0896, found 817.0891.

Synthesis of 2m and 2m': By following the general procedure, a mixture of C_{60} (0.04 mmol, 28.8 mg), Mg_3N_2 (0.20 mmol, 20.2 mg), **1m** (0.80 mmol, 57.7 mg), AgCl (0.04 mmol, 5.7 mg) and silica gel (36.0 mg) was milled vigorously (30 Hz) for 1 h to afford unreacted C_{60} (10.1 mg, 35%), **2m** (12.0 mg, 38%) and **2m′** (2.8 mg, 9%) as amorphous brown solids.

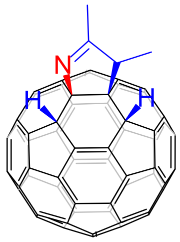

Spectral Data of 2m: ^1H NMR (500 MHz, $CS_2/C_2D_2Cl_4$) δ 6.10 (d, J = 1.8 Hz, 1H), 6.04 (d, J = 1.8 Hz, 1H), 4.17 (q, J = 7.6 Hz, 1H), 2.44 (s, 3H), 1.71 (d, J = 7.6 Hz, 3H); ^{13}C NMR (126 MHz, $CS_2/C_2D_2Cl_4$, all 1C unless indicated) δ 173.80 (*C*=N), 149.20, 148.86, 148.12, 148.06, 148.03, 147.27, 147.18, 147.15, 147.05, 146.20, 145.93, 145.80, 145.71, 145.55, 145.35, 145.26, 145.23, 145.12, 144.52, 144.42 (2C), 143.99, 143.96, 143.68, 143.65, 143.63, 143.48, 143.45, 143.26 (2C), 143.07, 142.95 (2C), 142.87, 142.82, 142.61, 142.49, 142.09, 141.95, 141.84, 141.76 (2C), 141.57, 141.50, 141.26, 141.17, 141.07, 140.93, 140.45, 140.20, 139.83, 137.67, 135.70, 135.15 (2C), 134.82, 90.12 (sp^3-*C* of C_{60}), 64.72, 63.69 (sp^3-*C* of C_{60}), 60.51 (sp^3-*C* of C_{60}), 55.17 (sp^3-*C* of C_{60}), 17.09, 14.44; FT-IR ν/cm^{-1} (KBr) 2969, 2839, 1603, 1580, 1460, 1426, 1324, 1255, 1200, 1161, 1136, 1066, 942, 916, 867, 830, 692, 673, 632, 606, 577, 527; UV–vis ($CHCl_3$) λ_{max}/nm (log ε) 256 (4.94), 330 (4.42), 431 (3.76), 706 (2.32); MALDI-TOF MS m/z calcd for $C_{64}H_9N$ $[M]^-$ 791.0740, found 791.0733.

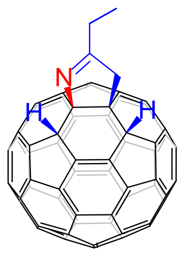

Spectral Data of 2m': ^{1}H NMR (500 MHz, $CS_2/C_2D_2Cl_4$) δ 6.14 (d, J = 1.8 Hz, 1H), 6.06 (d, J = 1.8 Hz, 1H), 4.22 (d, J = 18.6 Hz, 1H), 4.07 (d, J = 18.6 Hz, 1H), 2.89–2.70 (m, 2H), 1.52 (t, J = 7.5 Hz, 3H); ^{13}C NMR (126 MHz, $CS_2/C_2D_2Cl_4$, all 1C unless indicated) δ 174.68 (*C*=N), 149.38, 148.75, 148.01, 148.00, 147.98, 147.41, 147.24, 147.09, 147.04, 147.01, 146.14, 145.77, 145.68, 145.55, 145.50, 145.27, 145.16, 145.06 (2C), 144.47, 144.44, 143.96 (2C), 143.62, 143.61, 143.56, 143.44 (2C), 143.20, 143.10, 142.99 (2C), 142.94, 142.93, 142.88, 142.62, 142.42, 142.11, 142.09, 141.89, 141.76, 141.69, 141.57, 141.47, 141.23, 141.14, 141.06, 140.89, 140.39, 139.99, 139.84, 138.07, 135.52, 135.20, 134.96, 133.30, 92.67 (sp^3-*C* of C_{60}), 59.98, 59.54 (sp^3-*C* of C_{60}), 58.50 (sp^3-*C* of C_{60}), 55.49 (sp^3-*C* of C_{60}), 26.16, 10.02; FT-IR ν/cm^{-1} (KBr) 2963, 2921, 2898, 2850, 1648, 1457, 1418, 1182, 745, 559, 565, 530, 523, 520; UV–vis ($CHCl_3$) λ_{max}/nm (log ε) 256 (4.94), 330 (4.38), 431 (3.65), 706 (2.60); MALDI-TOF MS m/z calcd for $C_{64}H_9N$ [M]$^-$ 791.0740, found 791.0733.

Synthesis of 2n and 2n': By following the general procedure, a mixture of C_{60} (0.04 mmol, 28.8 mg), Mg_3N_2 (0.20 mmol, 20.2 mg), **1n** (0.60 mmol, 78.1 mg), AgCl (0.04 mmol, 5.7 mg) and silica gel (36.0 mg) was milled vigorously (35 Hz) for 1 h to afford unreacted C_{60} (15.2 mg, 53%), **2n** (7.5 mg, 22%) and **2n′** (6.3 mg, 19%) as amorphous brown solids.

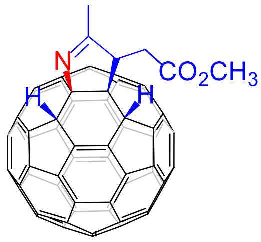

Spectral Data of 2n: ^{1}H NMR (500 MHz, $CS_2/C_2D_2Cl_4$) δ 6.36 (d, J = 1.8 Hz, 1H), 6.11 (d, J = 1.8 Hz, 1H), 4.65 (dd, J = 11.3, 3.8 Hz, 1H), 3.75 (s, 3H), 3.15 (dd, J = 17.5, 3.8 Hz, 1H), 2.86 (dd, J = 17.5, 11.3 Hz, 1H), 2.44 (s, 3H); ^{13}C NMR (101 MHz, $CS_2/C_2D_2Cl_4$, all 1C unless indicated) δ 171.56 (*C*=O), 170.36 (*C*=N), 150.23, 149.13, 148.14, 148.08, 148.01, 147.26, 147.21, 147.16, 147.11, 145.93, 145.76, 145.74, 145.68, 145.55, 145.45, 145.13 (2C), 144.56, 144.37, 144.26, 143.98, 143.70, 143.67, 143.59, 143.55, 143.51, 143.49, 143.34, 143.17, 143.14, 142.98, 142.96, 142.93, 142.69, 142.63 (2C), 142.17, 142.01, 141.99, 141.95, 141.81, 141.75, 141.56, 141.52, 141.23 (2C), 141.17, 140.90, 140.38, 140.18, 139.92, 137.62, 136.03, 135.32, 135.04, 134.45, 90.96 (sp^3-*C* of C_{60}), 65.46, 63.40 (sp^3-*C* of C_{60}), 60.62 (sp^3-*C* of C_{60}), 55.42 (sp^3-*C* of

C_{60}), 51.23, 33.90, 17.38; FT-IR ν/cm^{-1} (KBr) 2943, 2914, 2850, 1734, 1651, 1511, 1432, 1192, 1160, 578, 571, 566, 528, 520; UV–vis ($CHCl_3$) λ_{max}/nm (log ε) 257 (4.94), 333 (4.36), 431 (3.63), 706 (2.29); MALDI-TOF MS m/z calcd for $C_{66}H_{11}NO_2$ $[M]^-$ 849.0795, found 849.0787.

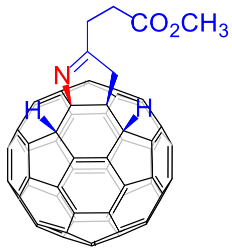

Spectral Data of 2n': ^{1}H NMR (400 MHz, $CS_2/C_2D_2Cl_4$) δ 6.07 (d, J = 1.7 Hz, 1H), 6.06 (d, J = 1.7 Hz, 1H), 4.23 (d, J = 18.6 Hz, 1H), 4.10 (d, J = 18.6 Hz, 1H), 3.74 (s, 3H), 3.14–3.03 (m, 2H), 3.03–2.85 (m, 2H); ^{13}C NMR (101 MHz, $CS_2/C_2D_2Cl_4$, all 1C unless indicated) δ 172.47 (*C*=O), 171.43 (*C*=N), 149.28, 148.78, 148.02, 148.01, 147.96, 147.27, 147.18, 147.10, 147.07, 147.05, 145.99 (2C), 145.78, 145.70, 145.55, 145.52, 145.30, 145.18, 145.07, 144.71, 144.49, 144.46, 143.97, 143.96, 143.66, 143.58 (2C), 143.46 (2C), 143.23, 143.09, 143.02 (2C), 142.94 (2C), 142.63, 142.46, 142.11 (2C), 141.93, 141.76, 141.70, 141.58, 141.49, 141.25, 141.15, 141.09, 140.86, 140.42, 140.02, 139.85, 138.05, 135.56, 135.18, 134.94, 133.40, 92.56 (sp^3-*C* of C_{60}), 60.57, 59.46 (sp^3-*C* of C_{60}), 58.64 (sp^3-*C* of C_{60}), 55.38 (sp^3-*C* of C_{60}), 50.47, 29.28, 27.25; FT-IR ν/cm^{-1} (KBr) 2954, 2923, 2848, 1731, 1648, 1421, 1190, 1041, 586, 566, 529, 527, 523, 520; UV–vis ($CHCl_3$) λ_{max}/nm (log ε) 256 (4.95), 331 (4.39), 430 (3.63), 707 (2.16); MALDI-TOF MS m/z calcd for $C_{66}H_{11}NO_2$ $[M]^-$ 849.0795, found 849.0789.

3. Control Experiment

A mixture of C_{60} (0.04 mmol, 28.8 mg), $NH_3 \cdot H_2O$ (0.40 mmol), **1a** (0.60 mmol, 72.1 mg), AgCl (0.04 mmol, 5.7 mg) and silica gel (36.0 mg) together with 4 stainless-steel balls (5 mm in diameter) was introduced into a stainless-steel jar (5 mL) and milled vigorously (35 Hz) in a GT 600 mixer mill at room temperature for 1 h. After that, the reaction mixture was extracted with CS_2 and separated by column chromatography on silica gel with CS_2 as the eluent to provide **2a** (1.0 mg, 3%).

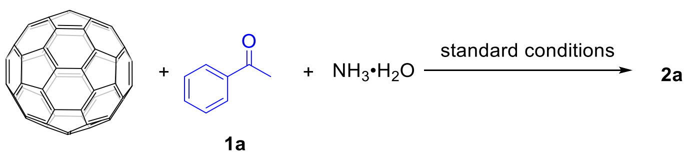

4. X-Ray Data of 2c

Black flake crystals of **2c** were obtained by slow diffusion of **2c** in CS_2/1,1,2,2-tetrachloroethane/CH_3OH solution at about 4 ºC. Single-crystal X-ray diffraction data were collected on a diffractometer (Gemini S Ultra, Agilent Technologies) equipped with a CCD area detector using graphite-monochromated CuKα radiation (λ = 1.54184 Å) in the scan range of 7.332° < 2θ < 145.828°. The structure was solved with intrinsic phasing using SHELXT and refined with full-matrix least-squares refinement using the SHELXL program within OLEX2. Crystallographic data have been deposited in the Cambridge Crystallographic Data Centre as deposition number CCDC 2525038.

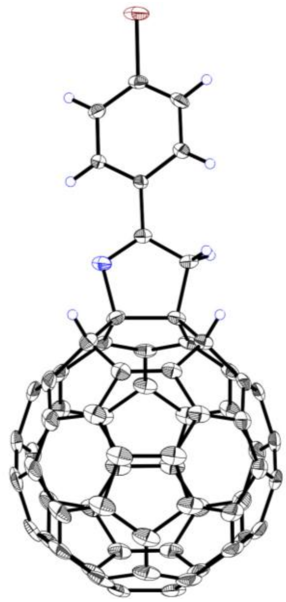

Fig. S2 ORTEP diagram for **2c** with 20% thermal ellipsoids. The solvent molecules are omitted for clarity.

Table S1 Crystal Data and Structure Refinement for **2c**.

Identification code	2525038
Empirical formula	$C_{70}H_{11}BrNOS_2$
Formula weight	1025.83
Temperature/K	293(2)
Crystal system	triclinic
Space group	P-1
a/Å	10.0033(4)
b/Å	12.9511(4)
c/Å	16.0243(5)
α/°	97.870(3)
β/°	91.414(3)
γ/°	109.580(3)
Volume/Å^3	1931.99(12)
Z	2
ρ_{calc}g/cm^3	1.763
μ/mm^{-1}	2.952
F(000)	1026.0
Crystal size/mm^3	0.18 × 0.09 × 0.03
Radiation	Cu Kα (λ = 1.54184)
2Θ range for data collection/°	7.332 to 145.828
Index ranges	-11 ≤ h ≤ 12, -15 ≤ k ≤ 16, -18 ≤ l ≤ 19
Reflections collected	14003
Independent reflections	7495 [R_{int} = 0.0278, R_{sigma} = 0.0351]
Data/restraints/parameters	7495/13/677
Goodness-of-fit on F^2	1.025
Final R indexes [I>=2σ (I)]	R_1 = 0.0687, wR_2 = 0.1939
Final R indexes [all data]	R_1 = 0.0816, wR_2 = 0.2095
Largest diff. peak/hole / e Å^{-3}	1.15/-0.88

5. Cyclic Voltammograms and Differential Pulse Voltammograms of 2a−n′

CV and DPV measurements were performed under an argon atmosphere at 25 ºC using a Shanghai Chenhua CHI630D workstation. A conventional three-electrode cell was used for CV and DPV measurements and consisted of a 2 mm-diameter platinum disc working electrode, a platinum wire auxiliary electrode, and a saturated calomel reference electrode (SCE). The SCE was separated from the bulk of the solution by a fritted-glass bridge of low porosity, which contained the solvent/supporting electrolyte mixture.

Cyclic Voltammograms Experimental Conditions: 1.0 mM **2a−n′** and 0.1 M *n*-Bu_4NClO_4 in anhydrous 1,2-$C_6H_4Cl_2$; reference electrode: saturated calomel electrode; working electrode: Pt disc (2 mm diameter); auxiliary electrode: Pt wire; scanning direction: from 0 V toward negative direction; scanning rate: 50 mV s^{-1}.

Differential Pulse Voltammograms Experimental Conditions: 1.0 mM **2a−n′** and 0.1 M *n*-Bu_4NClO_4 in anhydrous 1,2-$C_6H_4Cl_2$; reference electrode: saturated calomel electrode; working electrode: Pt disc (2 mm diameter); auxiliary electrode: Pt wire; scanning direction: from 1.0 V toward -2.0 V; pulse amplitude: 50 mV; pulse width: 50 ms; pulse period: 200 ms.

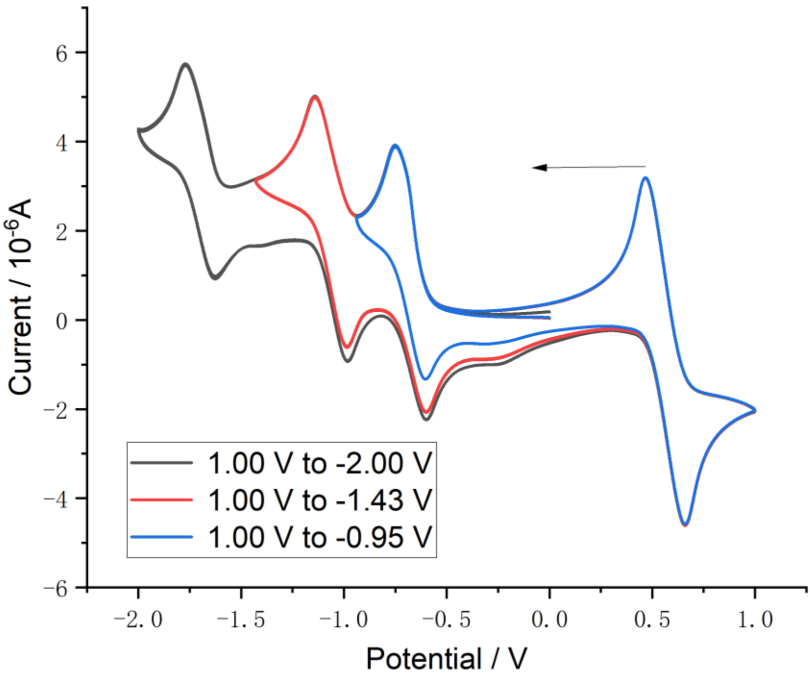

Fig. S3 Cyclic voltammogram of **2a** (scanning rate: 50 mV s^{-1})

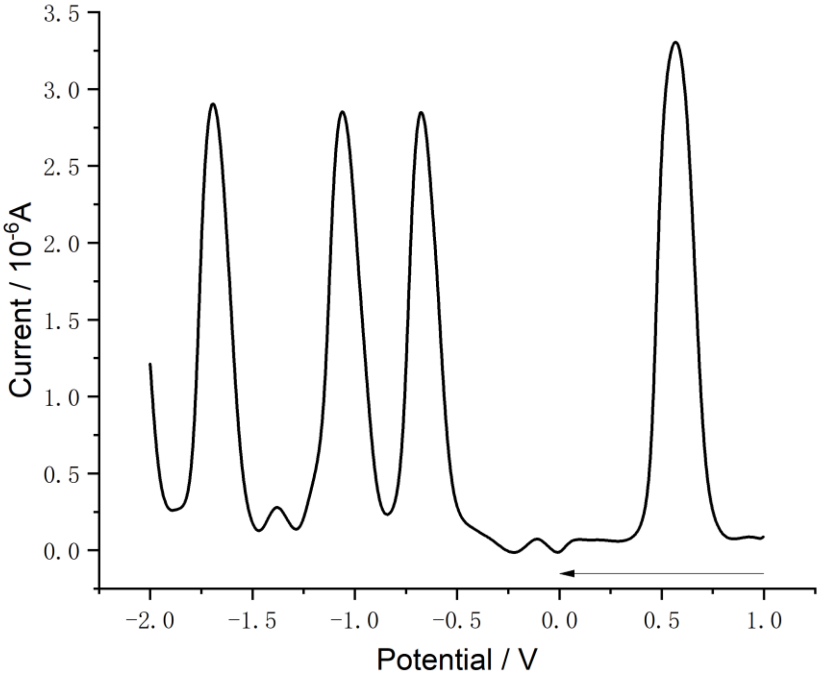

Fig. S4 Differential pulse voltammogram of **2a** (scanning rate: 50 mV s^{-1})

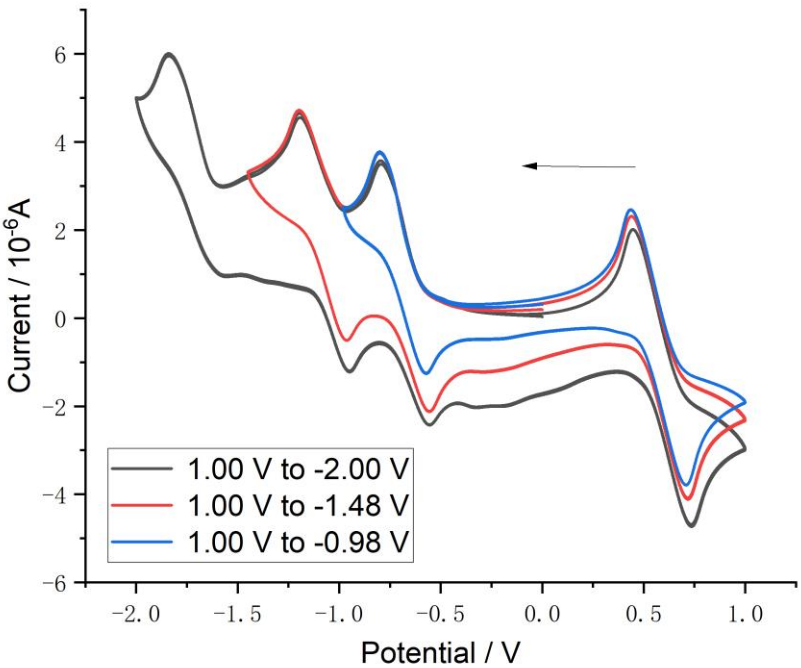

Fig. S5 Cyclic voltammogram of **2b** (scanning rate: 50 mV s^{-1})

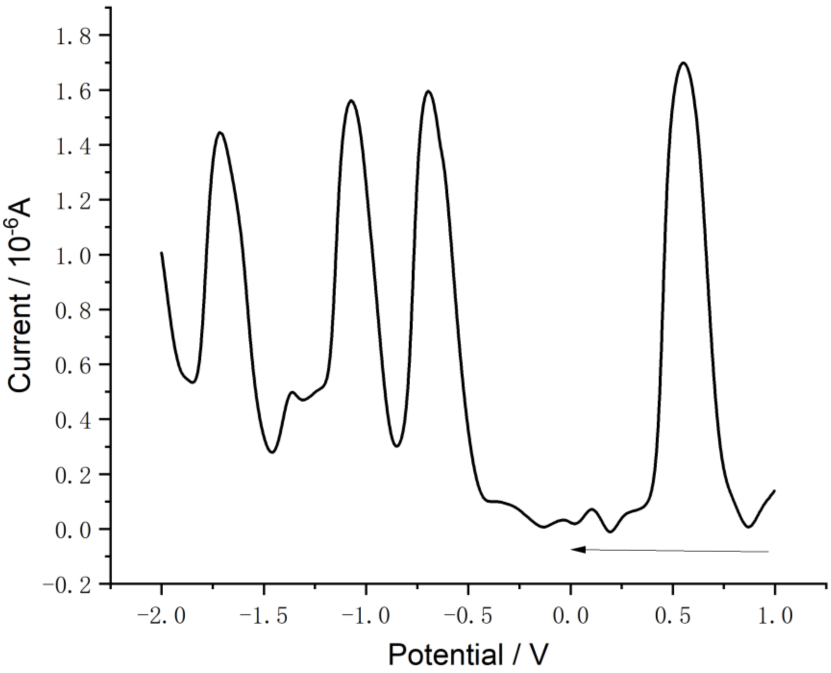

Fig. S6 Differential pulse voltammogram of **2b** (scanning rate: 50 mV s^{-1})

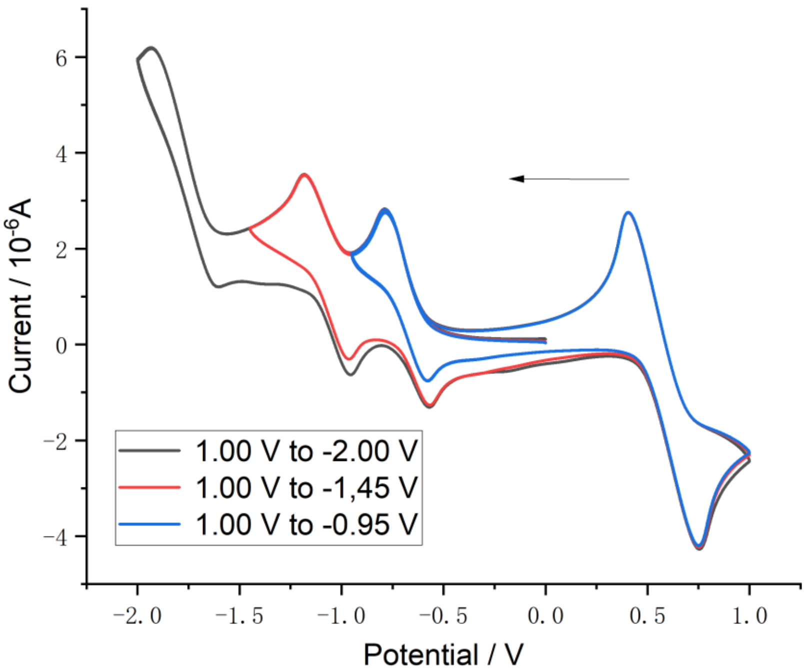

Fig. S7 Cyclic voltammogram of **2c** (scanning rate: 50 mV s^{-1})

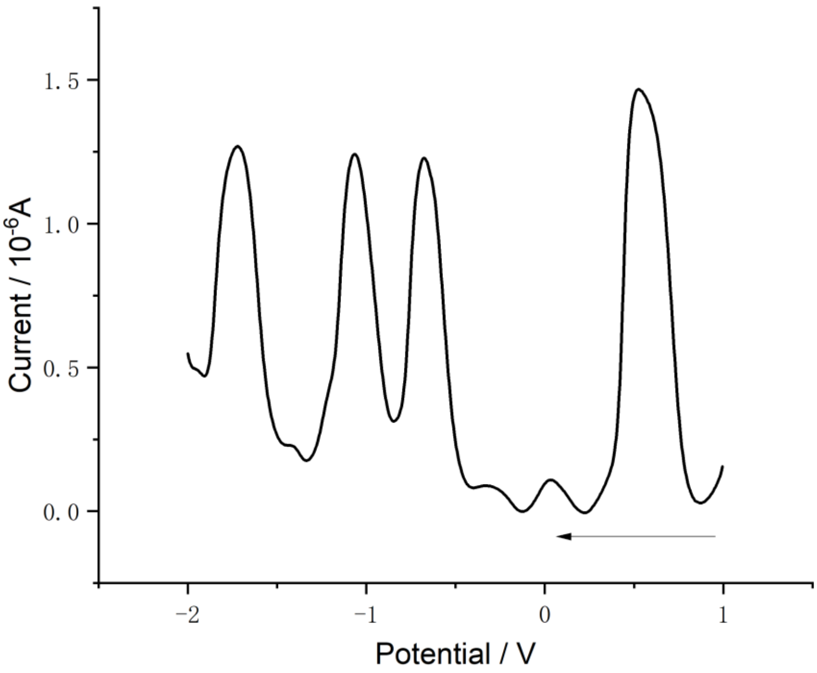

Fig. S8 Differential pulse voltammogram of **2c** (scanning rate: 50 mV s^{-1})

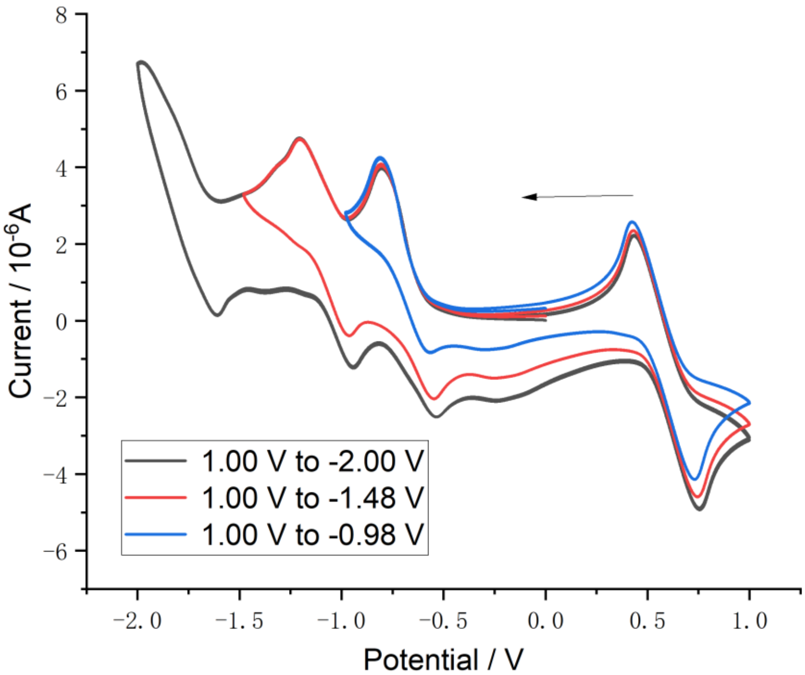

Fig. S9 Cyclic voltammogram of **2d** (scanning rate: 50 mV s^{-1})

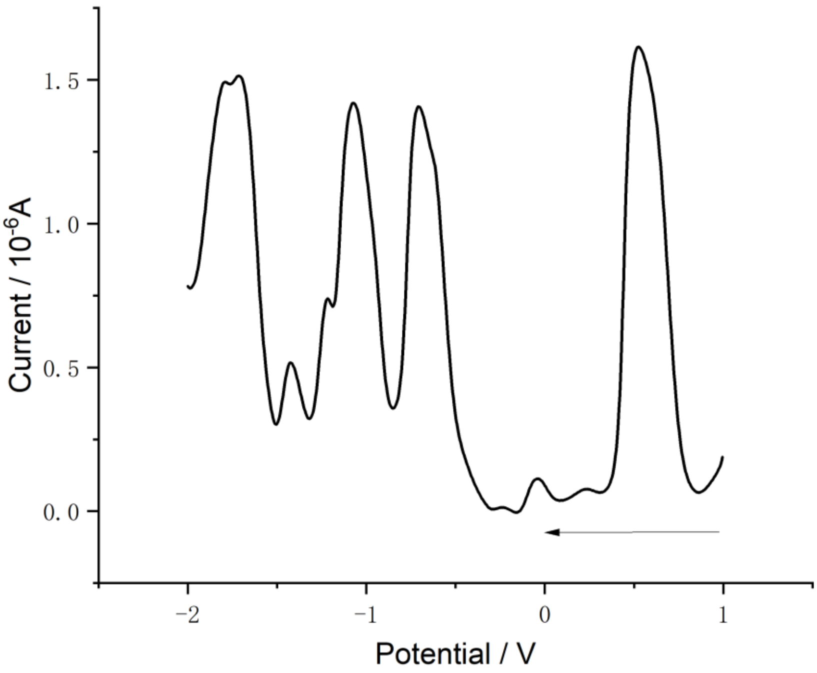

Fig. S10 Differential pulse voltammogram of **2d** (scanning rate: 50 mV s^{-1})

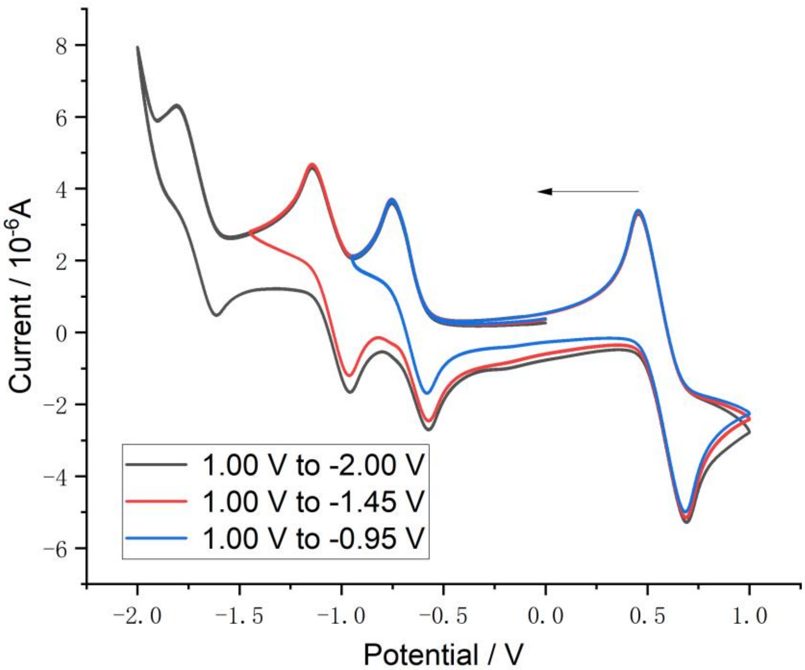

Fig. S11 Cyclic voltammogram of **2e** (scanning rate: 50 mV s^{-1})

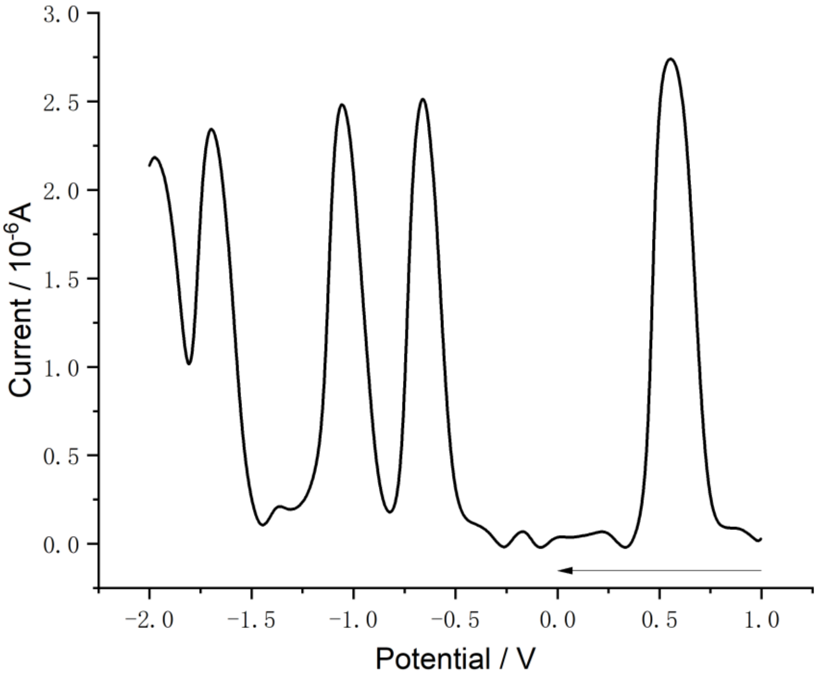

Fig. S12 Differential pulse voltammogram of **2e** (scanning rate: 50 mV s^{-1})

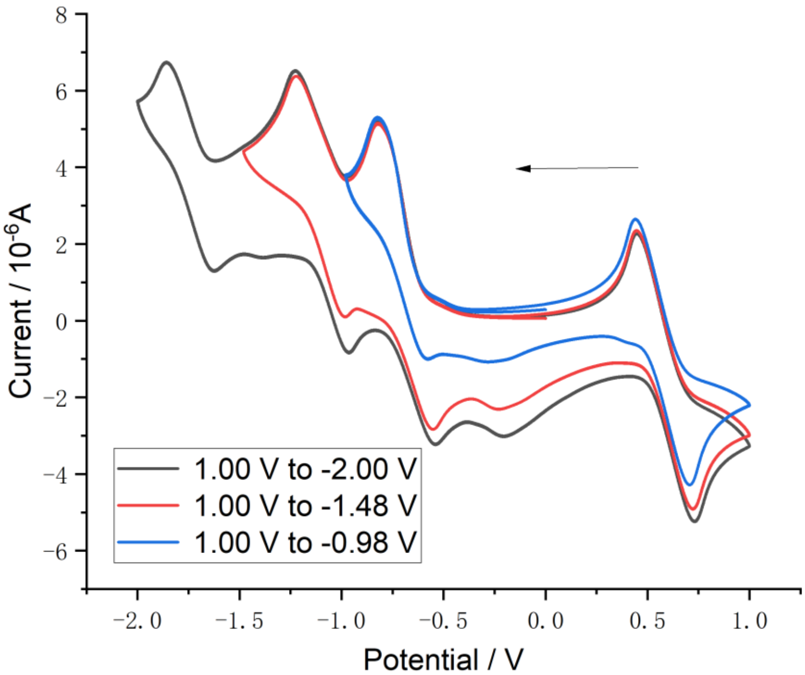

Fig. S13 Cyclic voltammogram of **2f** (scanning rate: 50 mV s^{-1})

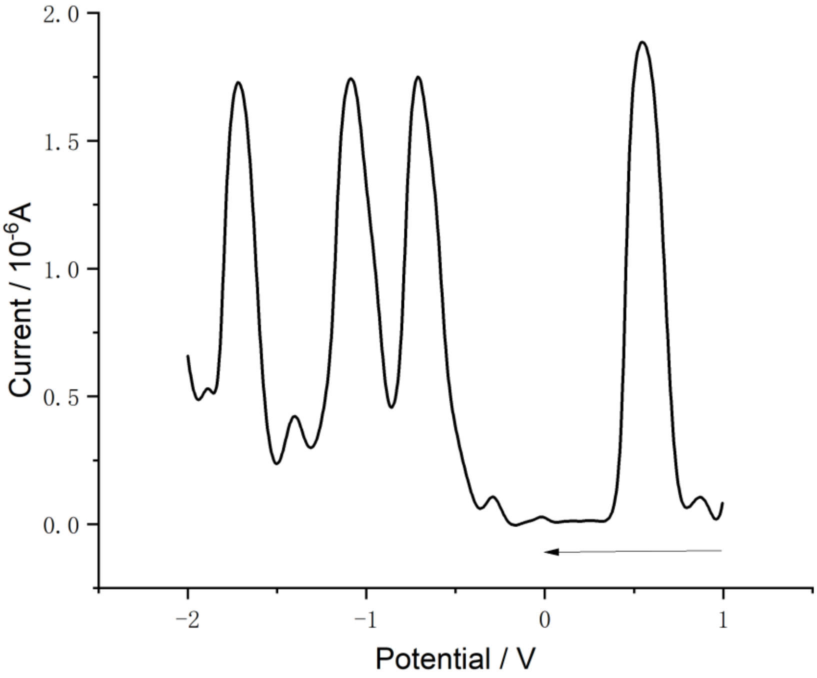

Fig. S14 Differential pulse voltammogram of **2f** (scanning rate: 50 mV s^{-1})

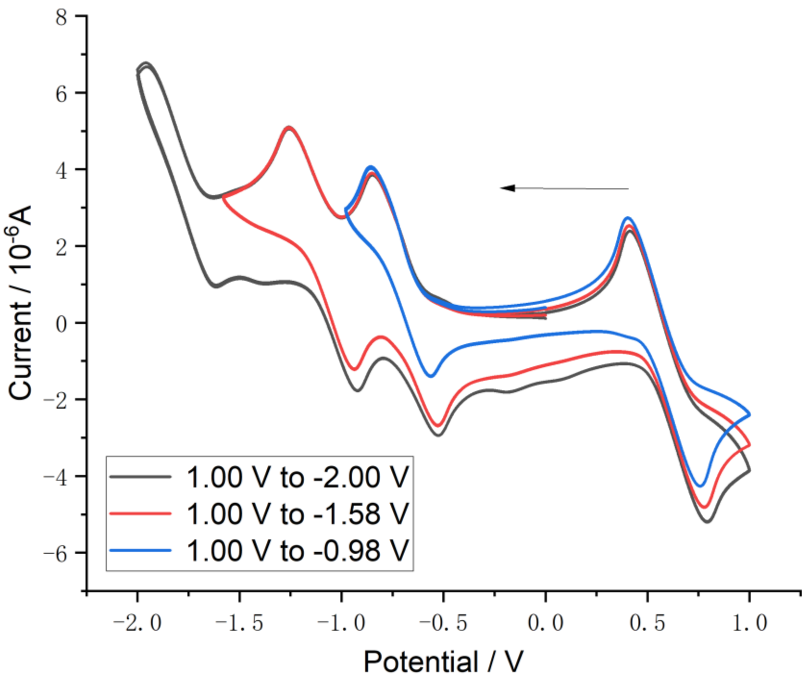

Fig. S15 Cyclic voltammogram of **2g** (scanning rate: 50 mV s^{-1})

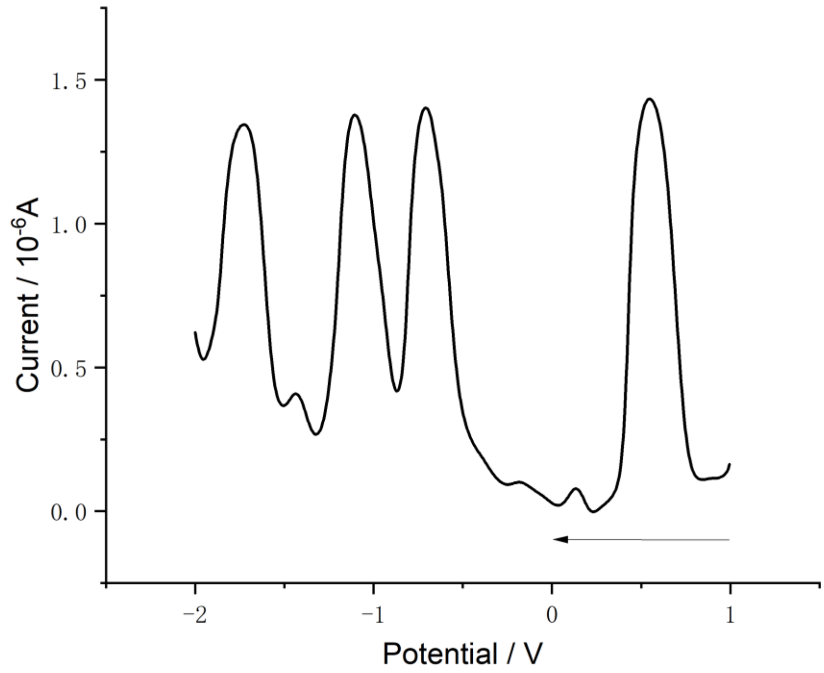

Fig. S16 Differential pulse voltammogram of **2g** (scanning rate: 50 mV s^{-1})

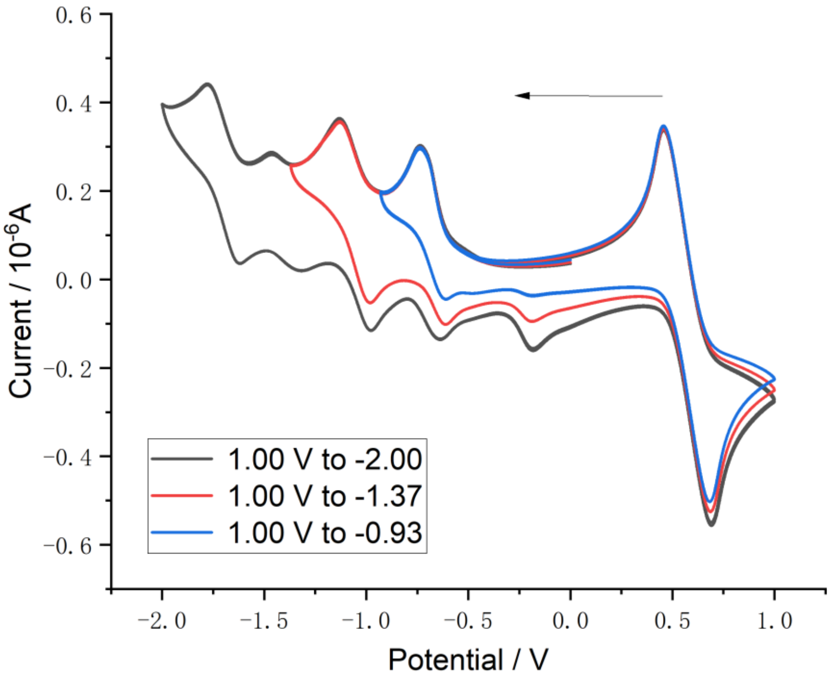

Fig. S17 Cyclic voltammogram of **2h** (scanning rate: 50 mV s^{-1})

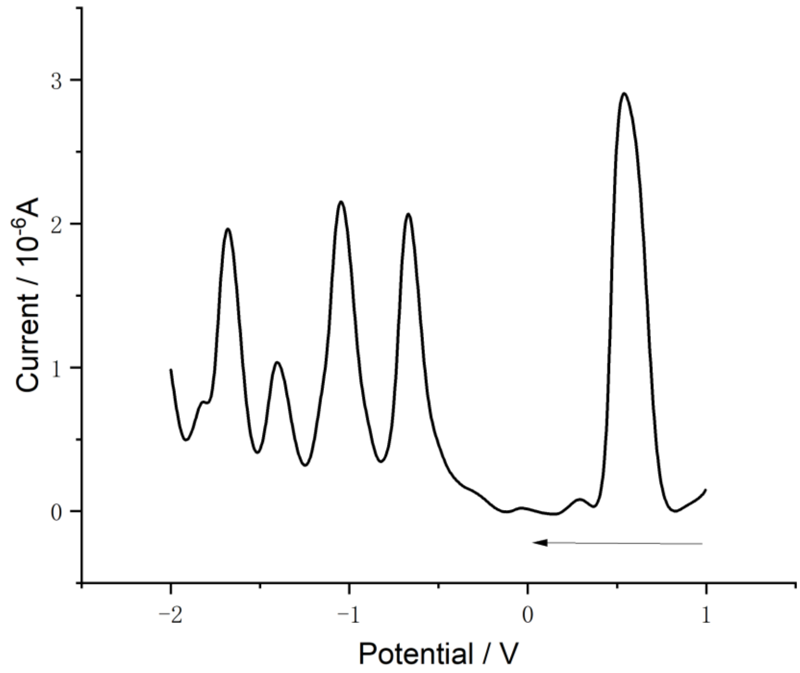

Fig. S18 Differential pulse voltammogram of **2h** (scanning rate: 50 mV s^{-1})

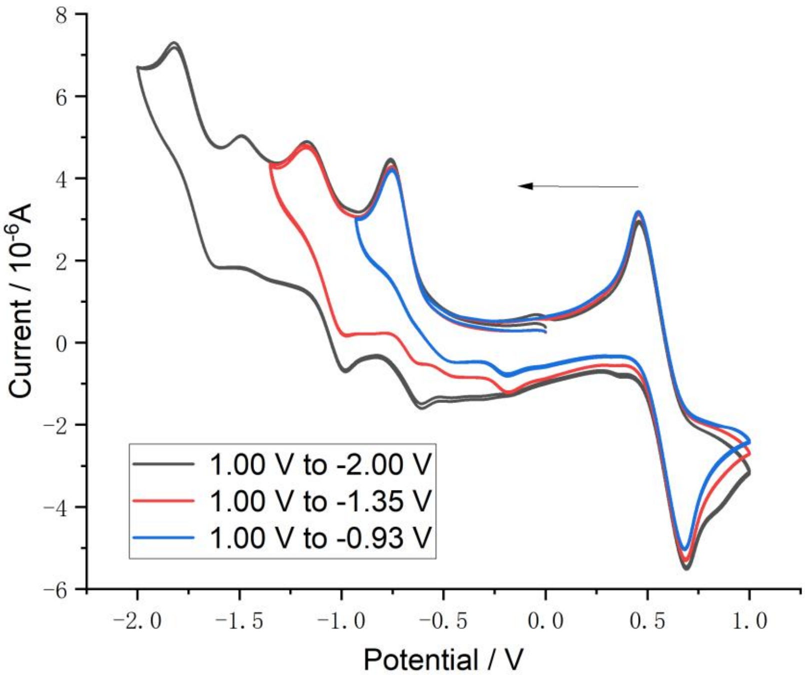

Fig. S19 Cyclic voltammogram of **2i** (scanning rate: 50 mV s^{-1})

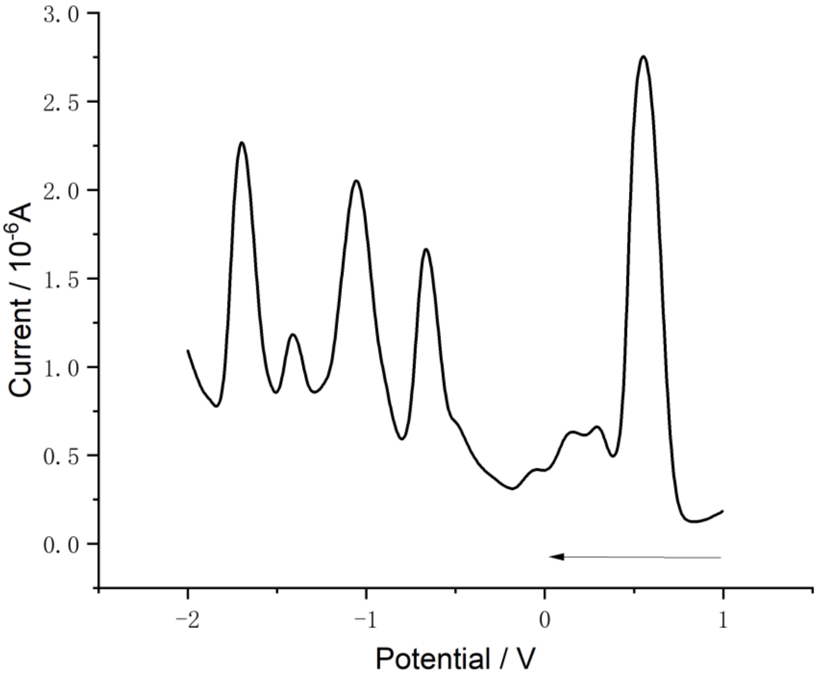

Fig. S20 Differential pulse voltammogram of **2i** (scanning rate: 50 mV s^{-1})

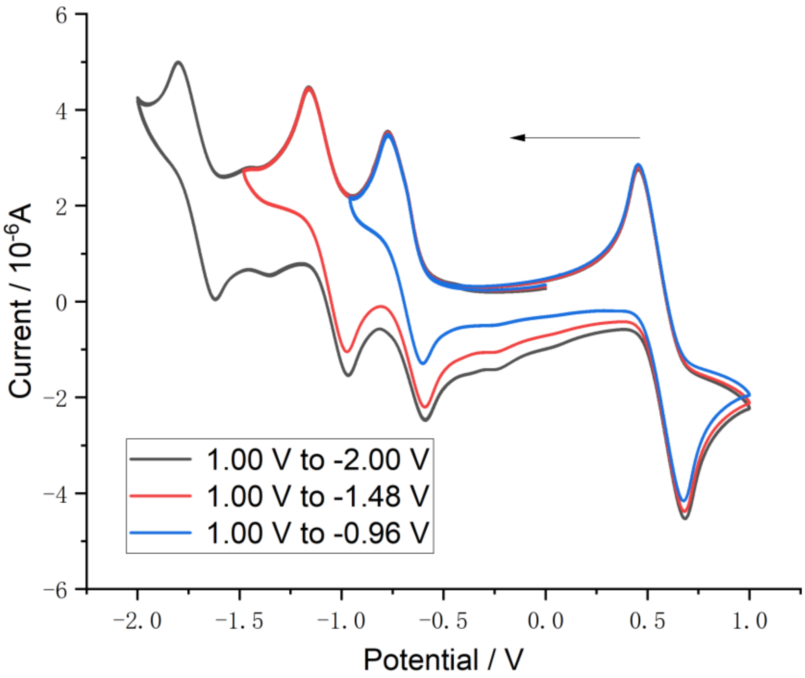

Fig. S21 Cyclic voltammogram of **2j** (scanning rate: 50 mV s^{-1})

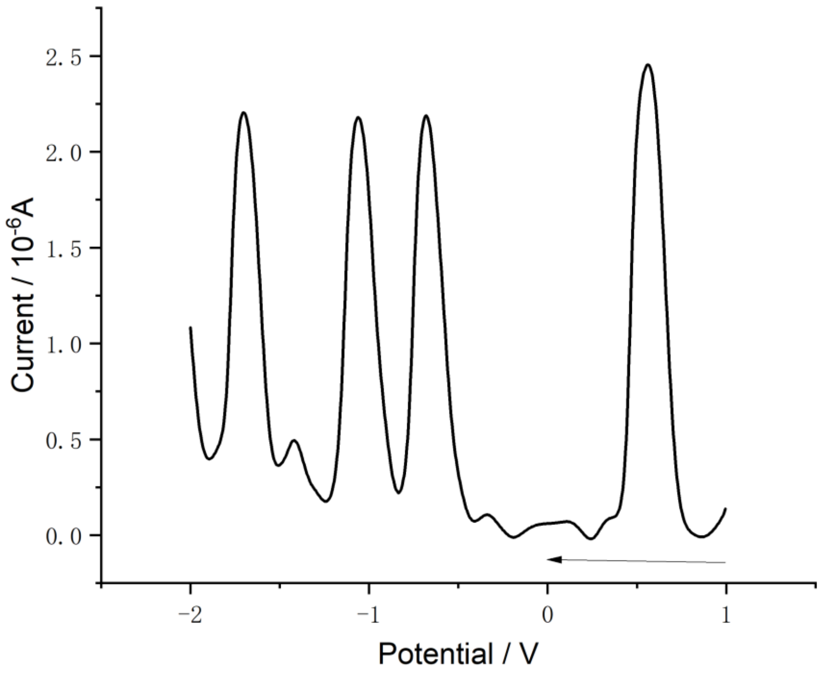

Fig. S22 Differential pulse voltammogram of **2j** (scanning rate: 50 mV s^{-1})

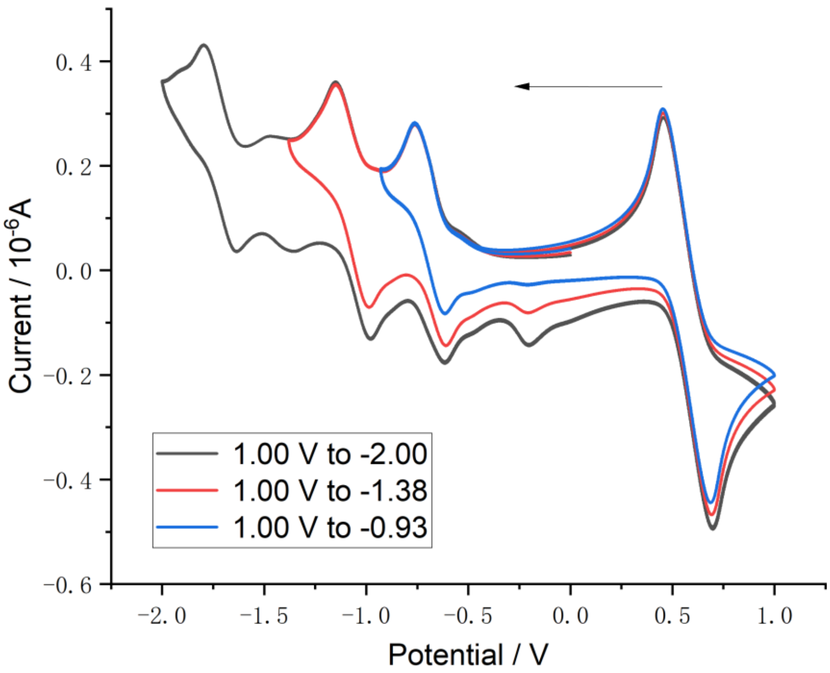

Fig. S23 Cyclic voltammogram of **2k** (scanning rate: 50 mV s^{-1})

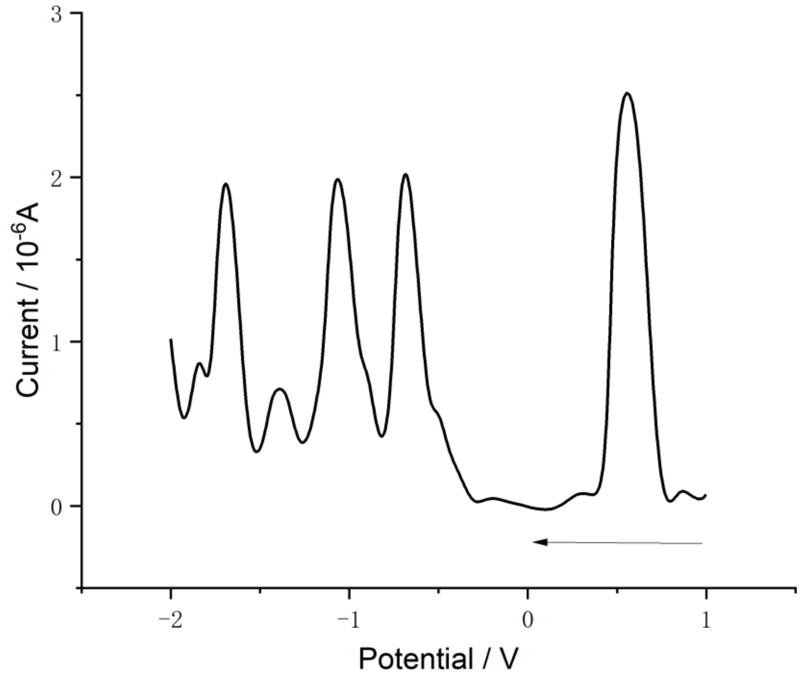

Fig. S24 Differential pulse voltammogram of **2k** (scanning rate: 50 mV s^{-1})

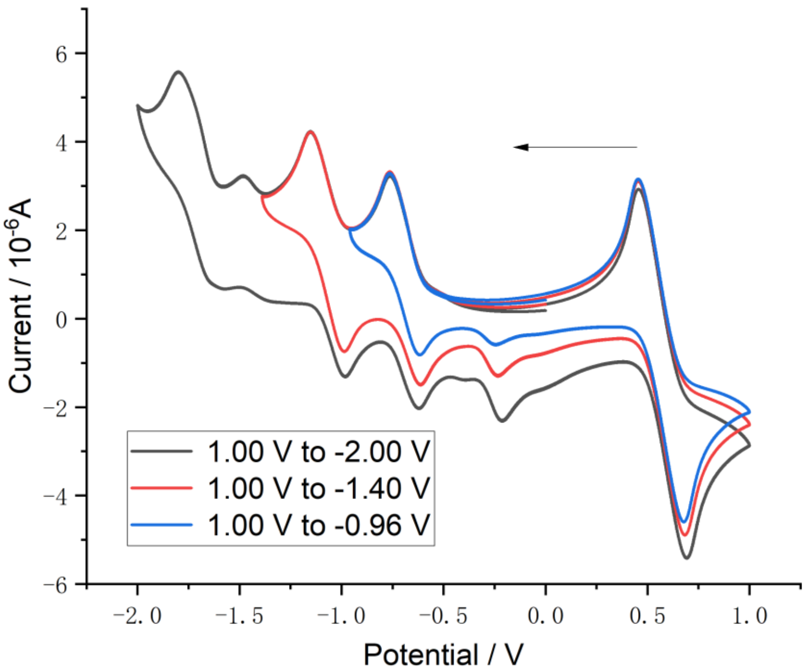

Fig. S25 Cyclic voltammogram of **2l** (scanning rate: 50 mV s^{-1})

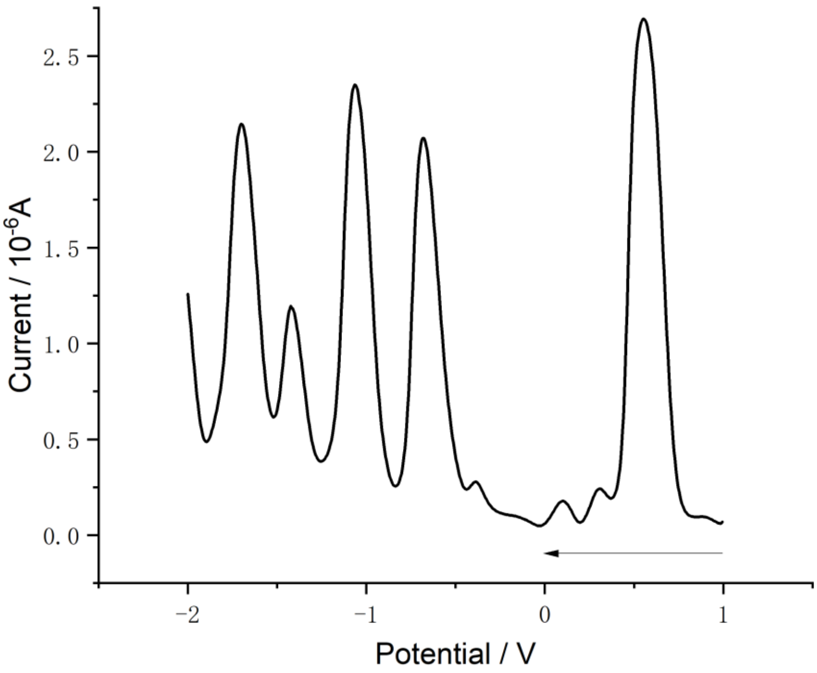

Fig. S26 Differential pulse voltammogram of **2l** (scanning rate: 50 mV s^{-1})

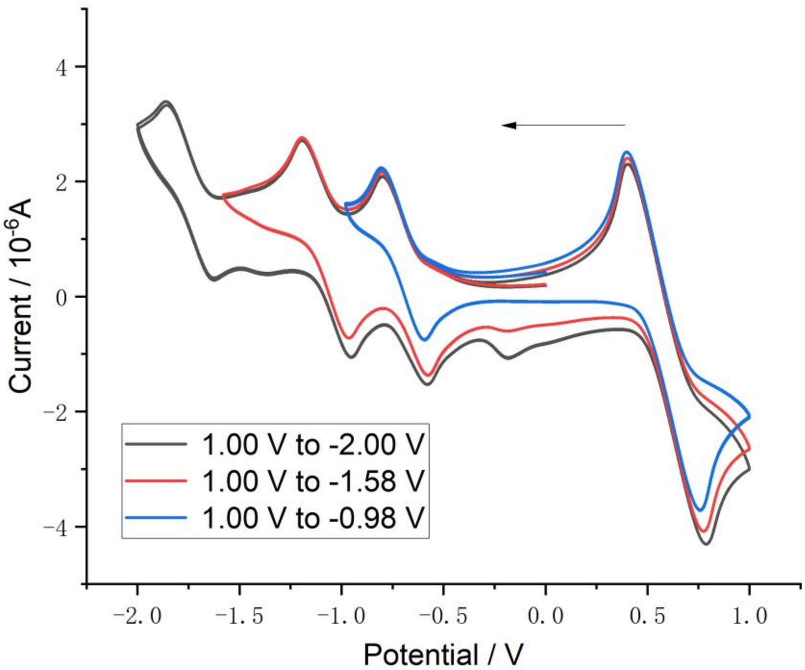

Fig. S27 Cyclic voltammogram of **2m** (scanning rate: 50 mV s^{-1})

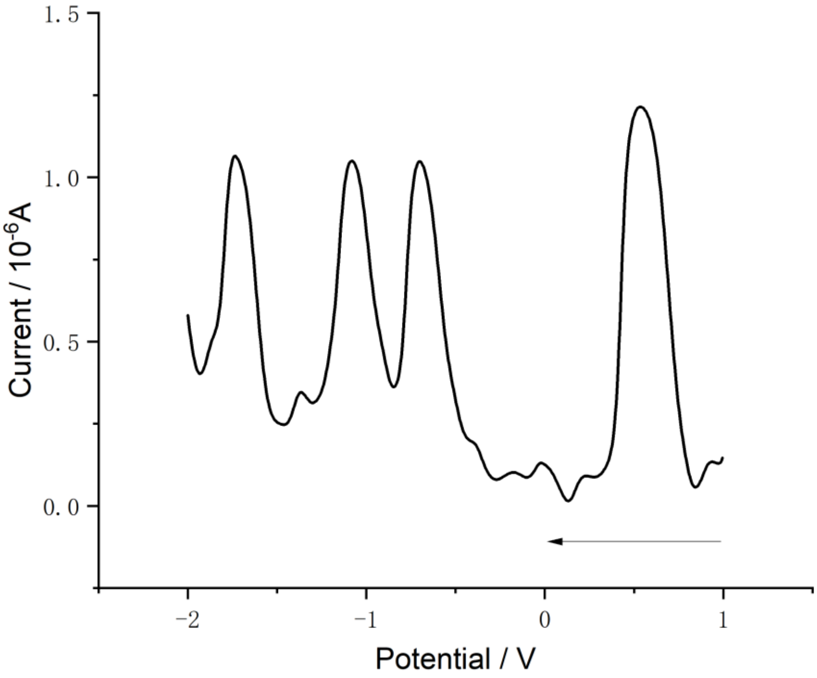

Fig. S28 Differential pulse voltammogram of **2m** (scanning rate: 50 mV s^{-1})

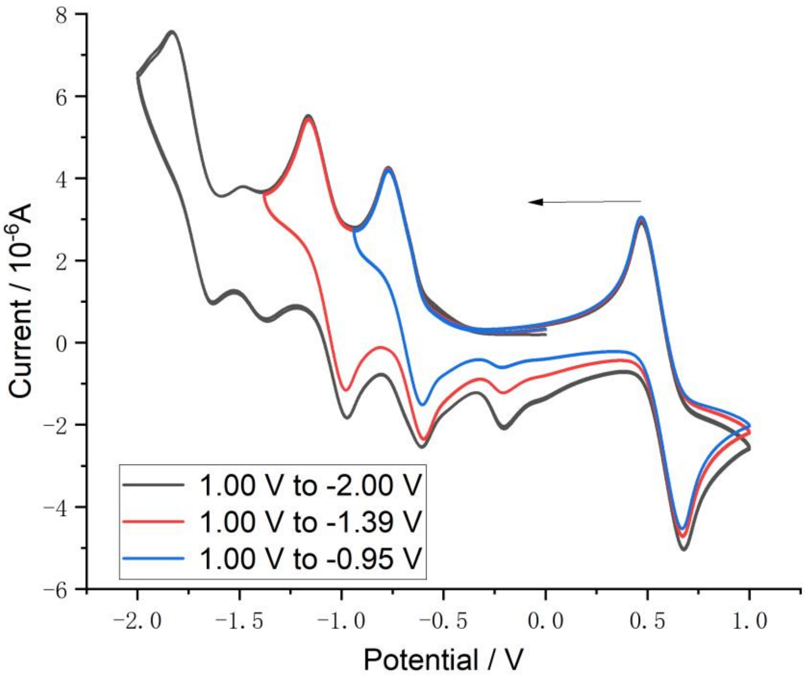

Fig. S29 Cyclic voltammogram of **2m′** (scanning rate: 50 mV s^{-1})

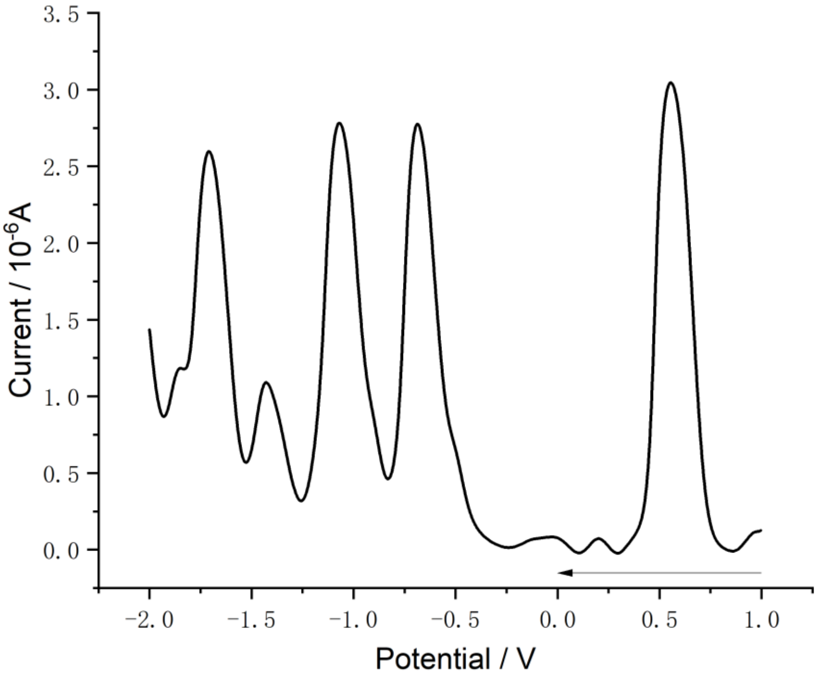

Fig. S30 Differential pulse voltammogram of **2m′** (scanning rate: 50 mV s^{-1})

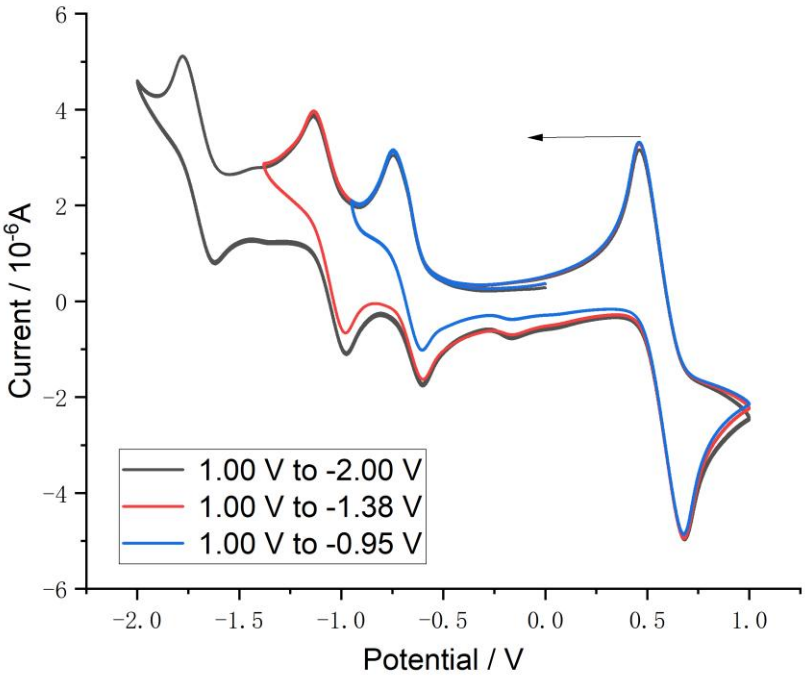

Fig. S31 Cyclic voltammogram of **2n** (scanning rate: 50 mV s^{-1})

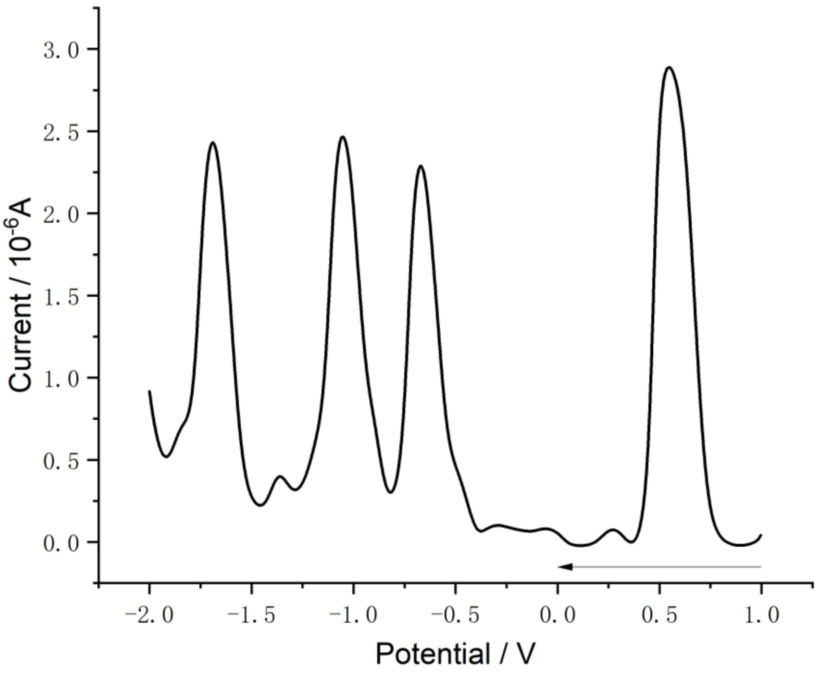

Fig. S32 Differential pulse voltammogram of **2n** (scanning rate: 50 mV s^{-1})

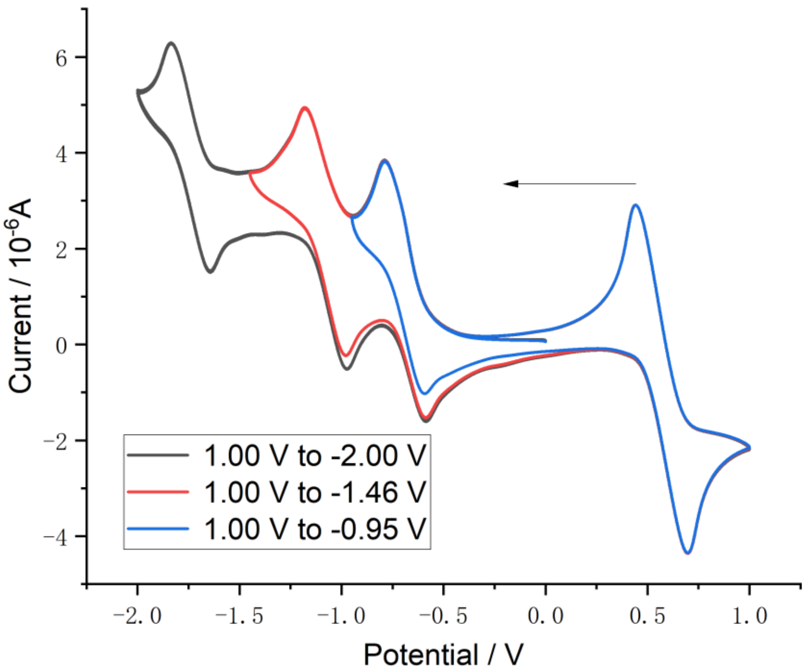

Fig. S33 Cyclic voltammogram of **2n′** (scanning rate: 50 mV s^{-1})

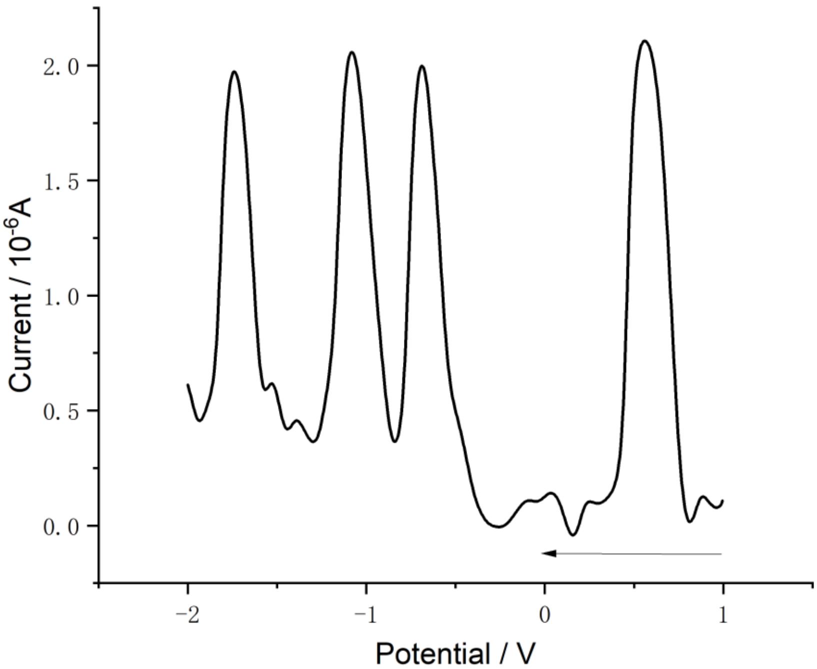

Fig. S34 Differential pulse voltammogram of **2n′** (scanning rate: 50 mV s^{-1})

Table S2. Half-Wave Reduction Potentials (V) of **2a–n′**.

Compd.	E_1	E_2	E_3
2a	-1.240	-1.628	-2.264
2b	-1.248	-1.624	-2.264
2c	-1.204	-1.592	-2.248
2d	-1.232	-1.596	-2.236
2e	-1.212	-1.612	-2.248
2f	-1.264	-1.636	-2.268
2g	-1.264	-1.660	-2.272
2h	-1.208	-1.588	-2.224
2i	-1.244	-1.616	-2.272
2j	-1.240	-1.620	-2.264
2k	-1.244	-1.620	-2.252
2l	-1.240	-1.620	-2.260
2m	-1.236	-1.616	-2.272
2m′	-1.240	-1.632	-2.264
2n	-1.220	-1.600	-2.236
2n′	-1.248	-1.640	-2.300

Versus ferrocene/ferrocenium. Experimental conditions: 1 mM of **2** and 0.1 M of *n*-Bu_4NClO_4 in anhydrous 1,2-dichlorobenzene; reference electrode: SCE; working electrode: 2-mm-diameter Pt disc; auxiliary electrode: Pt wire; scanning rate: 50 mV s^{-1}.

6. UV-vis Spectra of 2a–n′

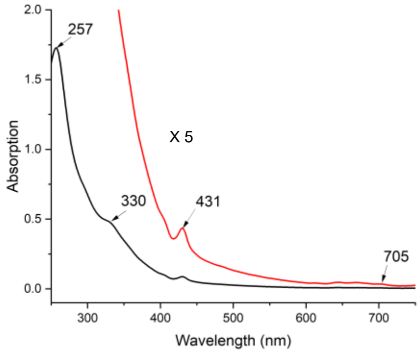

Fig. S35 UV-vis absorption of **2a**.

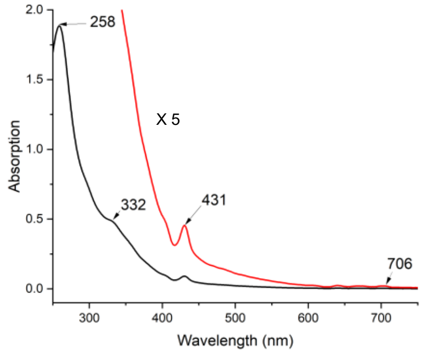

Fig. S36 UV-vis absorption of **2b**.

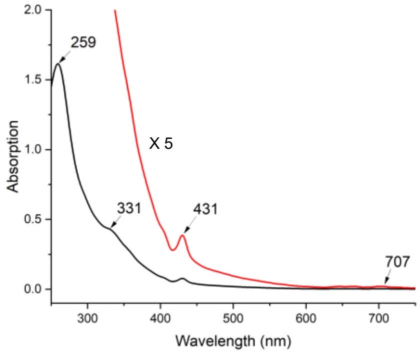

Fig. S37 UV-vis absorption of **2c**.

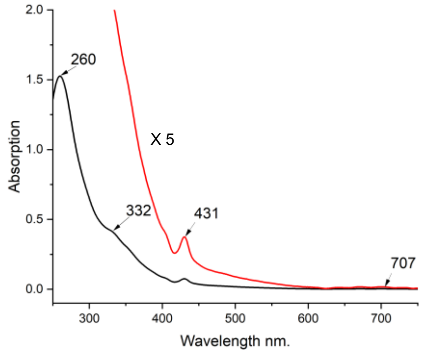

Fig. S38 UV-vis absorption of **2d**.

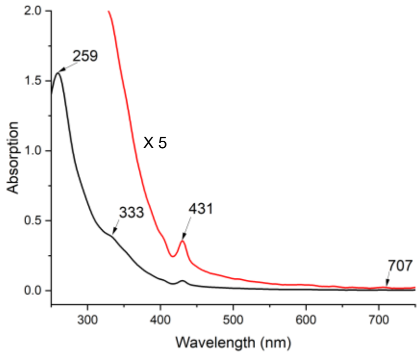

Fig. S39 UV-vis absorption of **2e**.

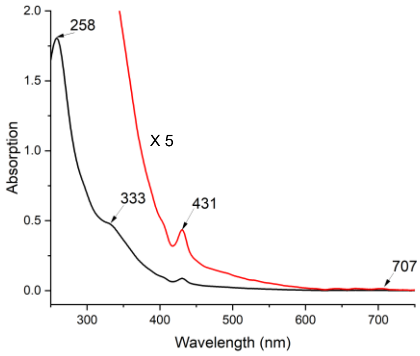

Fig. S40 UV-vis absorption of **2f**.

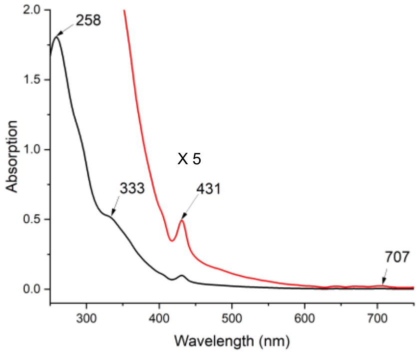

Fig. S41 UV-vis absorption of **2g**.

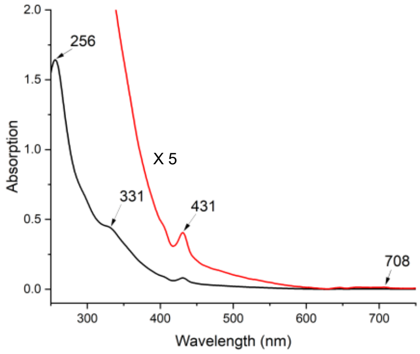

Fig. S42 UV-vis absorption of **2h**.

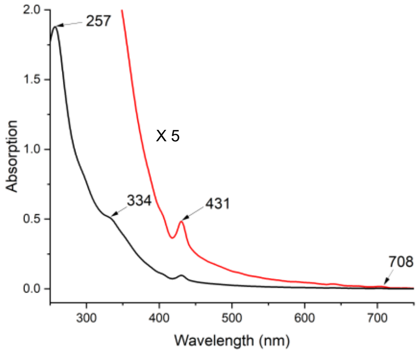

Fig. S43 UV-vis absorption of **2i**.

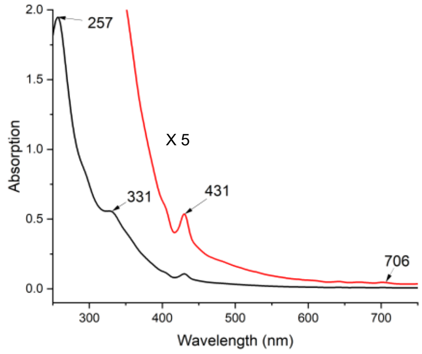

Fig. S44 UV-vis absorption of **2j**.

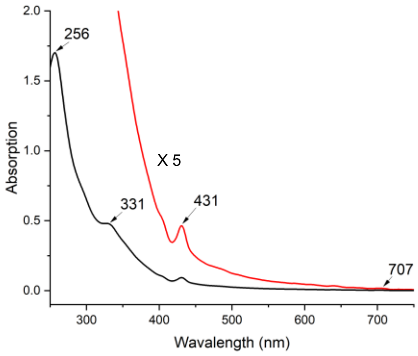

Fig. S45 UV-vis absorption of **2k**.

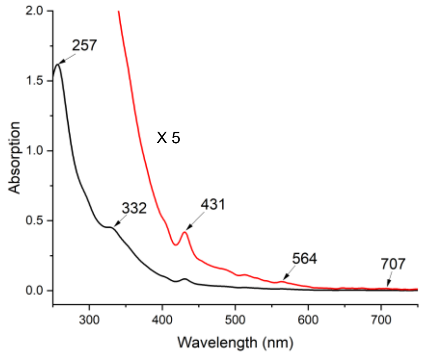

Fig. S46 UV-vis absorption of **2l**.

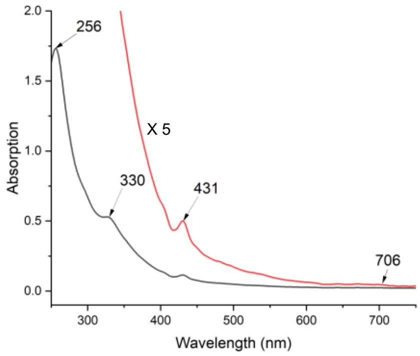

Fig. S47 UV-vis absorption of **2m**.

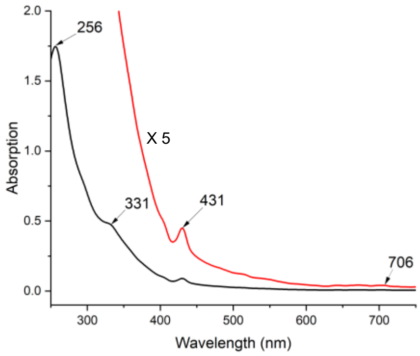

Fig. S48 UV-vis absorption of **2m′**.

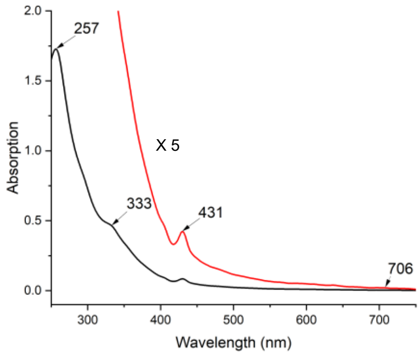

Fig. S49 UV-vis absorption of **2n**.

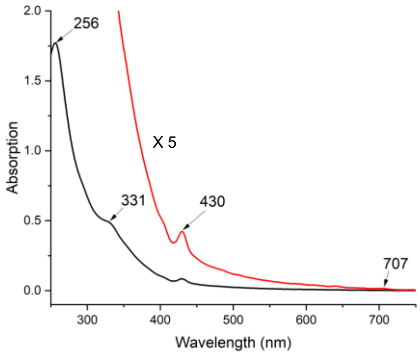

Fig. S50 UV-vis absorption of **2n′**.

7. NMR Spectra of 2a−n′

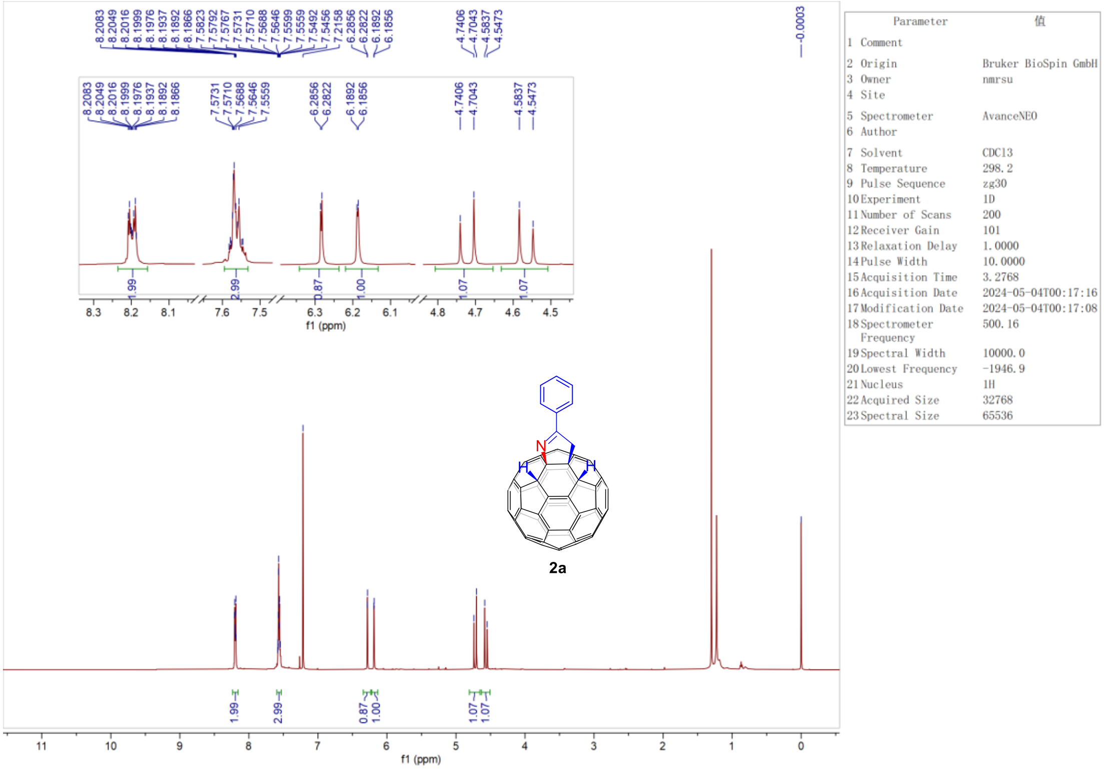

Fig. S51 ^{1}H NMR (500 MHz, $CS_2/CDCl_3$) of **2a**

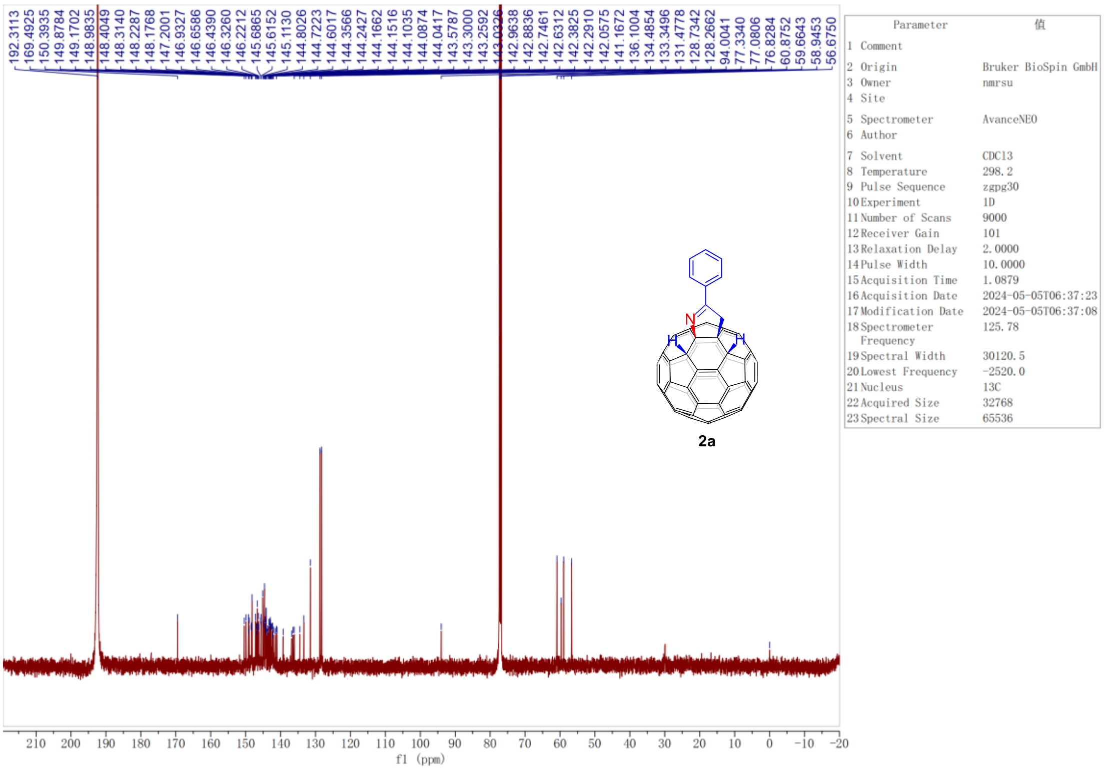

Fig. S52 ^{13}C NMR (126 MHz, $CS_2/CDCl_3$) of **2a**

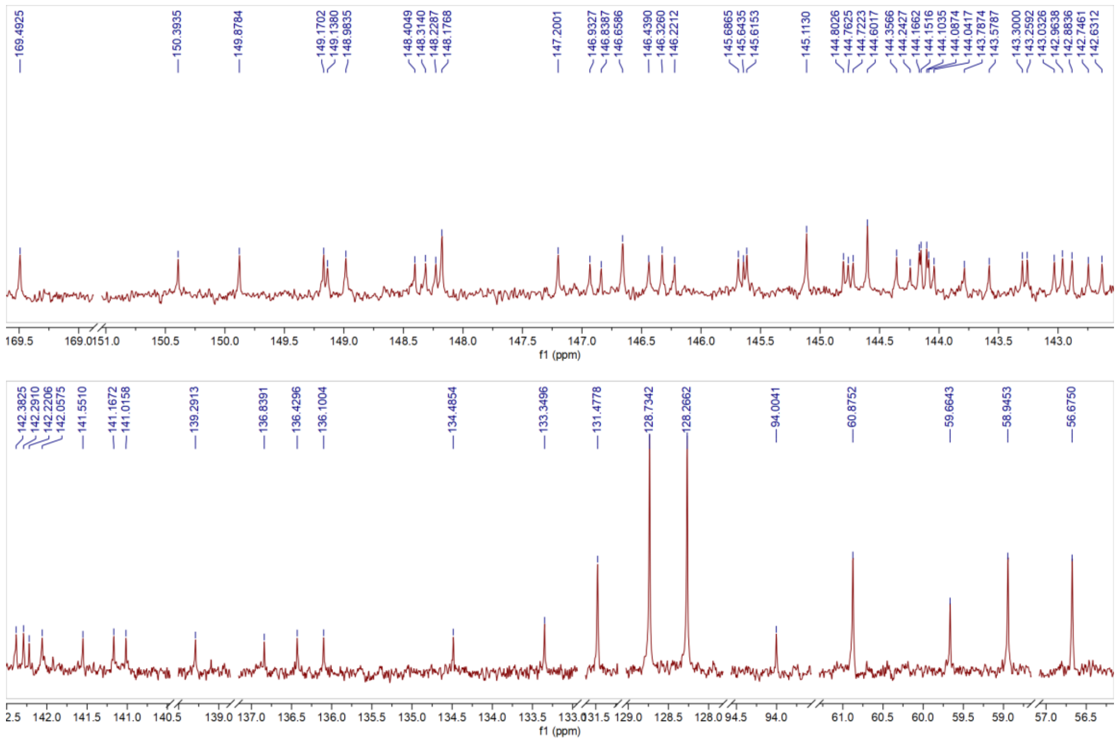

Fig. S53 Expanded ^{13}C NMR (126 MHz, $CS_2/CDCl_3$) of **2a**

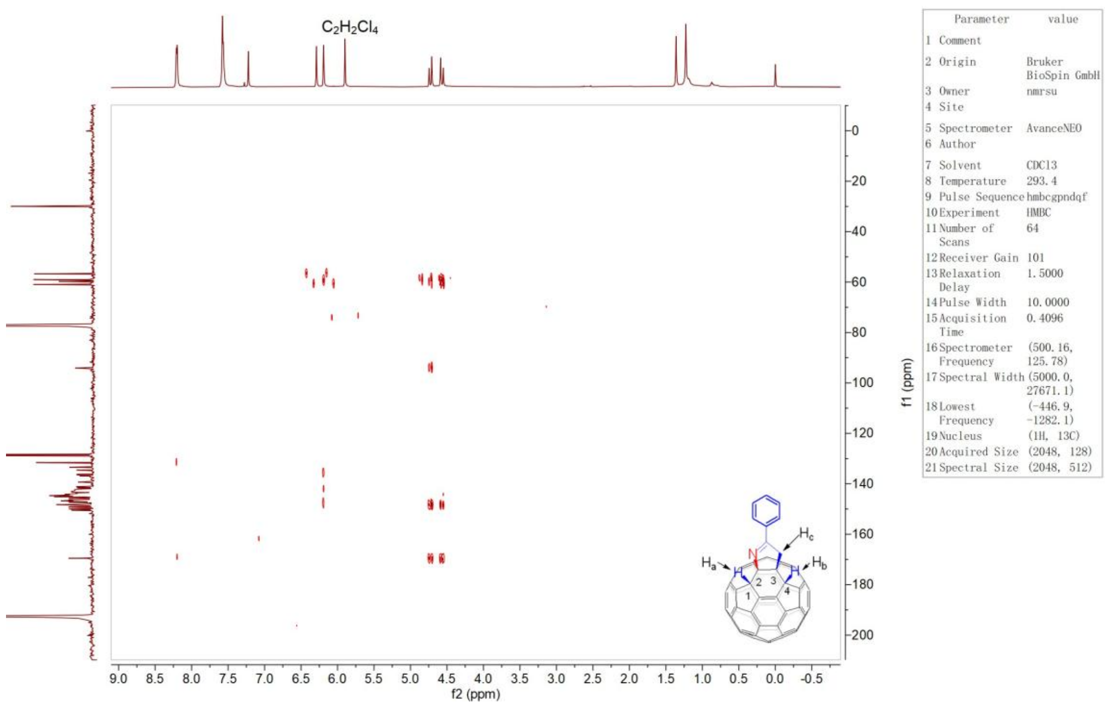

Fig. S54 HMBC (500/126 MHz, $CS_2/CDCl_3$) of **2a**

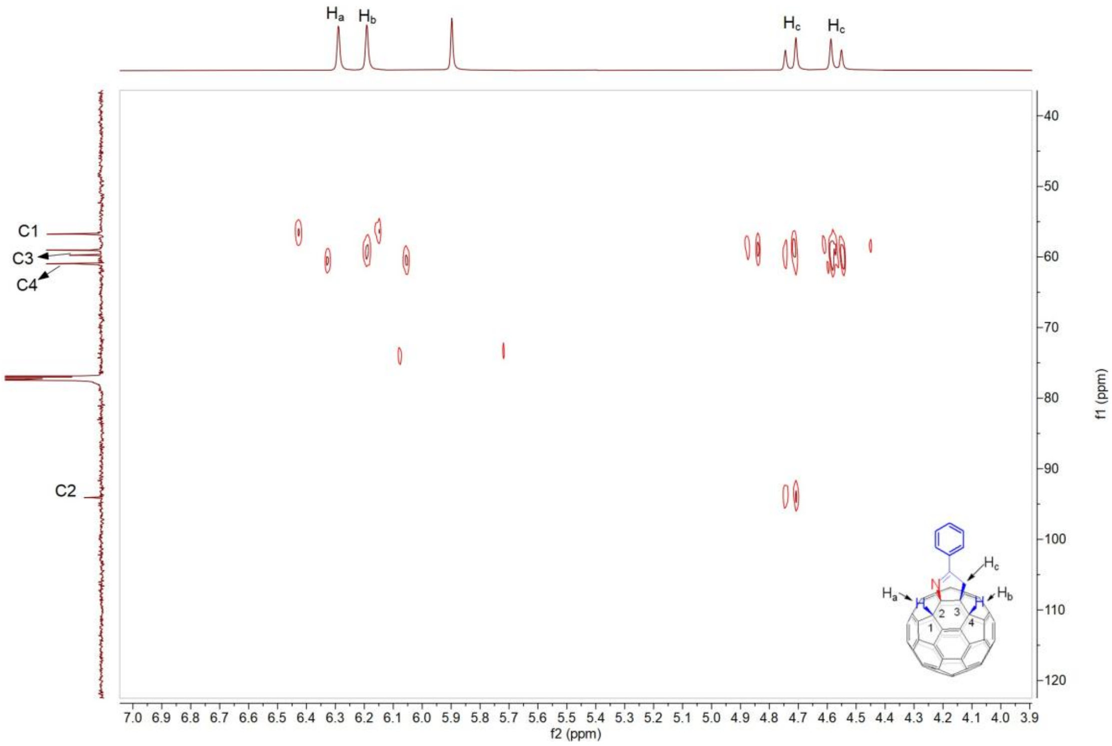

Fig. S55 Expanded HMBC (500/126 MHz, $CS_2/CDCl_3$) of **2a**

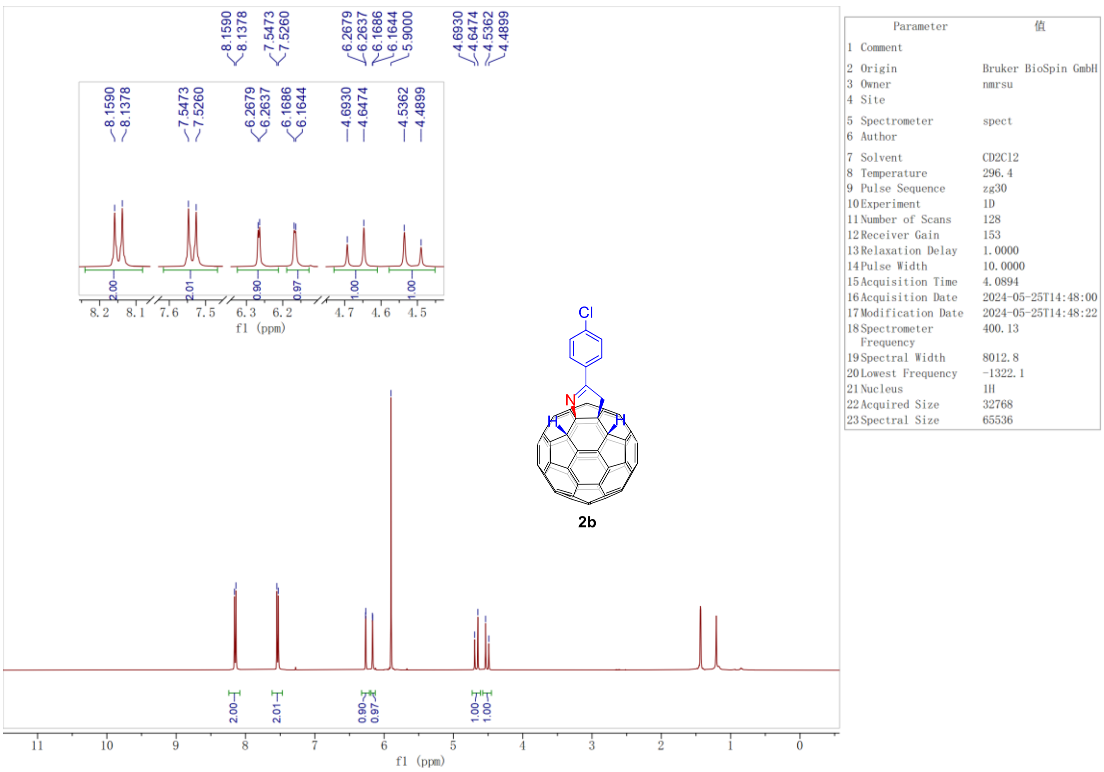

Fig. S56 ^1H NMR (400 MHz, $CS_2/C_2D_2Cl_4$) of **2b**

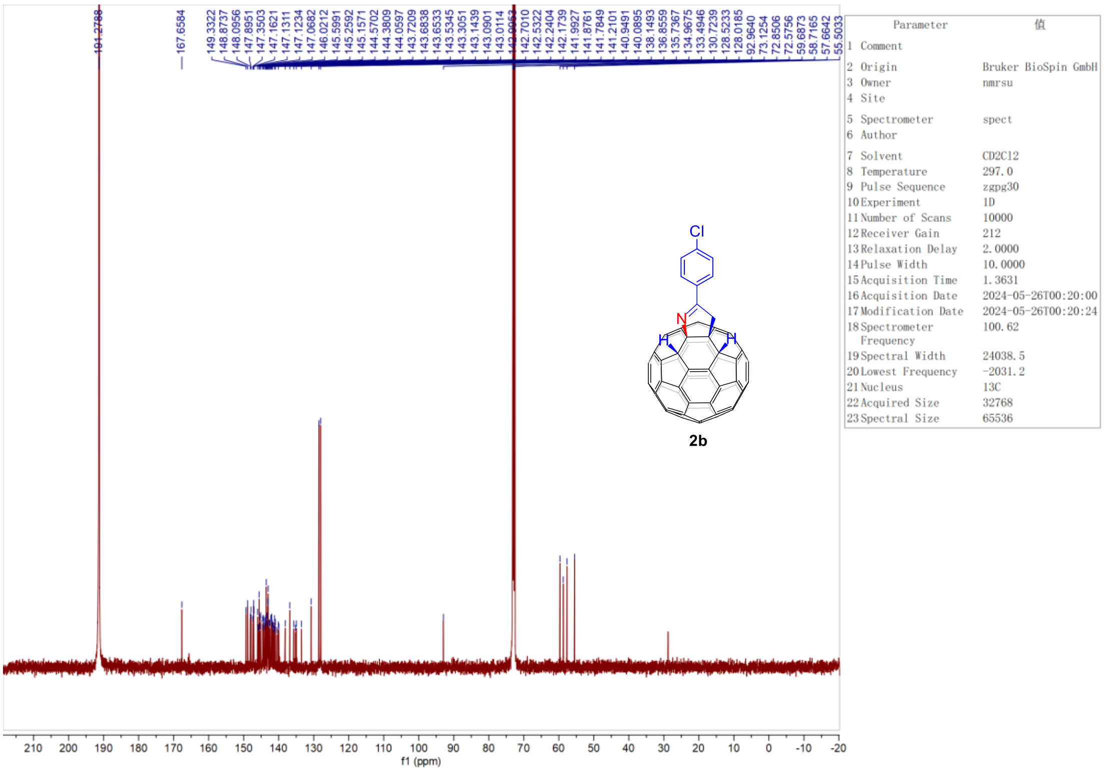

Fig. S57 ^{13}C NMR (101 MHz, $CS_2/C_2D_2Cl_4$) of **2b**

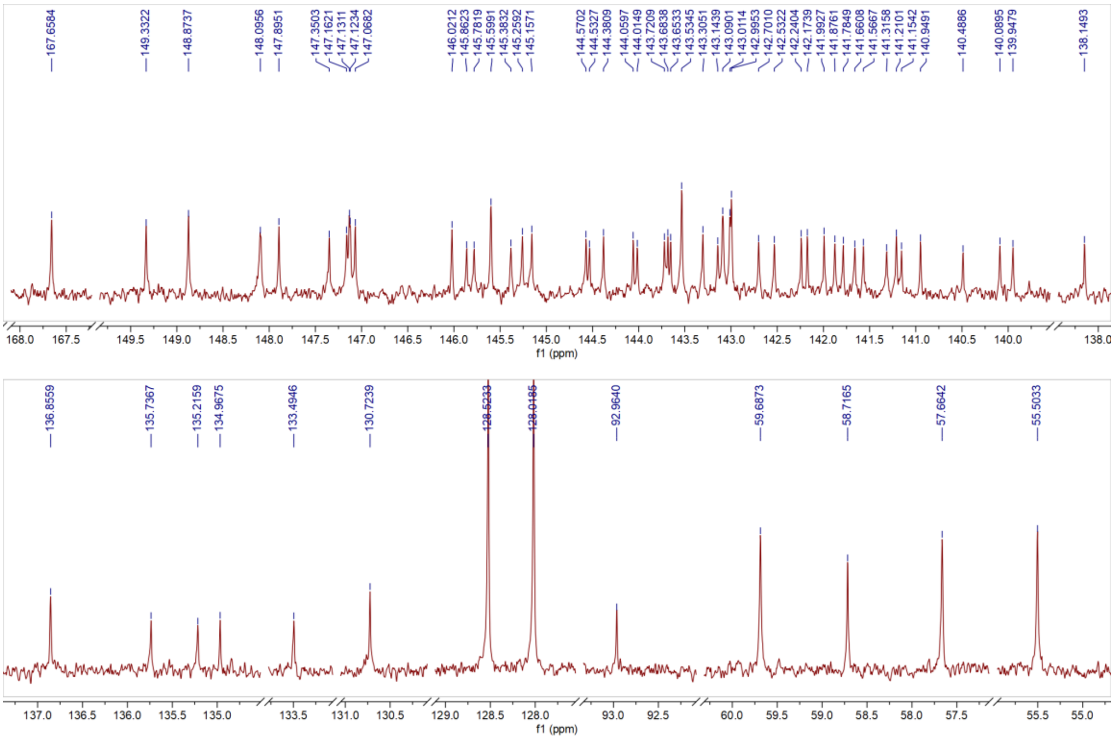

Fig. S58 Expanded ^{13}C NMR (101 MHz, $CS_2/C_2D_2Cl_4$) of **2b**

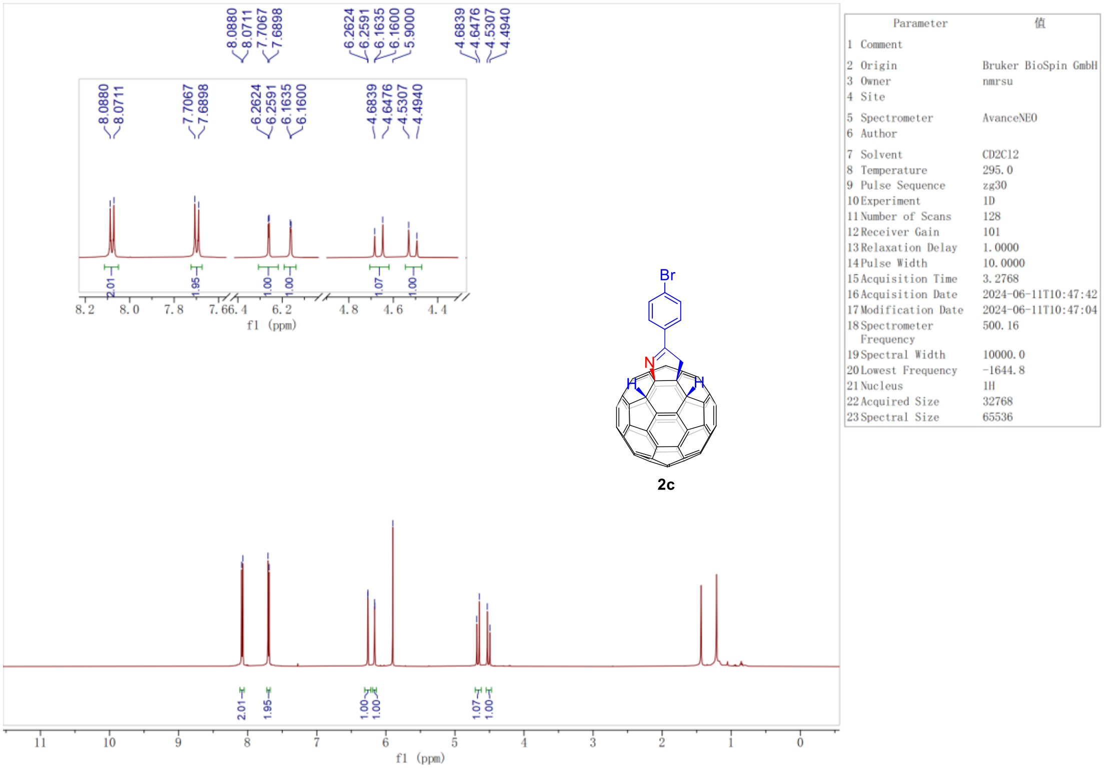

Fig. S59 ^{1}H NMR (500 MHz, $CS_2/C_2D_2Cl_4$) of **2c**

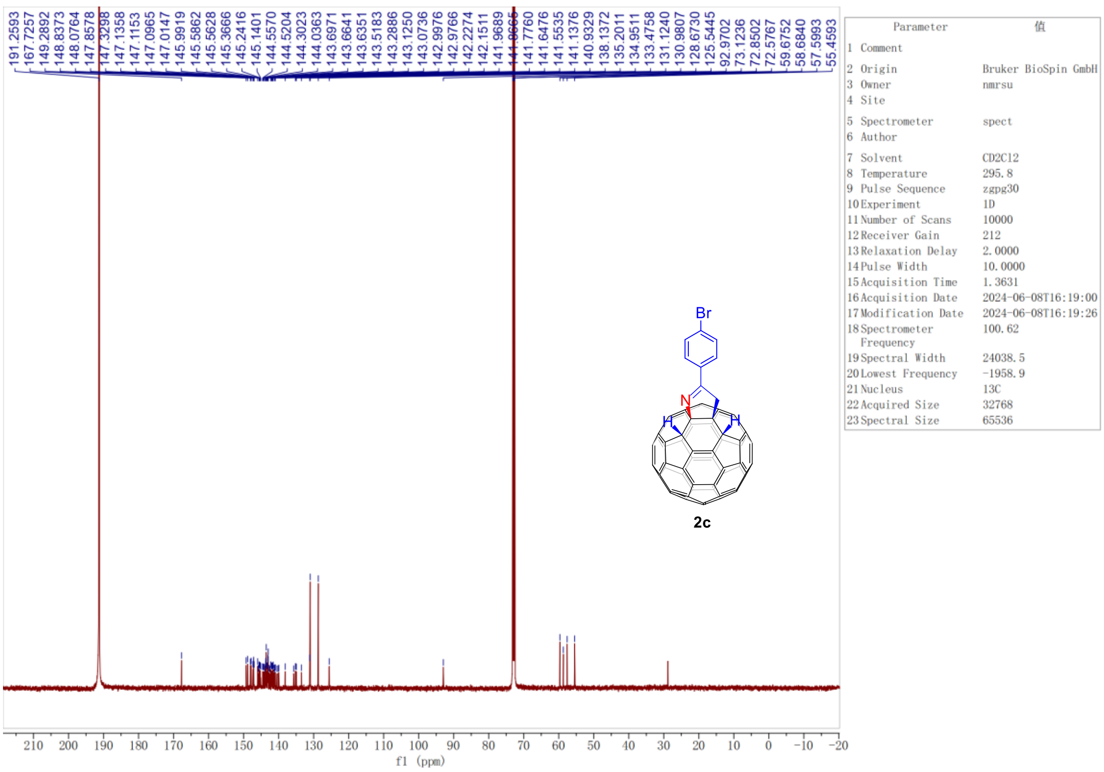

Fig. S60 ^{13}C NMR (101 MHz, $CS_2/C_2D_2Cl_4$) of **2c**

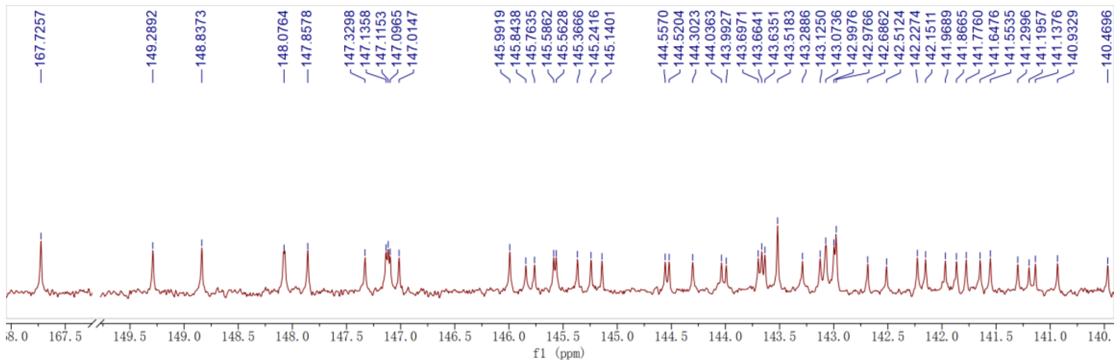

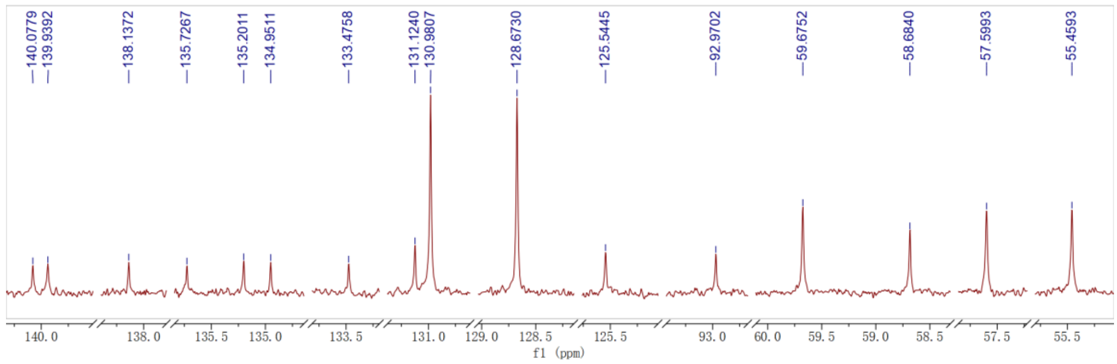

Fig. S61 Expanded ^{13}C NMR (101 MHz, $CS_2/C_2D_2Cl_4$) of **2c**

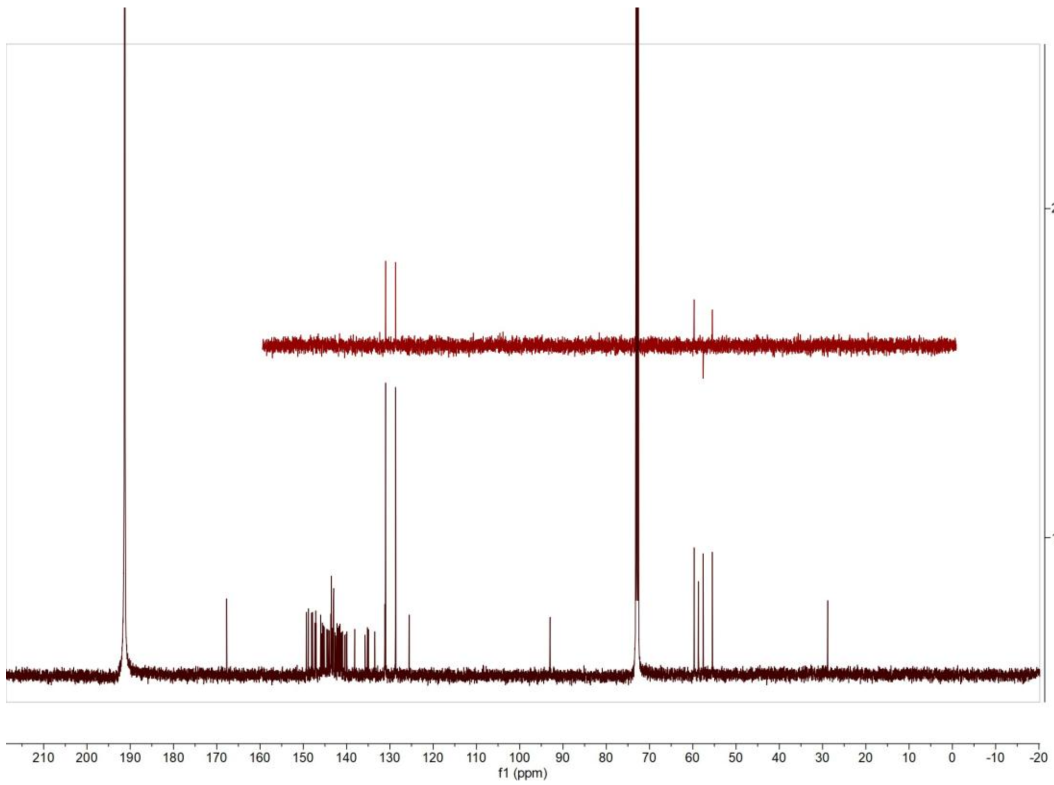

Fig. S62 DEPT-135 and ^{13}C NMR (101 MHz, $CS_2/C_2D_2Cl_4$) of **2c**

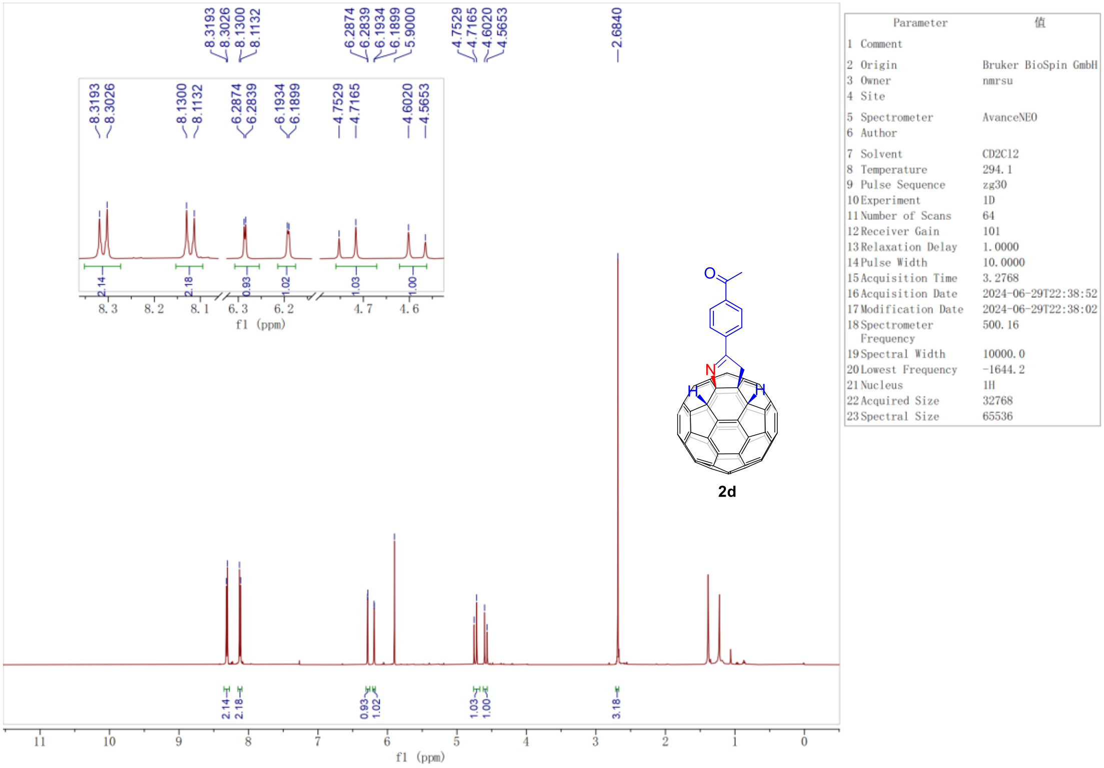

Fig. S63 ^{1}H NMR (500 MHz, $CS_2/C_2D_2Cl_4$) of **2d**

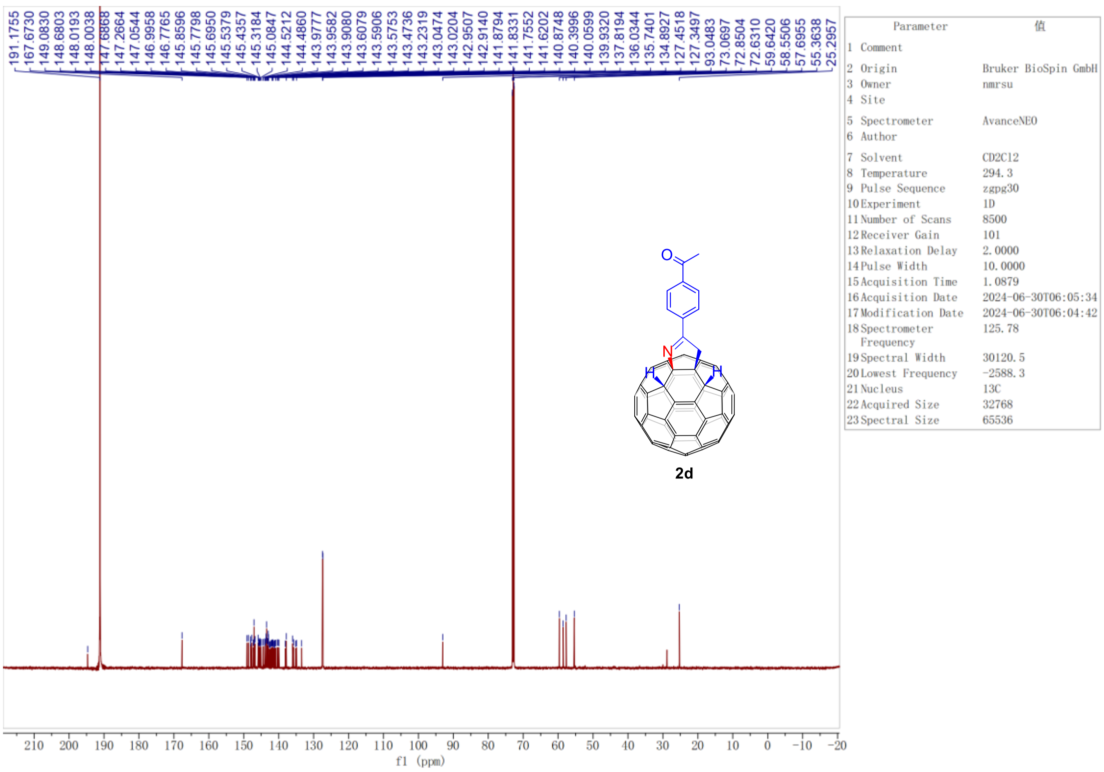

Fig. S64 ^{13}C NMR (126 MHz, $CS_2/C_2D_2Cl_4$) of **2d**

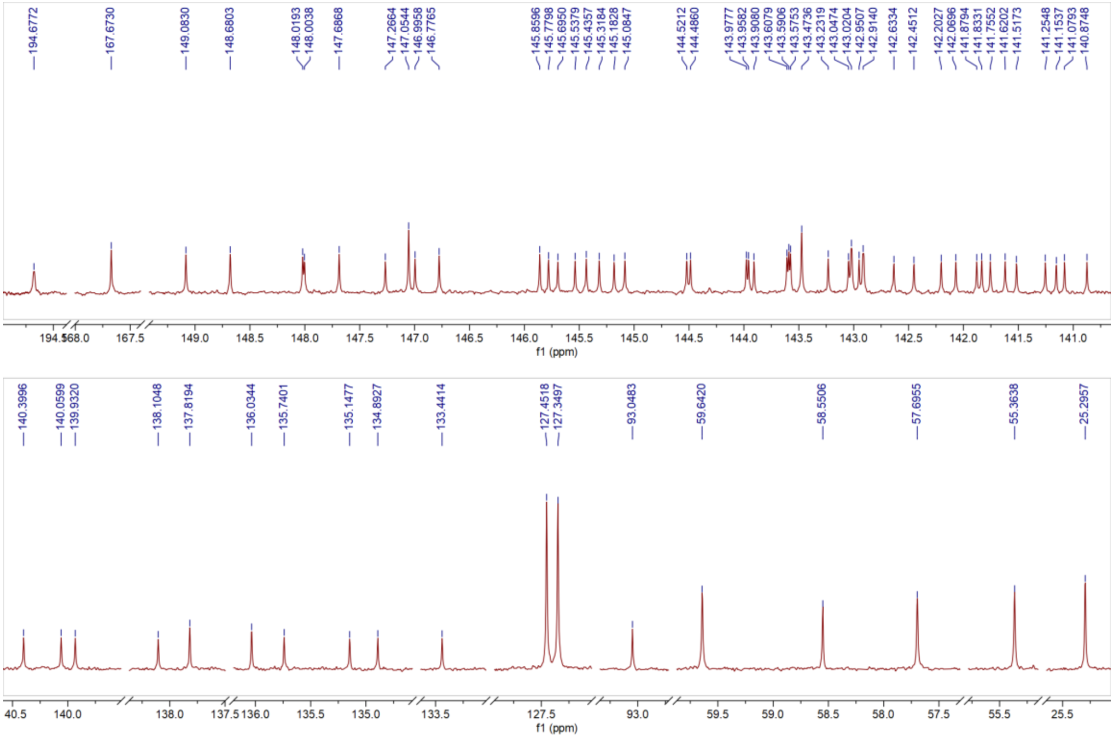

Fig. S65 Expanded ^{13}C NMR (126 MHz, $CS_2/C_2D_2Cl_4$) of **2d**

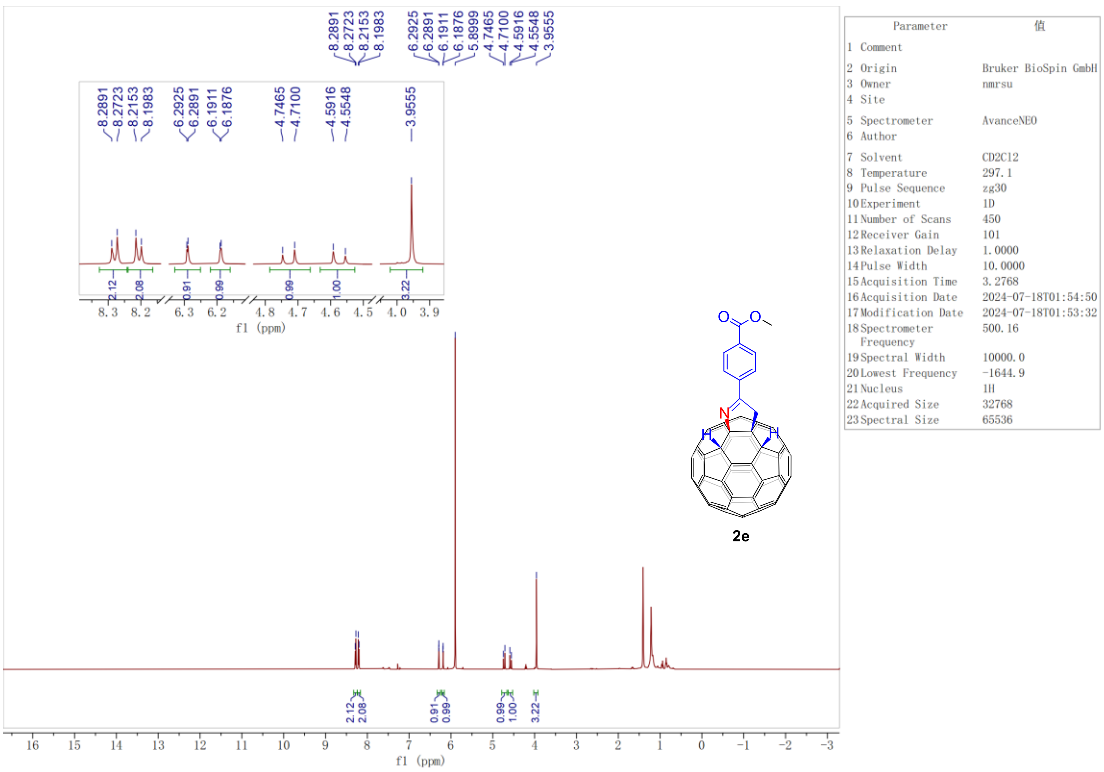

Fig. S66 ^{1}H NMR (500 MHz, $CS_2/C_2D_2Cl_4$) of **2e**

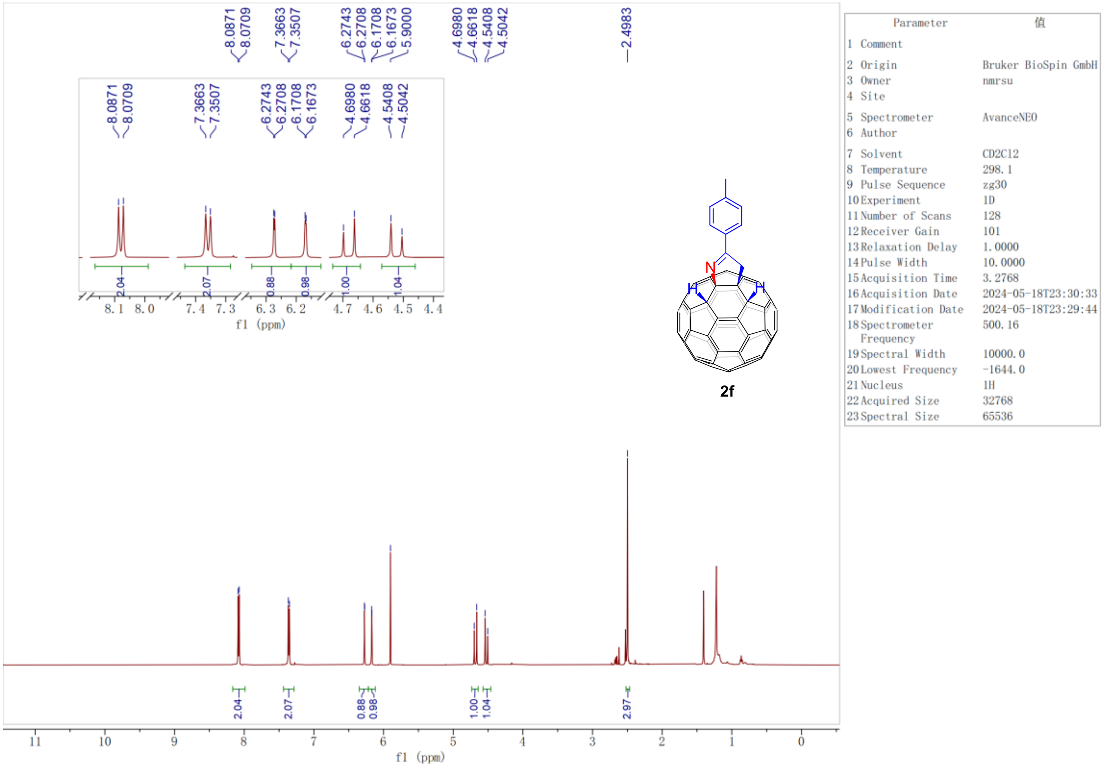

Fig. S67 ^{1}H NMR (500 MHz, $CS_2/C_2D_2Cl_4$) of **2f**

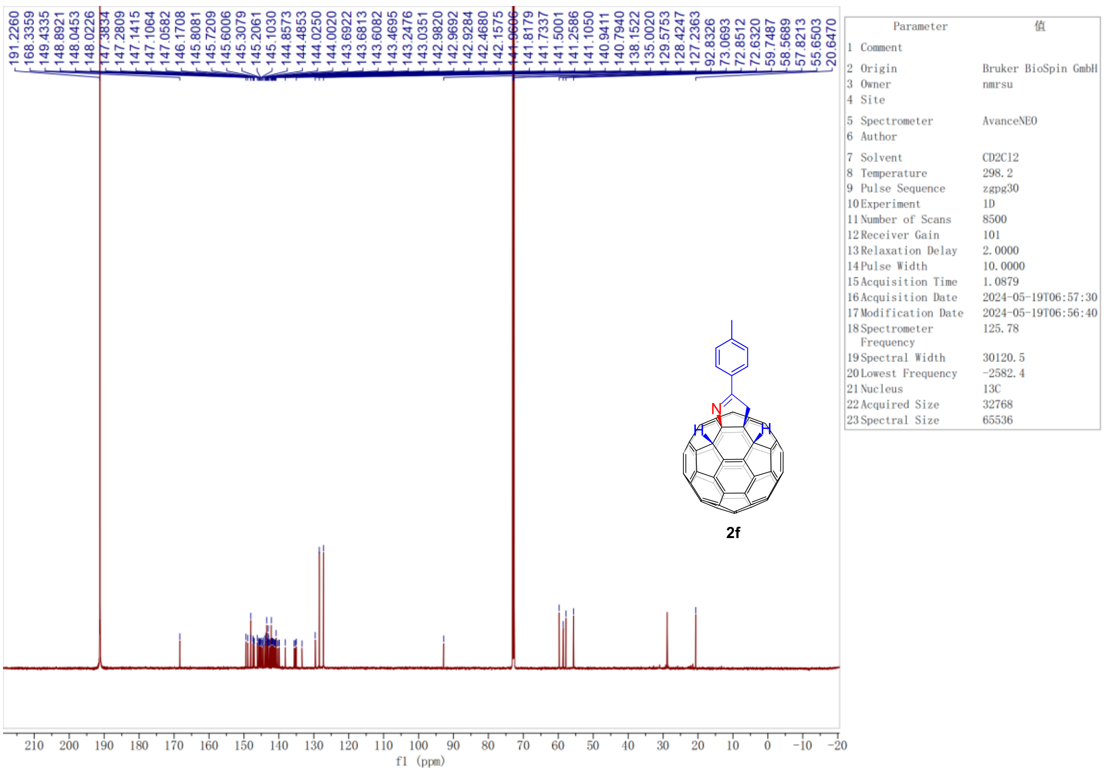

Fig. S68 ^{13}C NMR (126 MHz, $CS_2/C_2D_2Cl_4$) of **2f**

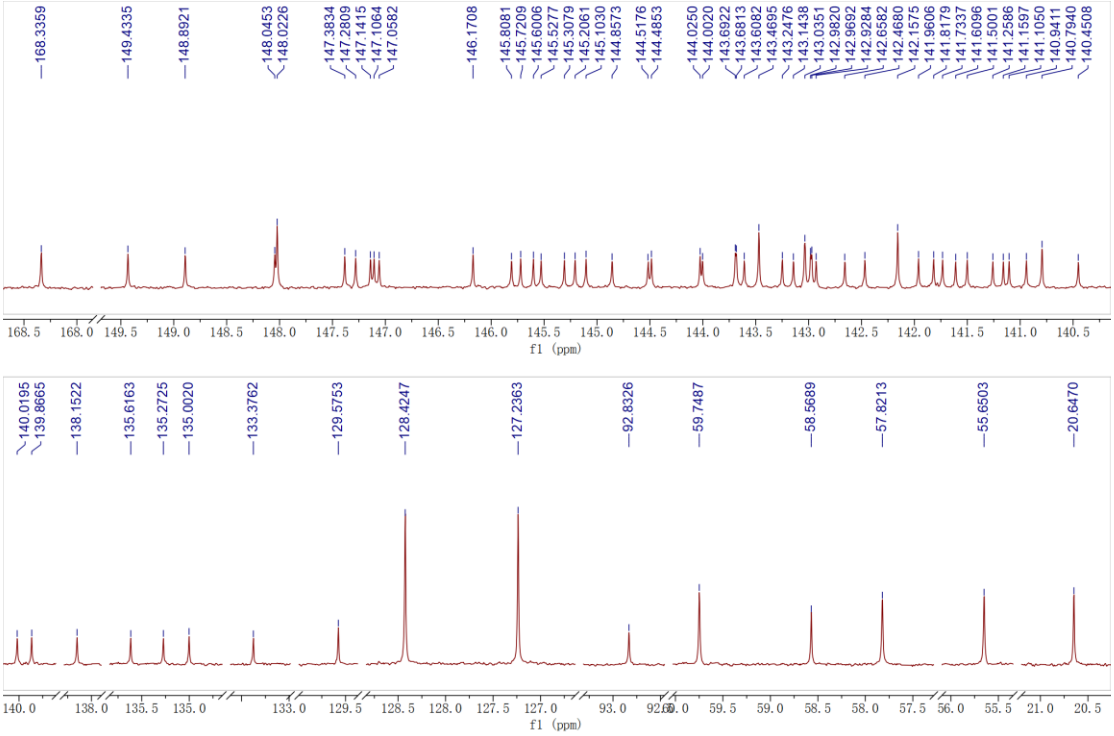

Fig. S69 Expanded ^{13}C NMR (126 MHz, $CS_2/C_2D_2Cl_4$) of **2f**

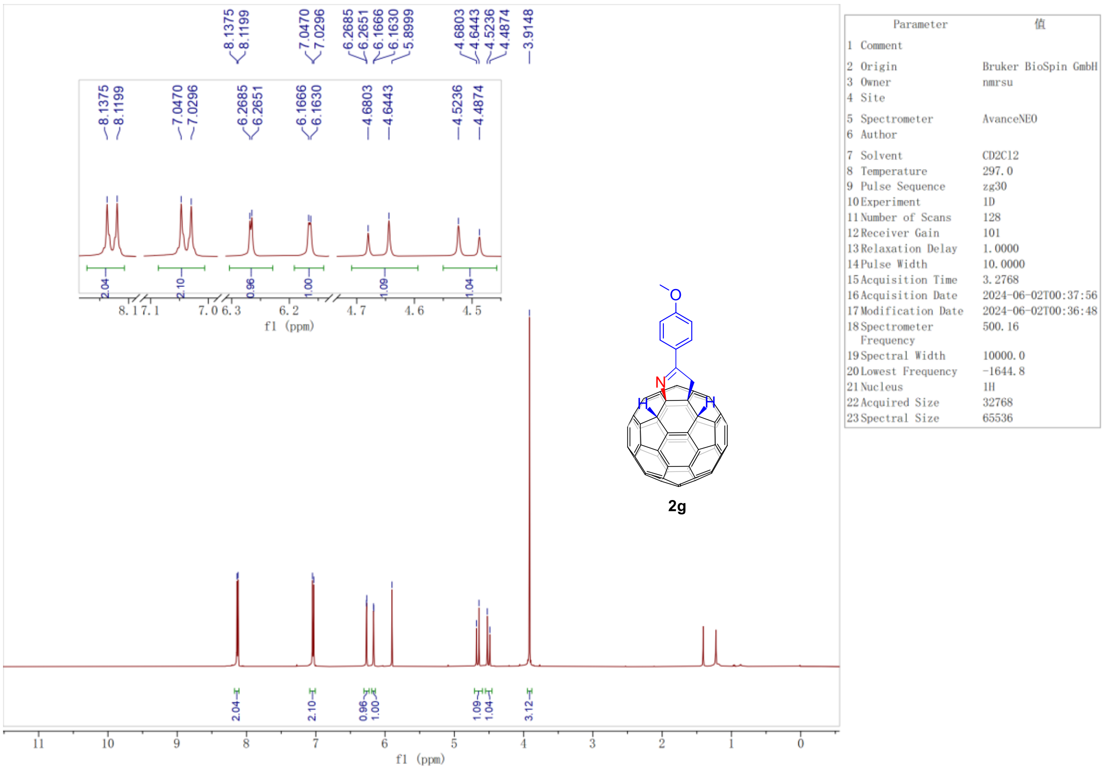

Fig. S70 ^{1}H NMR (500 MHz, $CS_2/C_2D_2Cl_4$) of **2g**

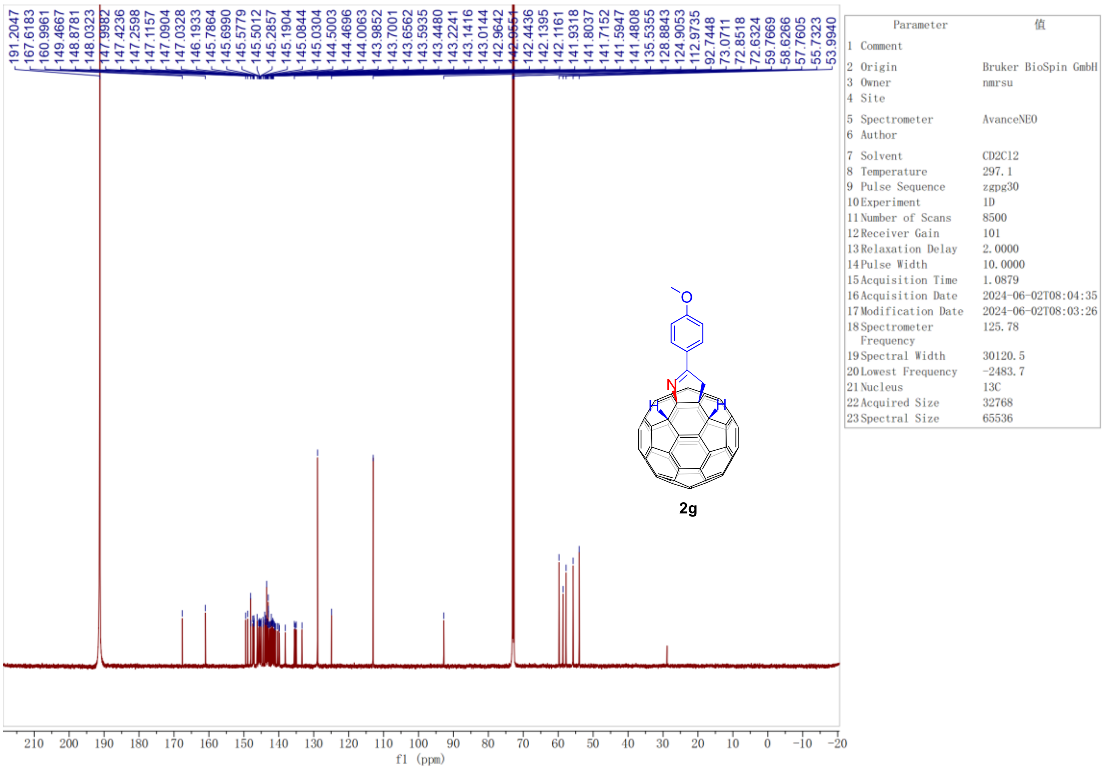

Fig. S71 ^{13}C NMR (126 MHz, $CS_2/C_2D_2Cl_4$) of **2g**

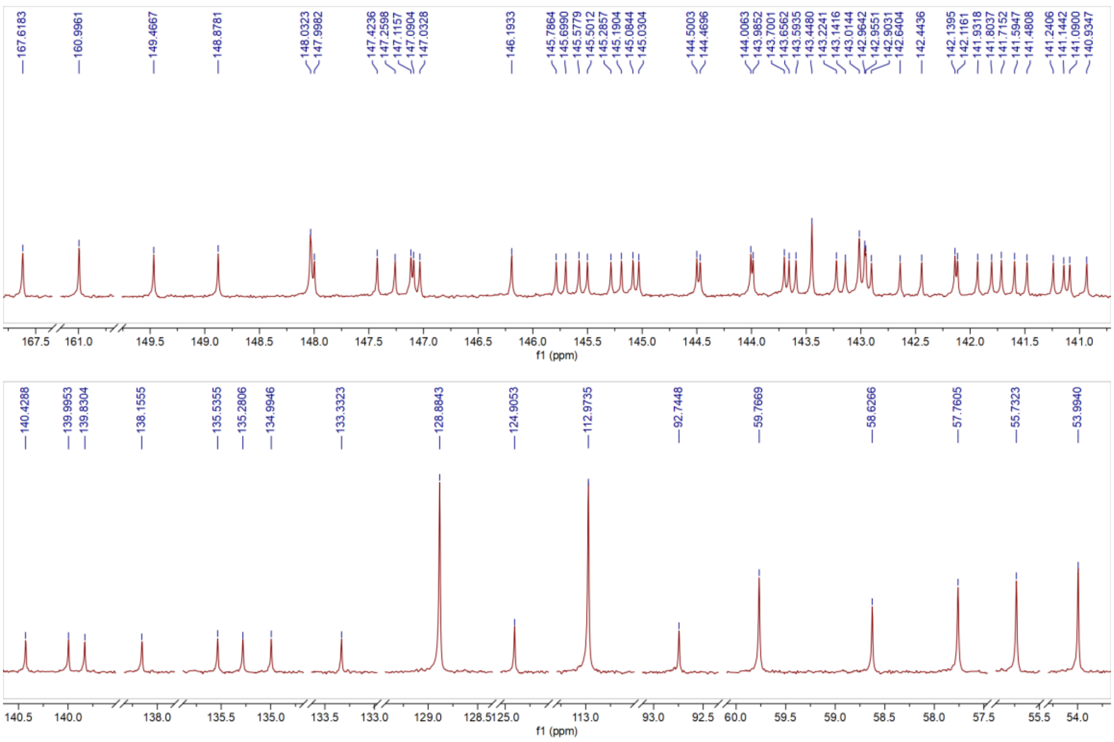

Fig. S72 Expanded ^{13}C NMR (126 MHz, $CS_2/C_2D_2Cl_4$) of **2g**

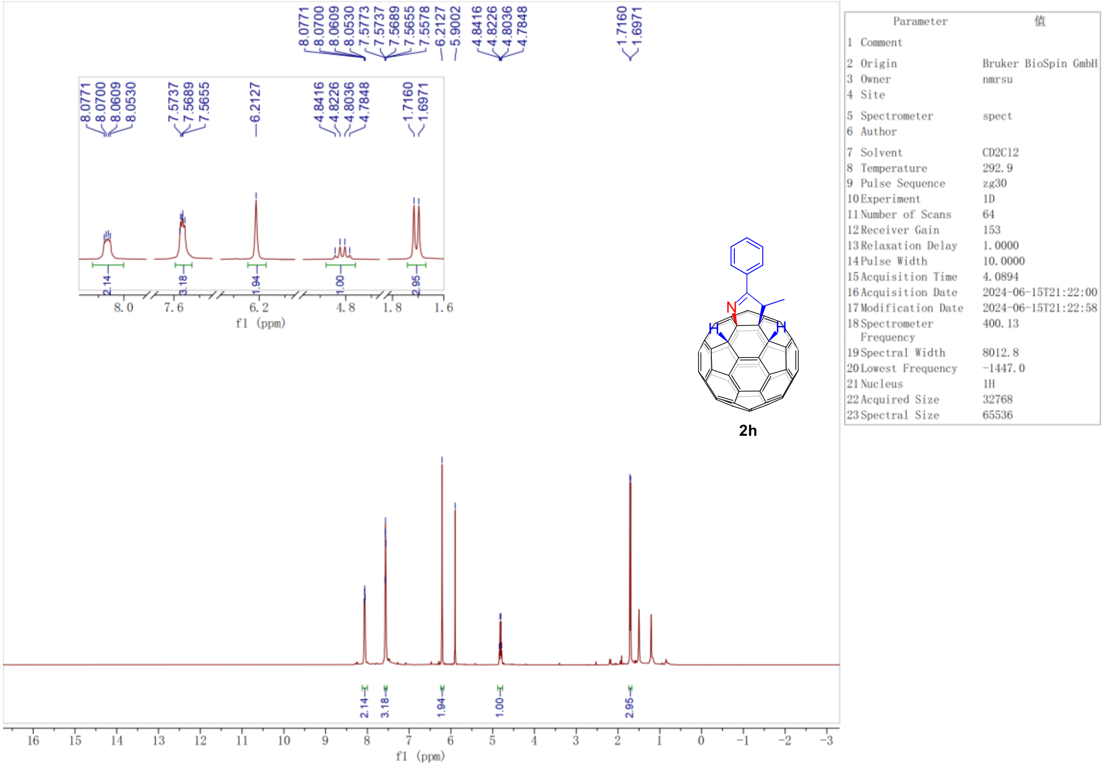

Fig. S73 ^{1}H NMR (400 MHz, $CS_2/C_2D_2Cl_4$) of **2h**

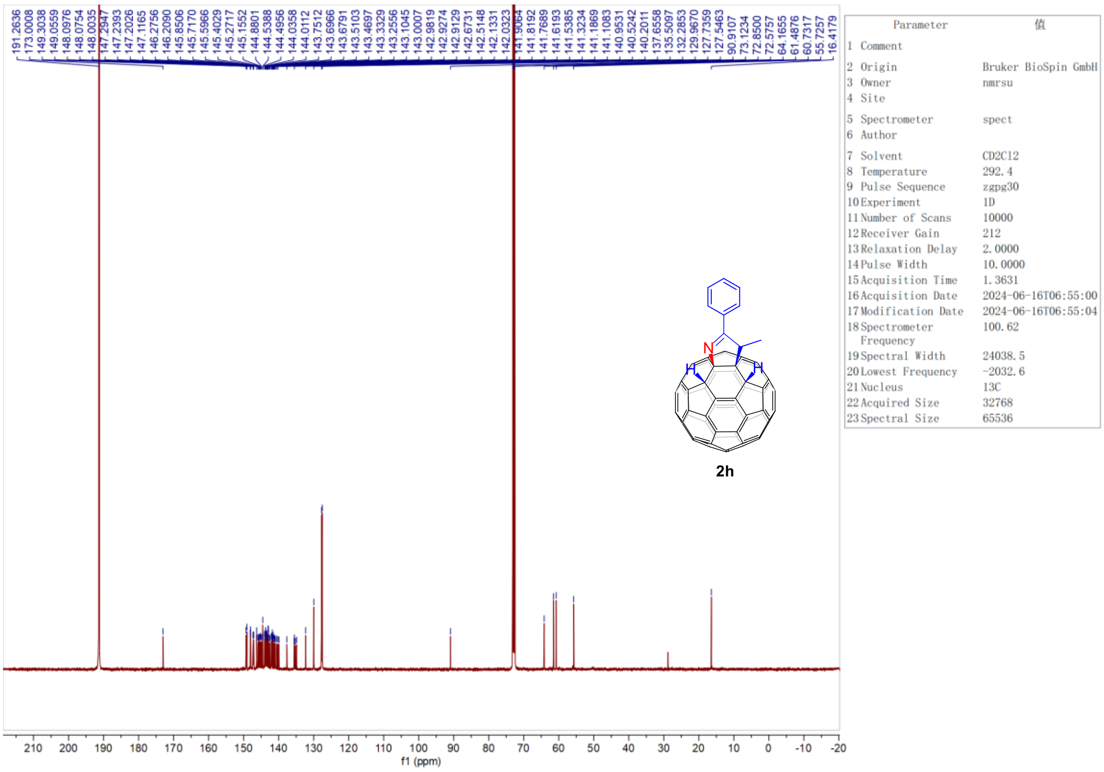

Fig. S74 ^{13}C NMR (101 MHz, $CS_2/C_2D_2Cl_4$) of **2h**

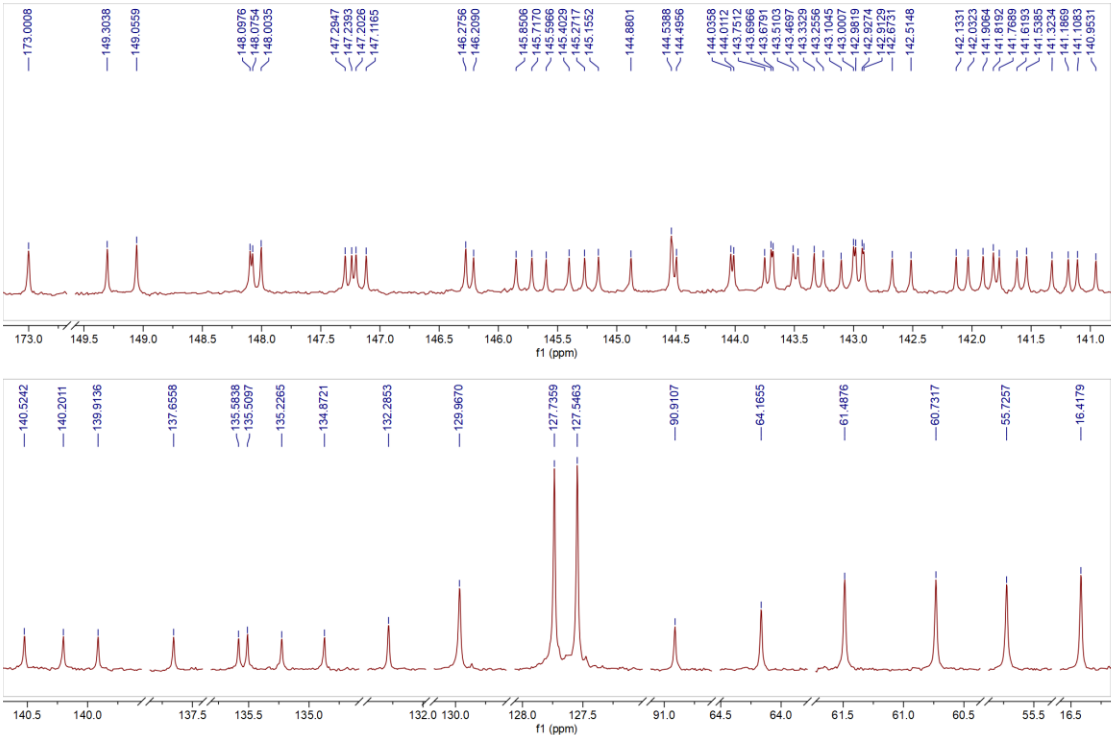

Fig. S75 Expanded ^{13}C NMR (101 MHz, $CS_2/C_2D_2Cl_4$) of **2h**

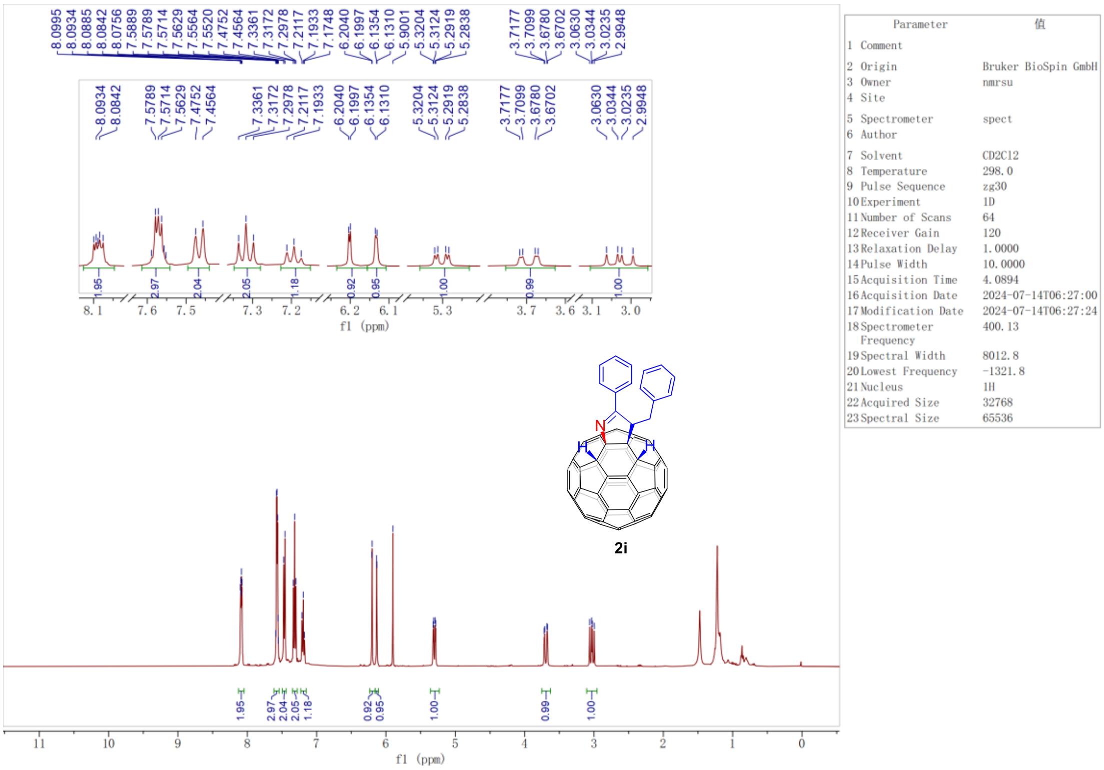

Fig. S76 ^{1}H NMR (400 MHz, $CS_2/C_2D_2Cl_4$) of **2i**

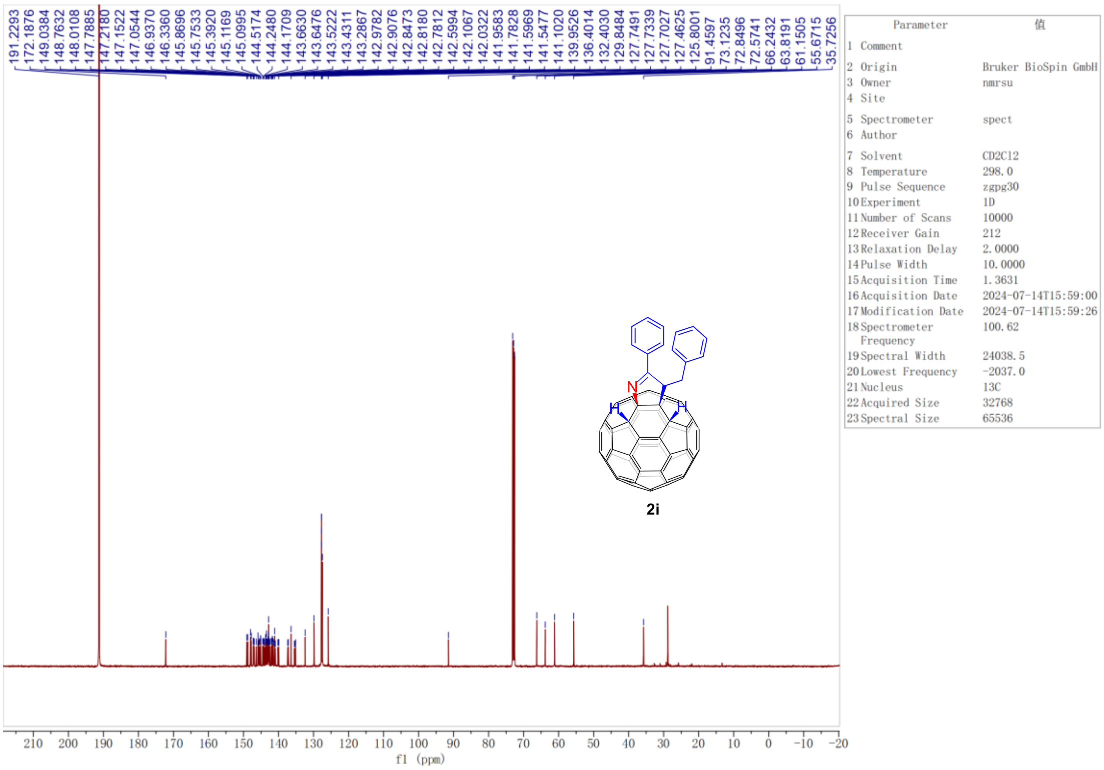

Fig. S77 ^{13}C NMR (101 MHz, $CS_2/C_2D_2Cl_4$) of **2i**

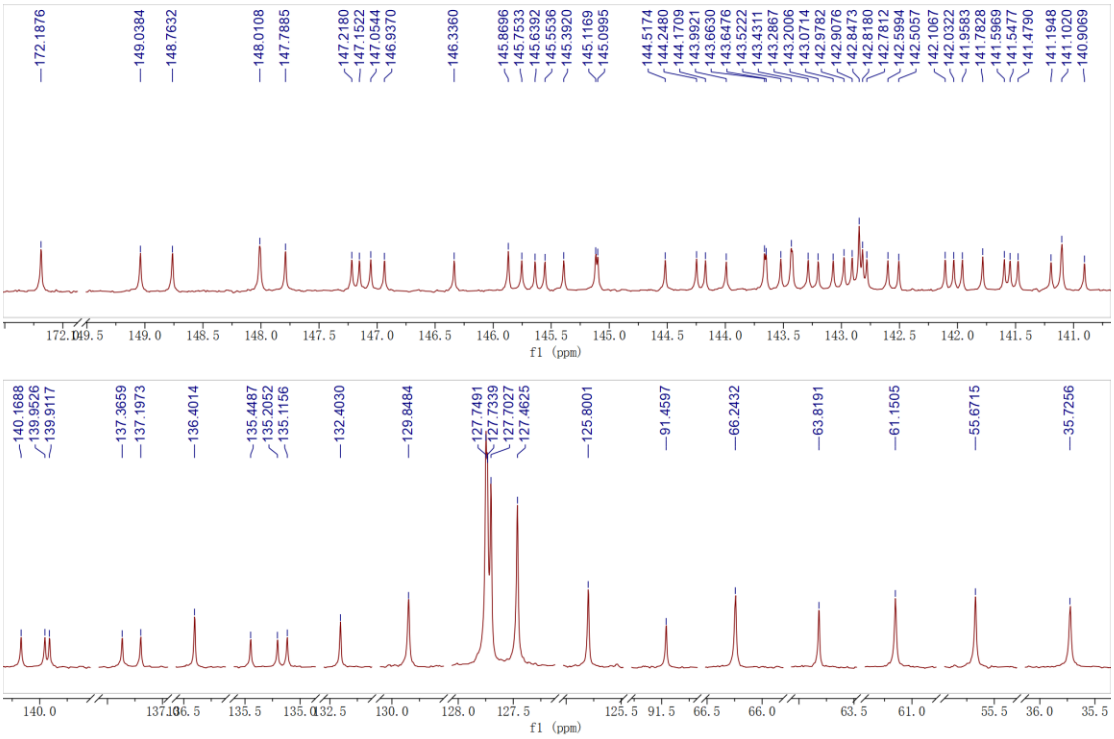

Fig. S78 Expanded ^{13}C NMR (101 MHz, $CS_2/C_2D_2Cl_4$) of **2i**

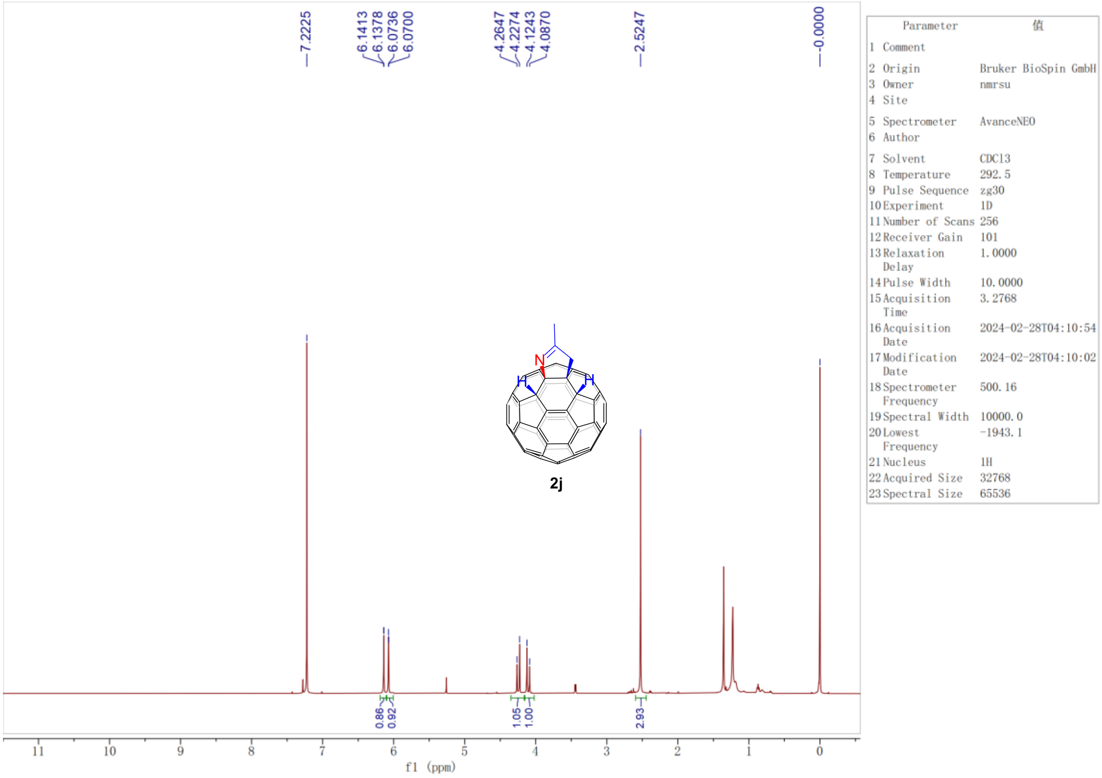

Fig. S79 ^{1}H NMR (500 MHz, CS_2/$CDCl_3$, $Cr(acac)_3$ as relaxation reagent) of **2j**

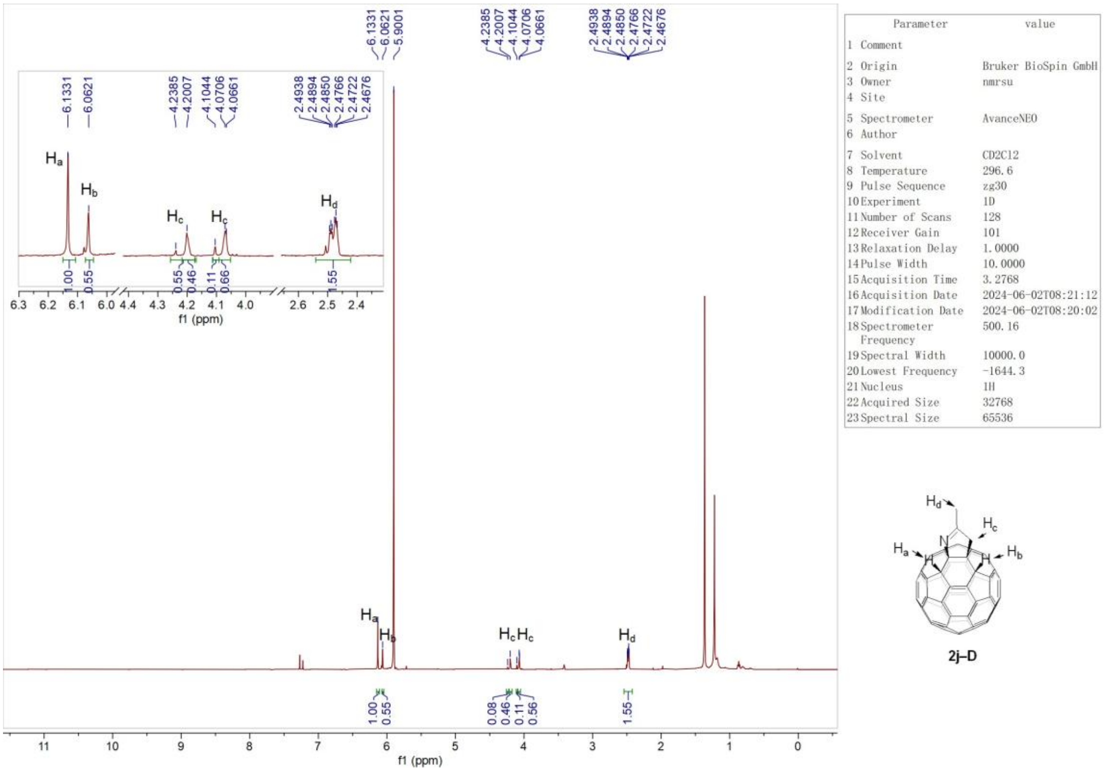

Fig. S80 ^{1}H NMR (500 MHz, CS_2/$C_2D_2Cl_4$) of **2j-D**

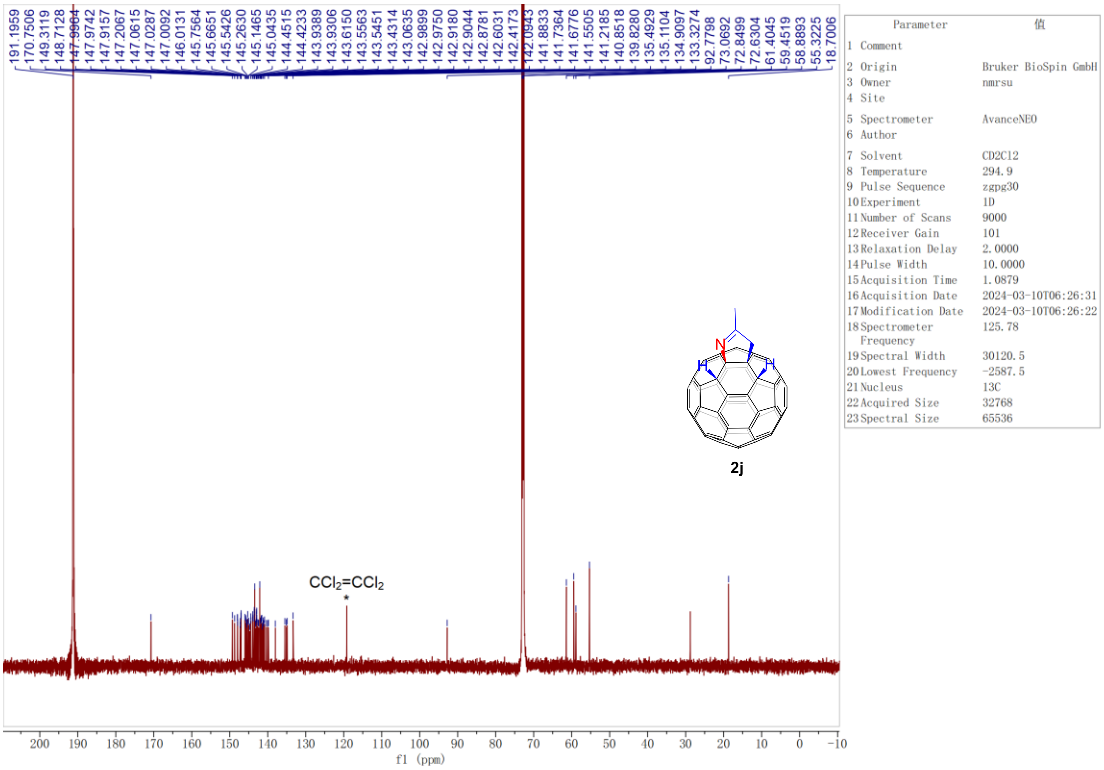

Fig. S81 ^{13}C NMR (126 MHz, $CS_2/C_2D_2Cl_4$, $Cr(acac)_3$ as relaxation reagent) of **2j**

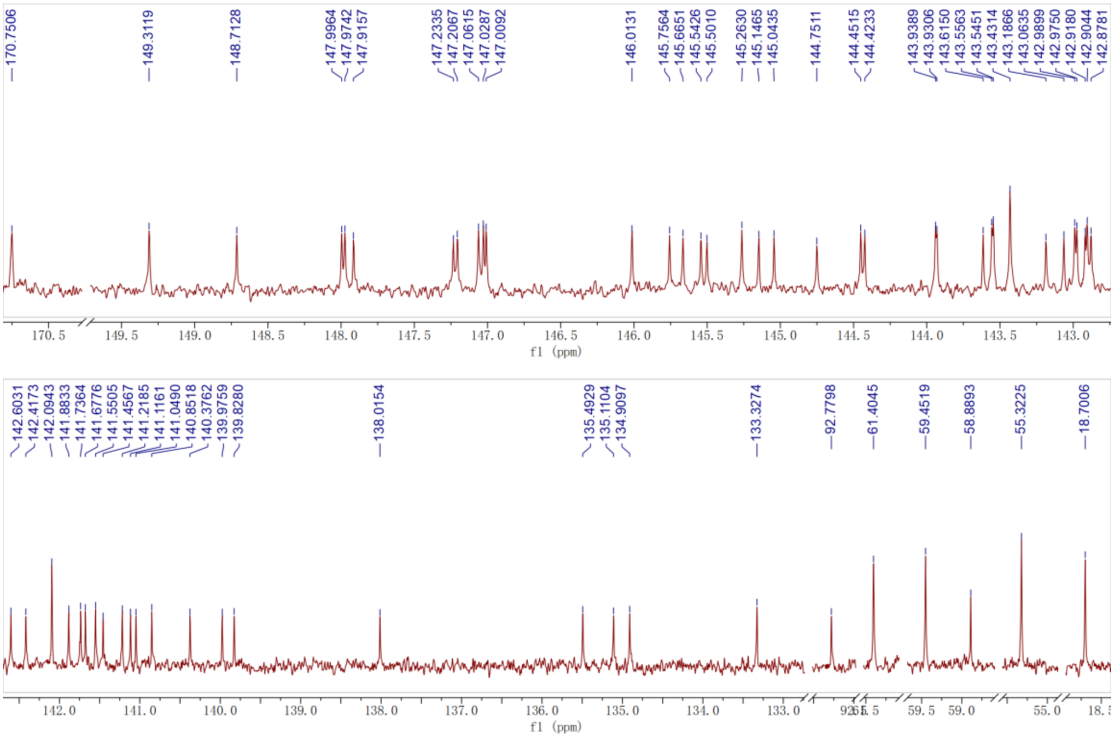

Fig. S82 Expanded ^{13}C NMR (126 MHz, $CS_2/C_2D_2Cl_4$, $Cr(acac)_3$ as relaxation reagent) of **2j**

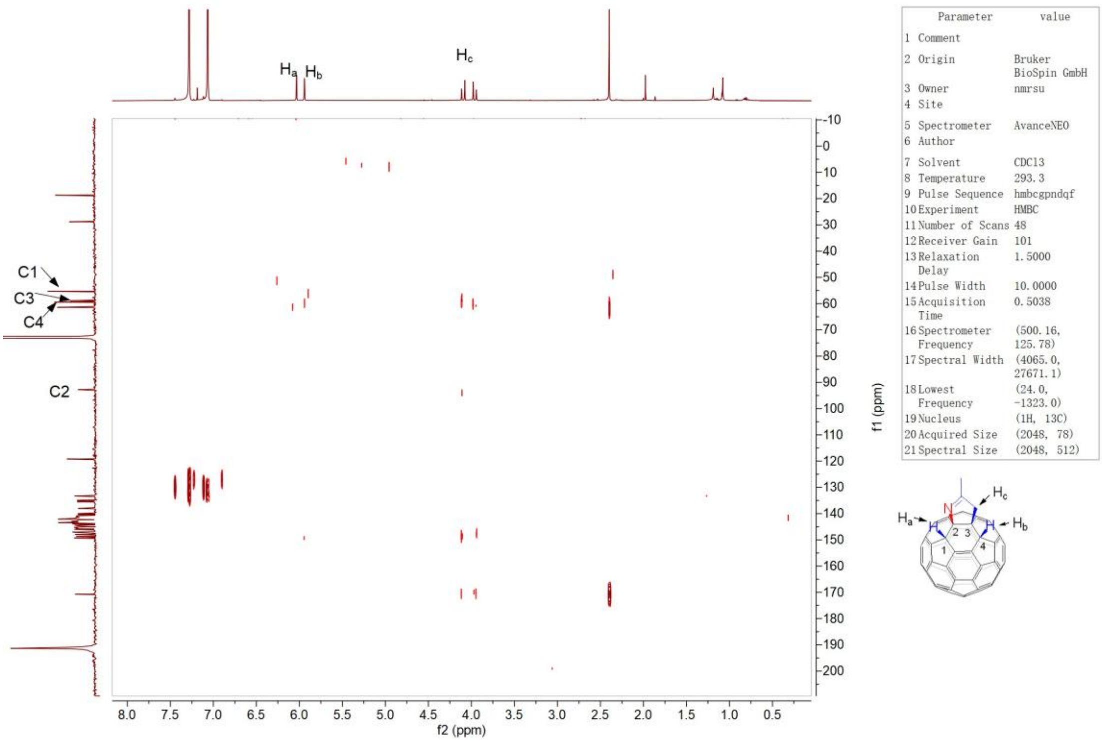

Fig. S83 HMBC (500/126 MHz, ^{1}H NMR was recorded in 4:1 CS_2/1,2-$C_6H_4Cl_2$-D_4, ^{13}C NMR was recorded in 2:1 CS_2/$C_2D_2Cl_4$) of compound **2j**

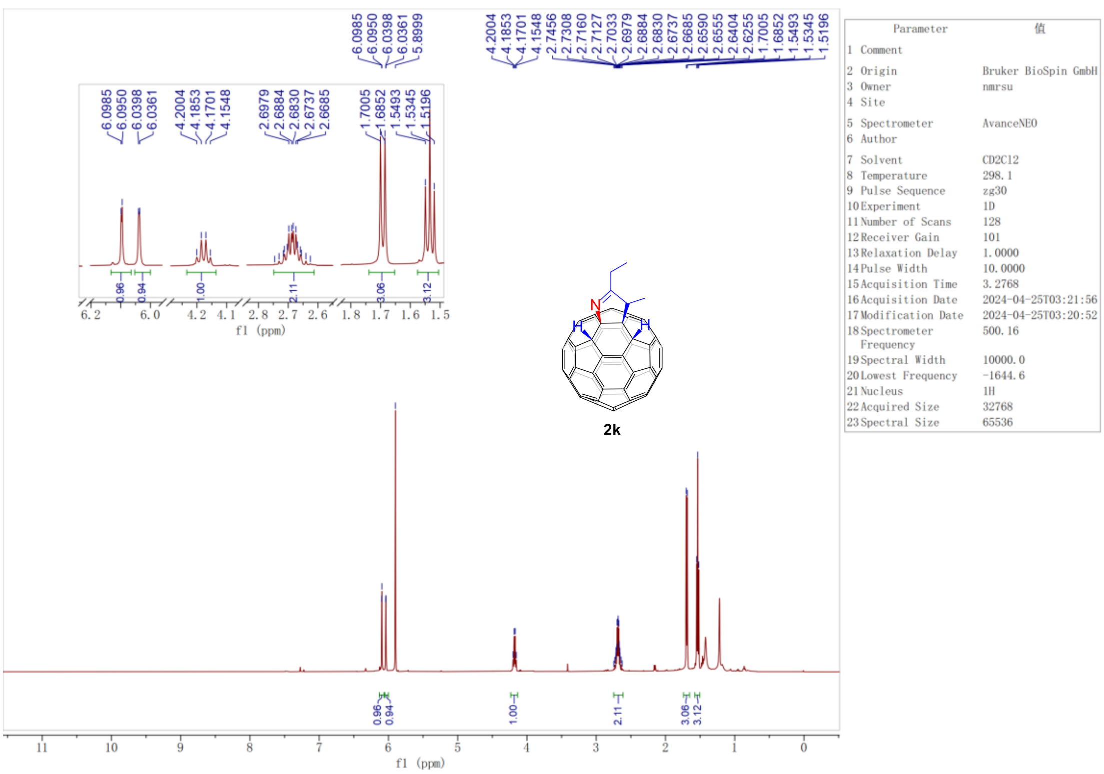

Fig. S84 ^{1}H NMR (500 MHz, CS_2/$C_2D_2Cl_4$) of **2k**

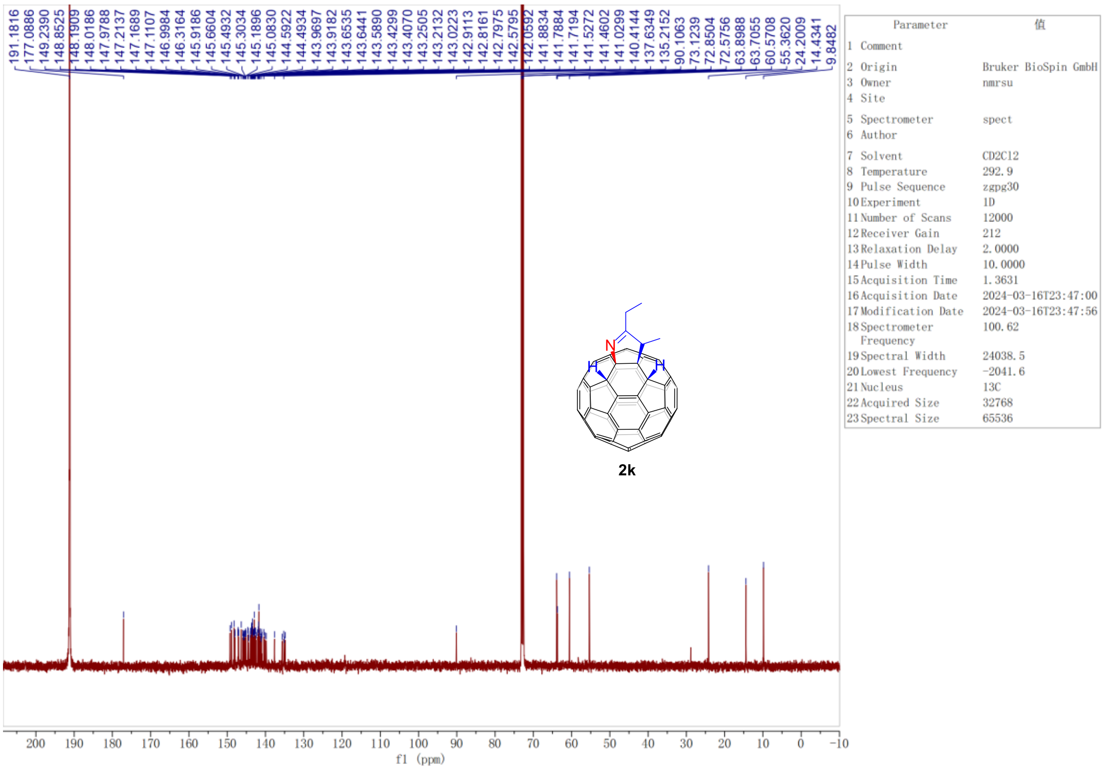

Fig. S85 ^{13}C NMR (101 MHz, $CS_2/C_2D_2Cl_4$) of **2k**

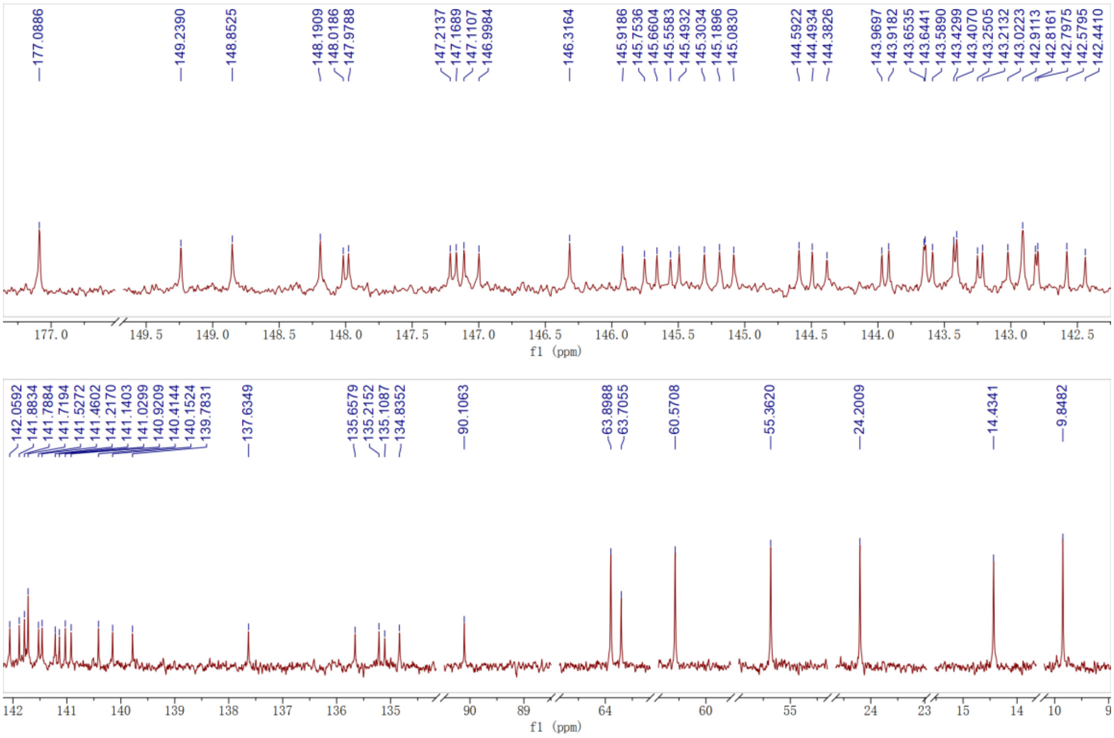

Fig. S86 Expanded ^{13}C NMR (101 MHz, $CS_2/C_2D_2Cl_4$) of **2k**

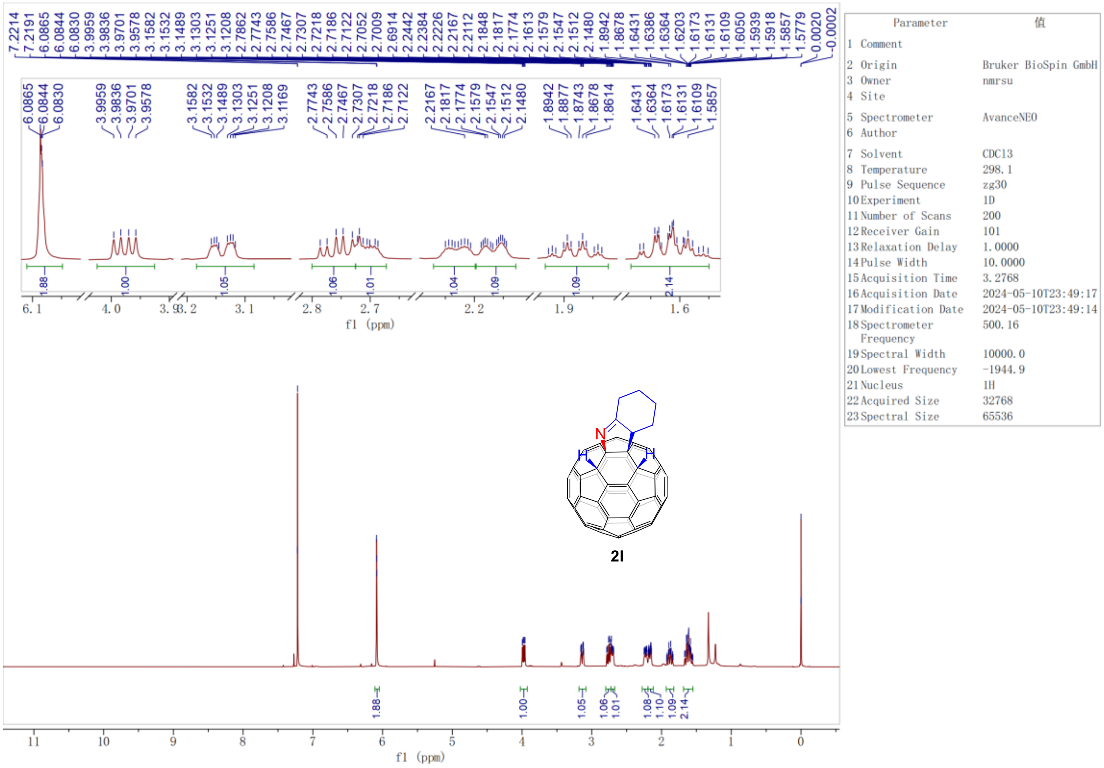

Fig. S87 ^{1}H NMR (500 MHz, $CS_2/CDCl_3$) of **2l**

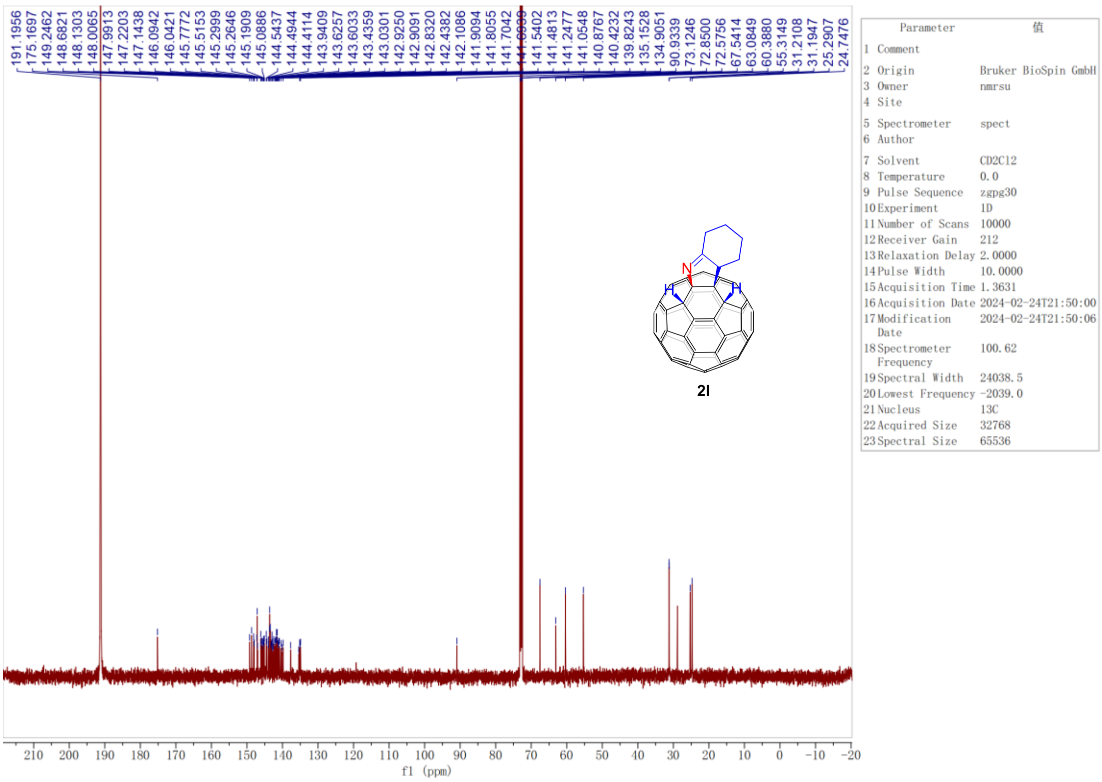

Fig. S88 ^{13}C NMR (101 MHz, $CS_2/C_2D_2Cl_4$) of **2l**

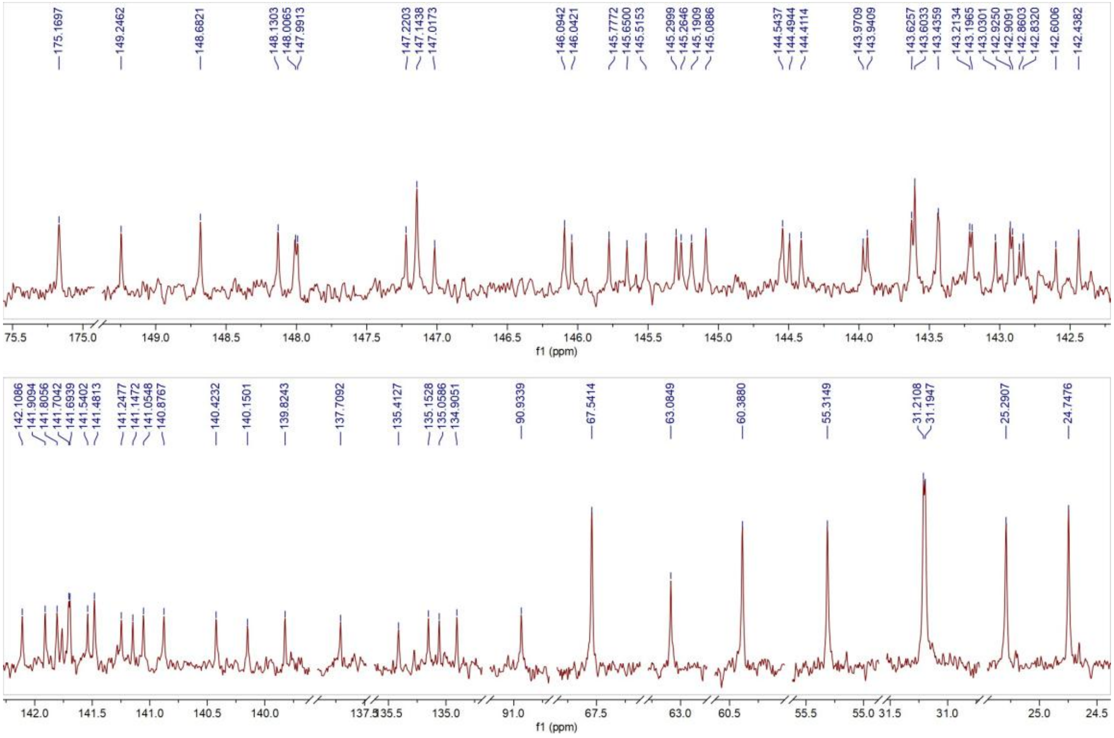

Fig. S89 Expanded ^{13}C NMR (101 MHz, $CS_2/C_2D_2Cl_4$) of **2l**

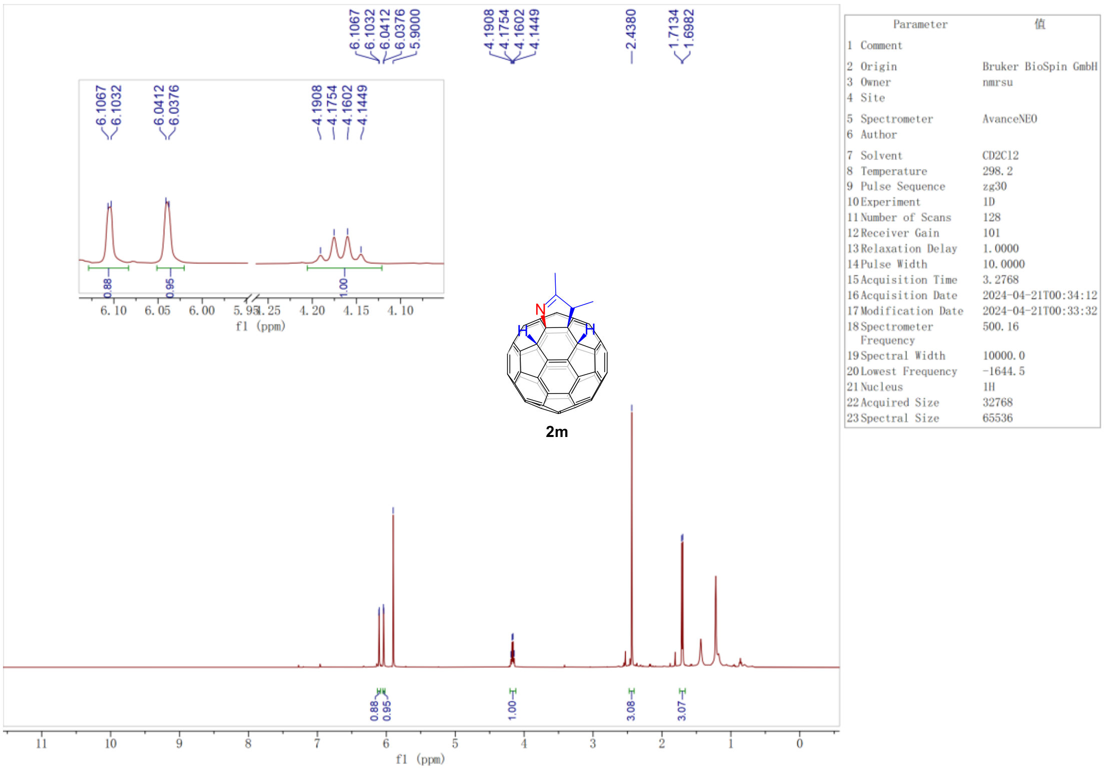

Fig. S90 ^{1}H NMR (500 MHz, $CS_2/C_2D_2Cl_4$) of **2m**

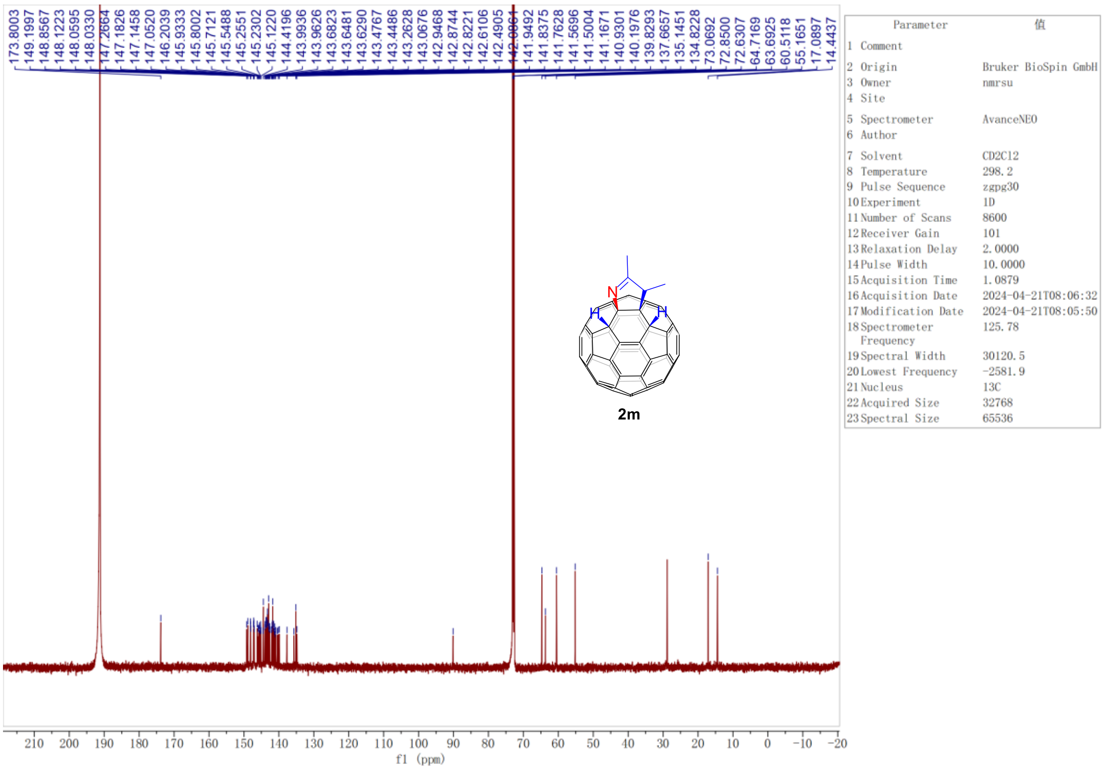

Fig. S91 [13]C NMR (126 MHz, $CS_2/C_2D_2Cl_4$) of **2m**

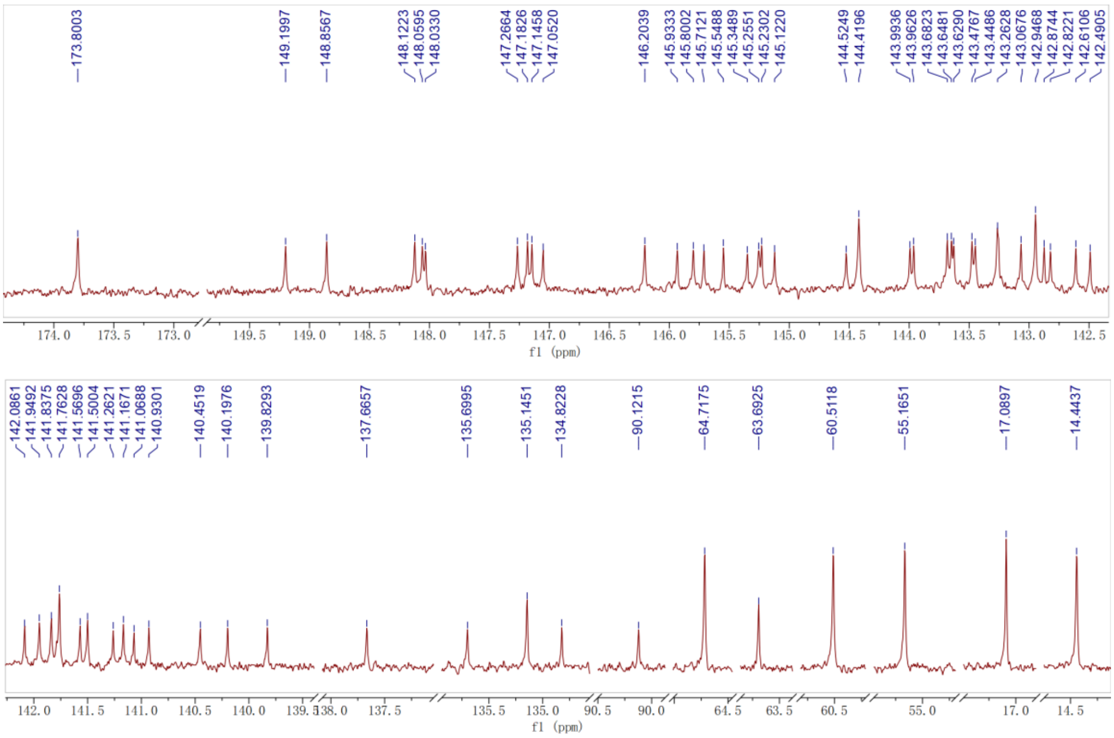

Fig. S92 Expanded [13]C NMR (126 MHz, $CS_2/C_2D_2Cl_4$) of **2m**

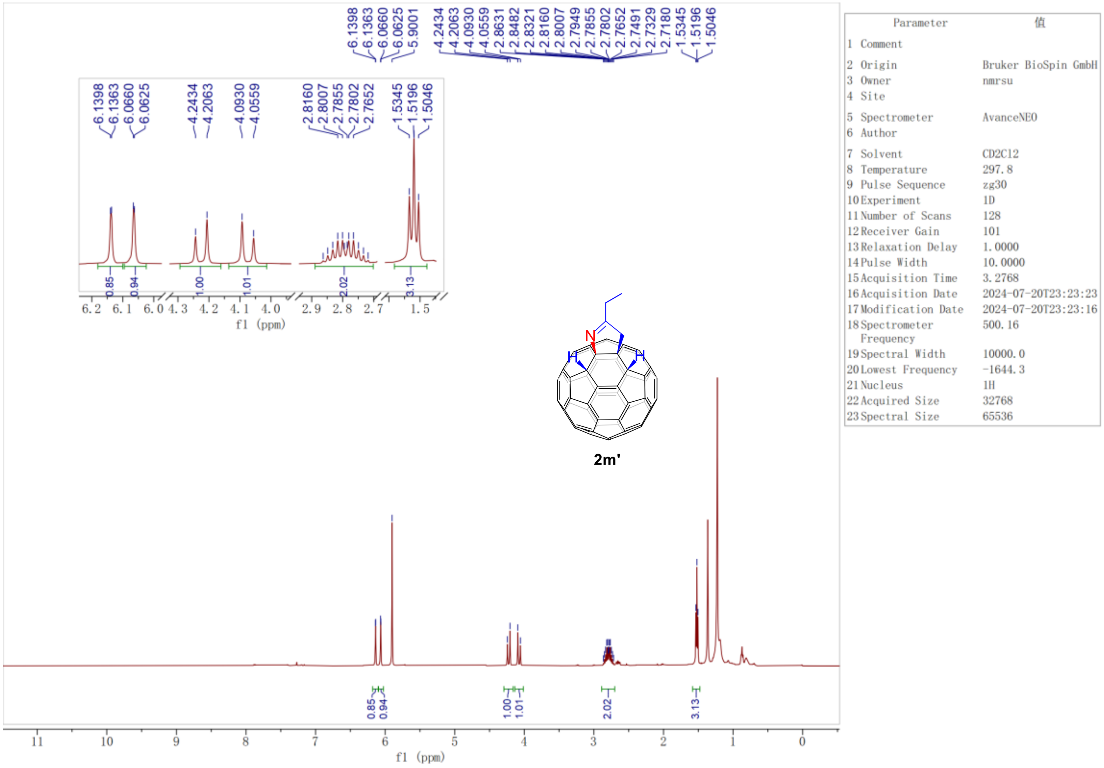

Fig. S93 ^{1}H NMR (500 MHz, $CS_2/C_2D_2Cl_4$) of **2m′**

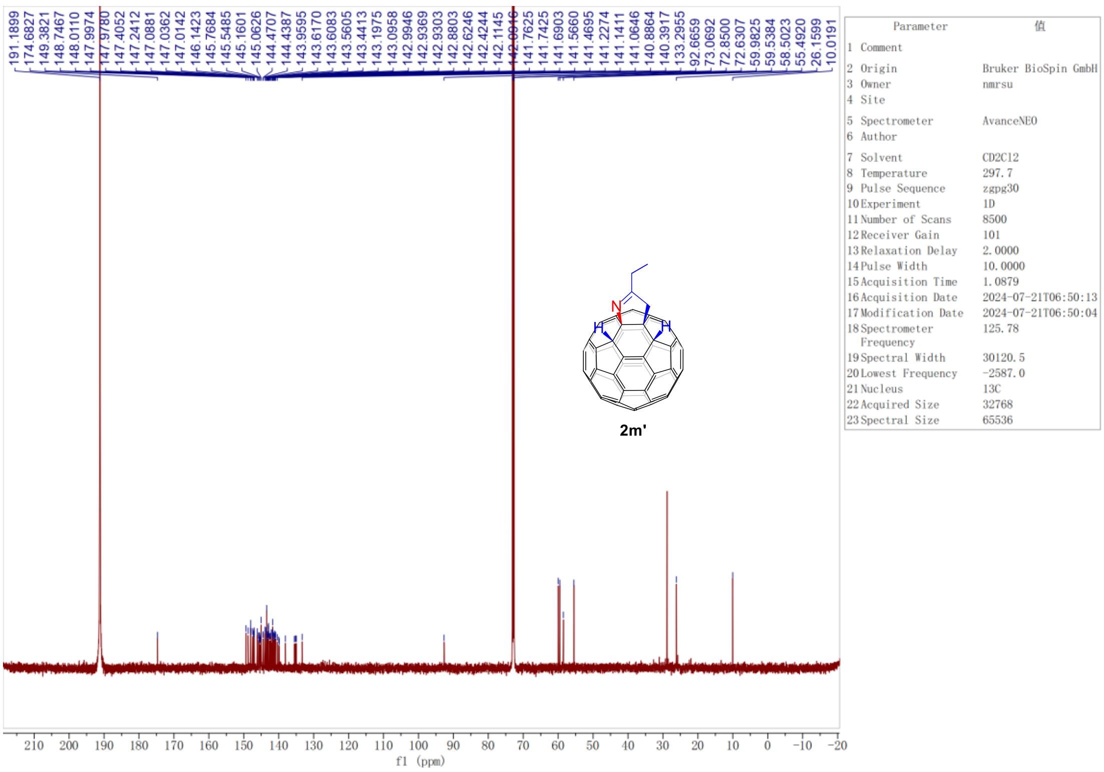

Fig. S94 ^{13}C NMR (126 MHz, $CS_2/C_2D_2Cl_4$) of **2m′**

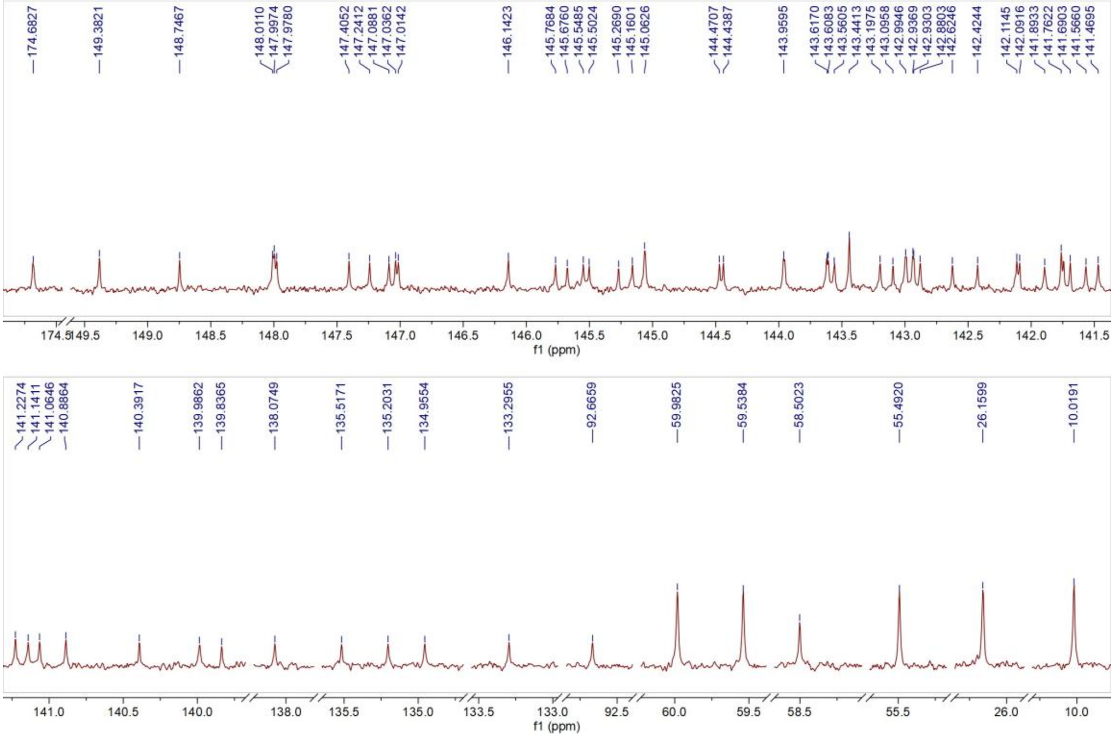

Fig. S95 Expanded ^{13}C NMR (126 MHz, $CS_2/C_2D_2Cl_4$) of **2m′**

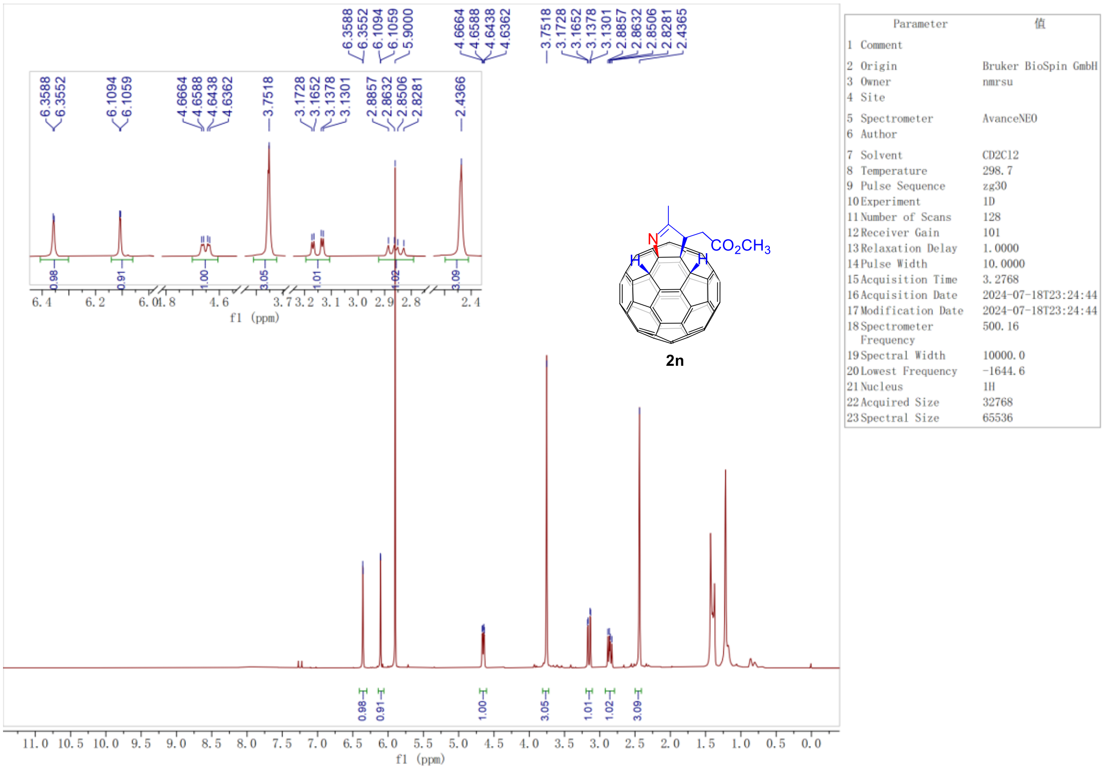

Fig. S96 ^{1}H NMR (500 MHz, $CS_2/C_2D_2Cl_4$) of **2n**

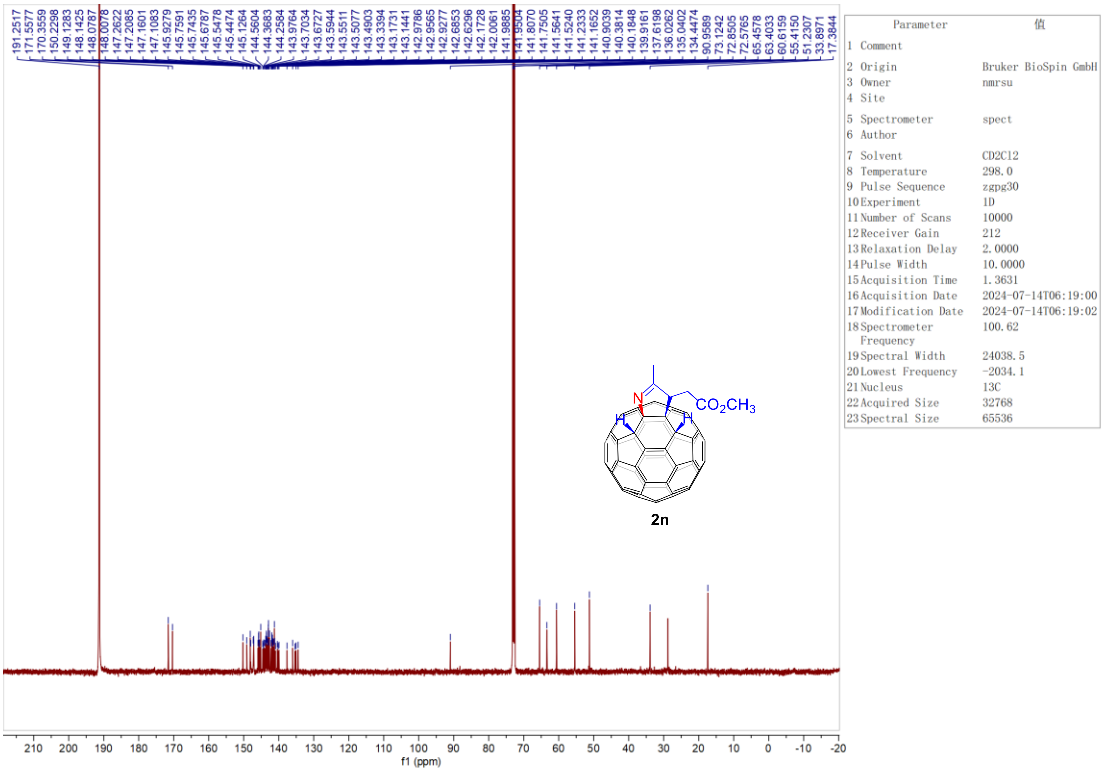

Fig. S97 ^{13}C NMR (101 MHz, $CS_2/C_2D_2Cl_4$) of **2n**

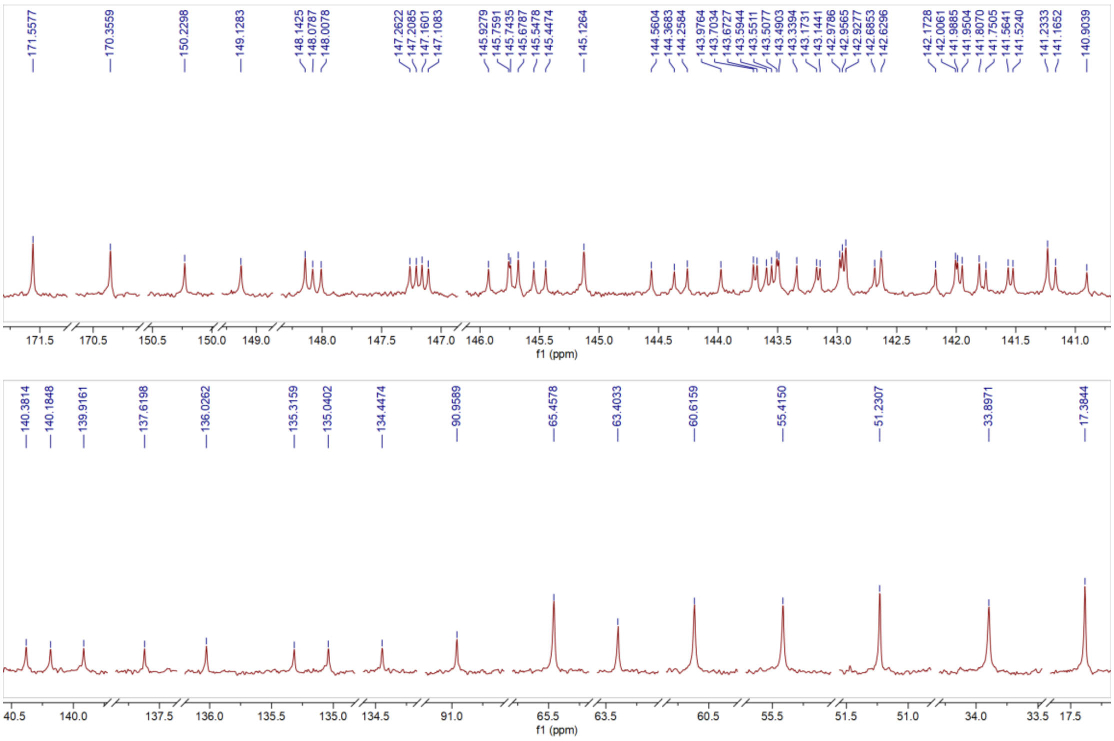

Fig. S98 Expanded ^{13}C NMR (101 MHz, $CS_2/C_2D_2Cl_4$) of **2n**

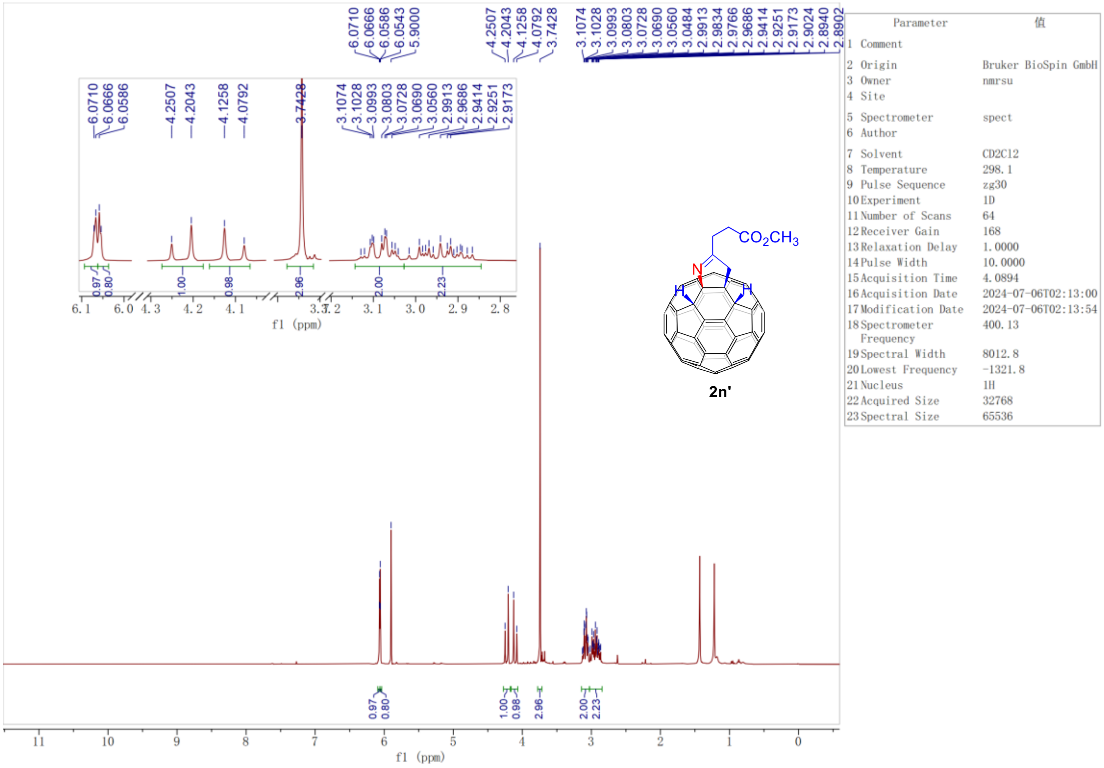

Fig. S99 ^{1}H NMR (400 MHz, $CS_2/C_2D_2Cl_4$) of s **2n′**

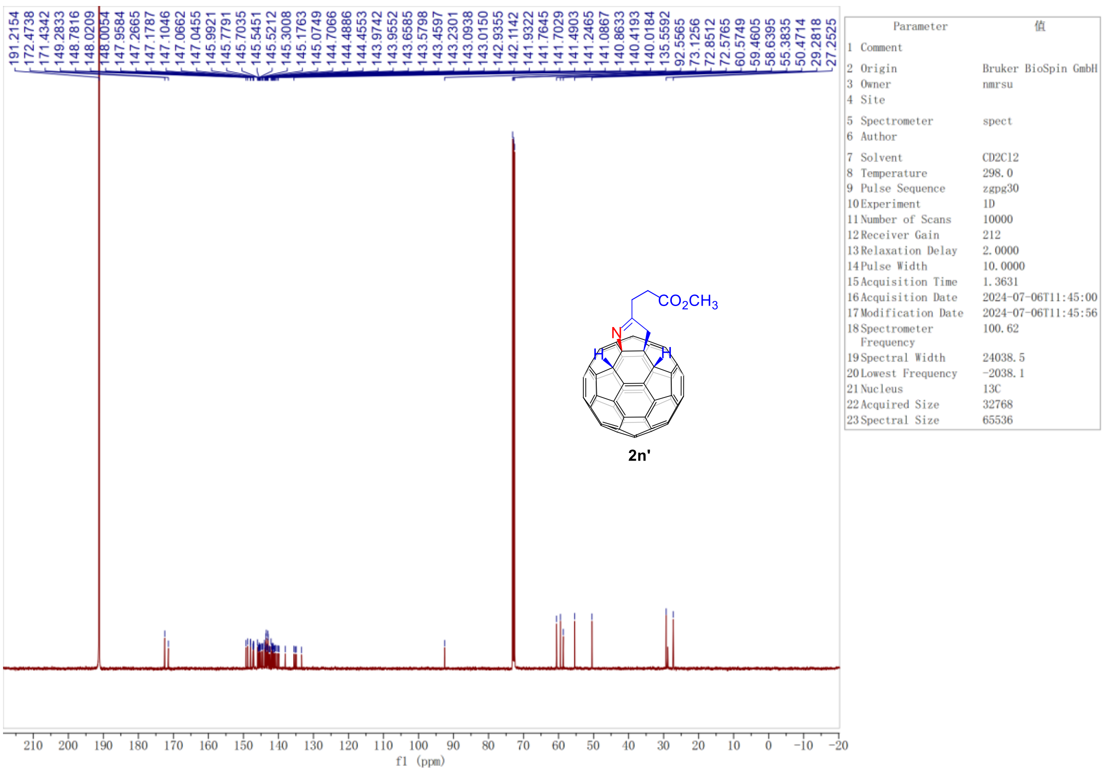

Fig. S100 ^{13}C NMR (101 MHz, $CS_2/C_2D_2Cl_4$) of **2n′**

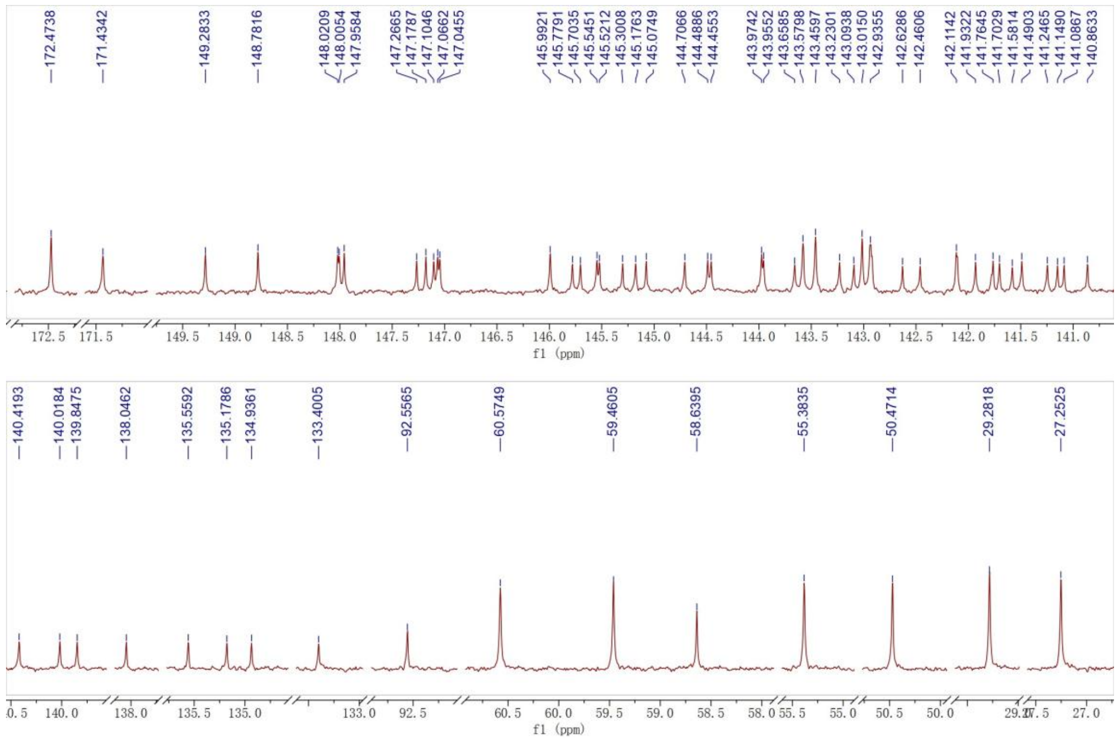

Fig. S101 Expanded ^{13}C NMR (101 MHz, $CS_2/C_2D_2Cl_4$) of **2n′**

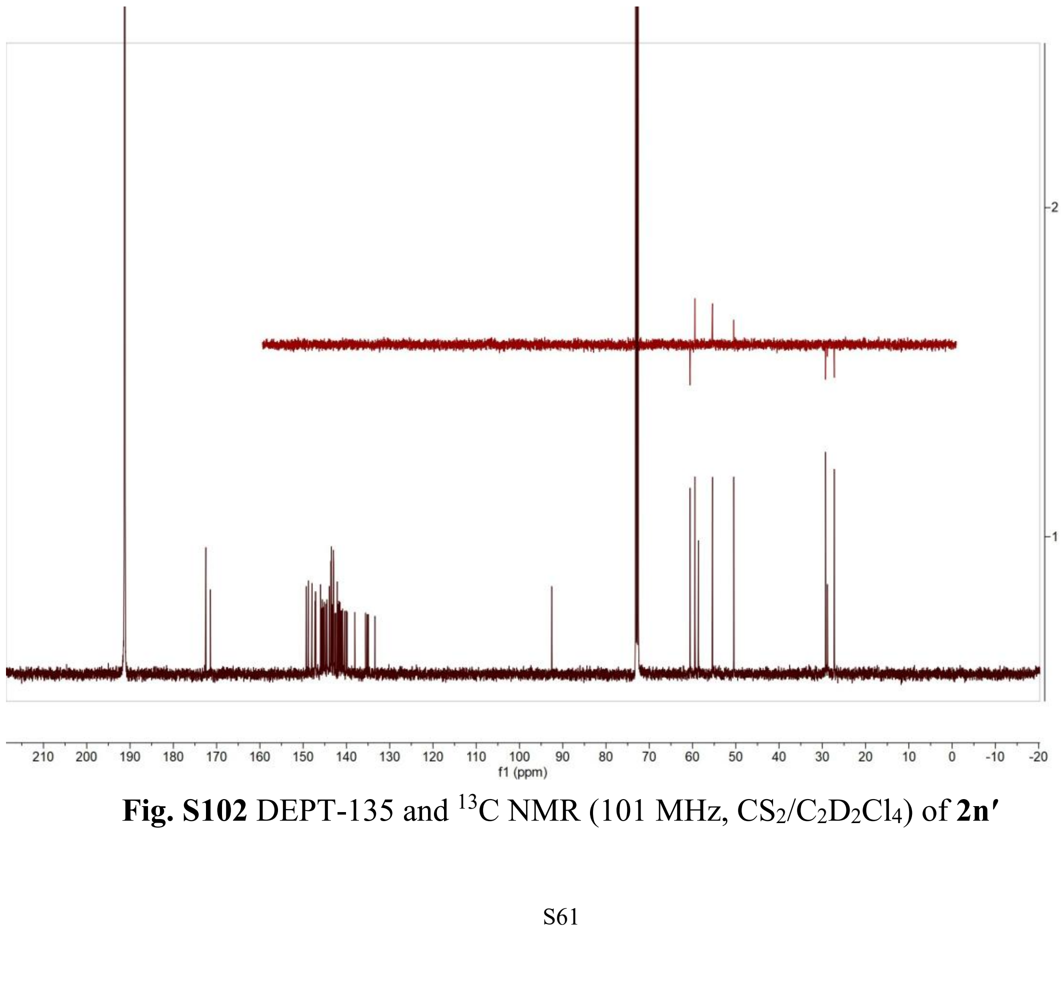

Fig. S102 DEPT-135 and ^{13}C NMR (101 MHz, $CS_2/C_2D_2Cl_4$) of **2n′**